

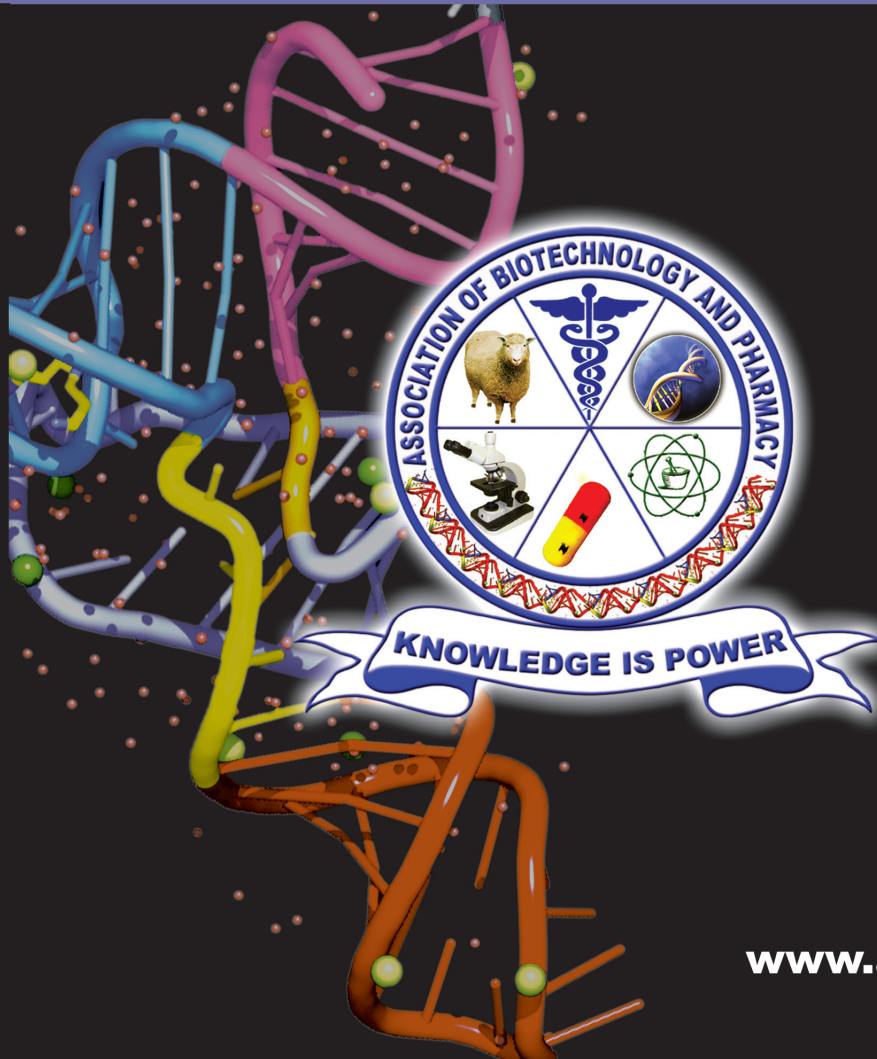
ISSN 0973-8916

Current Trends in Biotechnology and Pharmacy

Volume 12

Issue 2

April 2018



www.abap.co.in

Current Trends in Biotechnology and Pharmacy

ISSN 0973-8916 (Print), 2230-7303 (Online)

Editors

Prof.K.R.S. Sambasiva Rao, India
krssrao@abap.co.in

Prof. Karnam S. Murthy, USA
skarnam@vcu.edu

Editorial Board

Prof. Anil Kumar, India
Prof. P.Appa Rao, India
Prof. Bhaskara R.Jasti, USA
Prof. Chellu S. Chetty, USA
Dr. S.J.S. Flora, India
Prof. H.M. Heise, Germany
Prof. Jian-Jiang Zhong, China
Prof. Kanyaratt Supaibulwatana, Thailand
Prof. Jamila K. Adam, South Africa
Prof. P.Kondaiah, India
Prof. Madhavan P.N. Nair, USA
Prof. Mohammed Alzoghaibi, Saudi Arabia
Prof. Milan Franek, Czech Republic
Prof. Nelson Duran, Brazil
Prof. Mulchand S. Patel, USA
Dr. R.K. Patel, India
Prof. G.Raja Rami Reddy, India
Dr. Ramanjulu Sunkar, USA
Prof. B.J. Rao, India
Prof. Roman R. Ganta, USA
Prof. Sham S. Kakar, USA
Dr. N.Sreenivasulu, Germany
Prof. Sung Soo Kim, Korea
Prof. N. Udupa, India

Dr.P. Ananda Kumar, India
Prof. Aswani Kumar, India
Prof. Carola Severi, Italy
Prof. K.P.R. Chowdary, India
Dr. Govinder S. Flora, USA
Prof. Huangxian Ju, China
Dr. K.S.Jagannatha Rao, Panama
Prof. Juergen Backhaus, Germany
Prof. P.B.Kavi Kishor, India
Prof. M.Krishnan, India
Prof. M.Lakshmi Narasu, India
Prof. Mahendra Rai, India
Prof. T.V.Narayana, India
Dr. Prasada Rao S.Kodavanti, USA
Dr. C.N.Ramchand, India
Prof. P.Reddanna, India
Dr. Samuel J.K. Abraham, Japan
Dr. Shaji T. George, USA
Prof. Sehamuddin Galadari, UAE
Prof. B.Srinivasulu, India
Prof. B. Suresh, India
Prof. Swami Mruthinti, USA
Prof. Urmila Kodavanti, USA

Assistant Editors

Dr.Giridhar Mudduluru, Germany

Dr. Sridhar Kilaru, UK

Prof. Mohamed Ahmed El-Nabarawi, Egypt

Prof. Chitta Suresh Kumar, India

www.abap.co.in

ISSN 0973-8916

Current Trends in Biotechnology and Pharmacy

(An International Scientific Journal)

Volume 12

Issue 2

April 2018



www.abap.co.in

Indexed in Chemical Abstracts, EMBASE, ProQuest, Academic SearchTM, DOAJ, CAB Abstracts, Index Copernicus, Ulrich's Periodicals Directory, Open J-Gate Pharmoinfonet.in Indianjournals.com and Indian Science Abstracts.

Association of Biotechnology and Pharmacy (Regn. No. 28 OF 2007)

The *Association of Biotechnology and Pharmacy (ABAP)* was established for promoting the science of Biotechnology and Pharmacy. The objective of the Association is to advance and disseminate the knowledge and information in the areas of Biotechnology and Pharmacy by organising annual scientific meetings, seminars and symposia.

Members

The persons involved in research, teaching and work can become members of Association by paying membership fees to Association.

The members of the Association are allowed to write the title **MABAP** (Member of the Association of Biotechnology and Pharmacy) with their names.

Fellows

Every year, the Association will award Fellowships to the limited number of members of the Association with a distinguished academic and scientific career to be as Fellows of the Association during annual convention. The fellows can write the title **FABAP** (Fellow of the Association of Biotechnology and Pharmacy) with their names.

Membership details

(Membership and Journal)		India	SAARC	Others
Individuals	– 1 year	Rs. 600	Rs. 1000	\$100
	LifeMember	Rs. 4000	Rs. 6000	\$500
Institutions (Journal only)	– 1 year	Rs. 1500	Rs. 2000	\$200
	Life member	Rs.10000	Rs.12000	\$1200

Individuals can pay in two instalments, however the membership certificate will be issued on payment of full amount. All the members and Fellows will receive a copy of the journal free.

Association of Biotechnology and Pharmacy
(Regn. No. 28 OF 2007)
#5-69-64; 6/19, Brodipet
Guntur – 522 002, Andhra Pradesh, India

Current Trends in Biotechnology and Pharmacy

ISSN 0973-8916

Volume 12 (2)	CONTENTS	April 2018
Research Papers		
	Characterization of Akhanaphou, an unique landrace from North-East India and its RIL population for rice leaf and neck blast resistance <i>Supriya Babasaheb Aglawe, Umakanth Bangale, S J S Rama Devi, Vishalakshi Baliya, Vijay Pal Bhadana, Susheel Kumar Sharma, Sudhir Kumar, M. Srinivas Prasad and Maganti Sheshu Madhav</i>	118-127
	Phytochemical screening, antioxidant and antimicrobial efficacy of <i>Protorhus longifolia</i> (Bernh. Ex C. krauss) Engl. (Anacardiaceae) seed extracts <i>Nonsikelolo Yvonne Mhlongo, Krishna Suresh Babu Naidu, Reddy Kandappa Himakar, Sershen, Abdelkrim Cheriti and Patrick Govender</i>	128-138
	Determination of adipocyte cell size by H & E stained adipose tissue and collagenase digested isolated adipocytes <i>Devaligoda Gamage Kalpani Yashodara Perera, Hemantha Senanayake, Tharanga Thoradeniya</i>	139-146
	Spectroscopic studies, Antioxidant and Anticancer attributes of diffusible eumelanin produced by marine <i>Streptomyces roche</i> <i>Satheesh Periyasamy, Shalini Devi.S , Preethi Kathirvel</i>	147-158
	Optimization of process parameters for Poly Hydroxy Butyrate Production from Isolated <i>Acinetobacter nosocomialis</i> RR20 through Submerged Fermentation <i>A. Ranganadha Reddy, T.C. Venkateswarulu, P. Sudhakar, S. Krupanidhi, K. Vidya Prabhakar</i>	159-168
	<i>In-Vivo</i> Evaluation of Rifampicin Loaded Nanospheres: Biodistribution and <i>Mycobacterium</i> Screening Studies <i>Vishnu Vardhan Reddy Beeram, Krupanidhi S & Venkata Nadh R</i>	169-176
	System Modeling of Akt using Linear and Robust Regression Analysis <i>Shruti Jain</i>	177-186
	Molecular Taxonomy of Associated Microbes From Sea Slug <i>Kalinga Ornata</i> and its bioactivity <i>M. Mohanraj, N. Sri Kumaran and S. Bragadeeeswaran</i>	187-195
	Review Papers	
	Targeting Cancer cell metabolism via Target of Rapamycin <i>Ankita Awasthi, Vikrant Nain, Himanshi Singh, Pavan Kumar, Rekha Puria</i>	196-205
	From Natural products to therapeutically important antifungals <i>Neelabh and Karuna Singh</i>	206-211
	<i>News Item</i>	i - vi

Information to Authors

The *Current Trends in Biotechnology and Pharmacy* is an official international journal of *Association of Biotechnology and Pharmacy*. It is a peer reviewed quarterly journal dedicated to publish high quality original research articles in biotechnology and pharmacy. The journal will accept contributions from all areas of biotechnology and pharmacy including plant, animal, industrial, microbial, medical, pharmaceutical and analytical biotechnologies, immunology, proteomics, genomics, metabolomics, bioinformatics and different areas in pharmacy such as, pharmaceuticals, pharmacology, pharmaceutical chemistry, pharma analysis and pharmacognosy. In addition to the original research papers, review articles in the above mentioned fields will also be considered.

Call for papers

The Association is inviting original research or review papers and short communications in any of the above mentioned research areas for publication in *Current Trends in Biotechnology and Pharmacy*. The manuscripts should be concise, typed in double space in a general format containing a title page with a short running title and the names and addresses of the authors for correspondence followed by Abstract (350 words), 3 – 5 key words, Introduction, Materials and Methods, Results and Discussion, Conclusion, References, followed by the tables, figures and graphs on separate sheets. For quoting references in the text one has to follow the numbering of references in parentheses and full references with appropriate numbers at the end of the text in the same order. References have to be cited in the format below.

Mahavadi, S., Rao, R.S.S.K. and Murthy, K.S. (2007). Cross-regulation of VAPC2 receptor internalization by m2 receptors via c-Src-mediated phosphorylation of GRK2. *Regulatory Peptides*, 139: 109-114.

Lehninger, A.L., Nelson, D.L. and Cox, M.M. (2004). *Lehninger Principles of Biochemistry*, (4th edition), W.H. Freeman & Co., New York, USA, pp. 73-111.

Authors have to submit the figures, graphs and tables of the related research paper/article in Adobe Photoshop of the latest version for good illumination and alignment.

Authors can submit their papers and articles either to the editor or any of the editorial board members for onward transmission to the editorial office. Members of the editorial board are authorized to accept papers and can recommend for publication after the peer reviewing process. The email address of editorial board members are available in website www.abap.in. For submission of the articles directly, the authors are advised to submit by email to krssrao@abap.co.in or krssrao@yahoo.com.

Authors are solely responsible for the data, presentation and conclusions made in their articles/research papers. It is the responsibility of the advertisers for the statements made in the advertisements. No part of the journal can be reproduced without the permission of the editorial office.

Characterization of Akhanaphou, an unique landrace from North-East India and its RIL population for rice leaf and neck blast resistance

Supriya Babasaheb Aglawe¹, Umakanth Bangale¹, S J S Rama Devi¹, Vishalakshi Balija¹, Vijay Pal Bhadana¹, Susheel Kumar Sharma², Sudhir Kumar³, M. Srinivas Prasad¹ and Maganti Sheshu Madhav^{1*}

¹Biotechnology Division, Indian Institute of Rice Research, Rajendranagar, Hyderabad-500 030

²Plant Pathology Division, ICAR Research Complex for NEH Region, Manipur Centre, Imphal-795 004

³Crop Improvement Division, ICAR Research Complex for NEH Region, Manipur Centre, Imphal-795 004

* For Correspondence - sheshu24@gmail.com, sheshu_24@yahoo.com

Abstract

Rice blast continues to be the major constraint in sustainable rice production throughout the world. Although many genetic resources harboring single R-genes are available for blast resistance, wide genetic variations exist in the blast fungus lead to breakdown of these resistant varieties soon after its release. To control such a deadly disease, there is a need to identify QTLs which offer durable partial resistance. In this endeavor, we identified Akhanaphou, a unique rice landrace of Manipur showing a high level of resistance to leaf and neck blast across various locations. Upon genetic characterization, we found resistance in Akhanaphou governed by QTLs and two major genes *i.e* *Pi38* and *Pitp*. Three best stabilized recombinant inbred lines (RILs) showing resistance for leaf and neck blast and having significant homozygosity at various loci were identified based on gene profiling, phenotyping, and agronomic evaluation studies. The shortlisted RILs are valuable genetic resources for the development of blast resistance in rice improvement programs.

Keywords: Akhanaphou, Neck blast, Gene profiling, *Pi38* and *Pitp*

Introduction

In rice, since from the identification of *Pia*, the first blast-R gene (1), more than 100 blast resistance genes and more than 350 QTLs for blast resistance have been identified in various germplasm (2). The wide genetic variation available in *Magnaporthe* may be the driving force in the evolution of rice blast R-genes. Use of resistant cultivar is the primary and most economical approach to control blast disease (3). But increments of novel pathotypes have been reported to cause a breakdown of resistant rice varieties soon after its release (1, 4). Identification of novel R-genes/QTLs or mining the new alleles of blast R-genes with broad spectrum resistance and pyramiding different R-genes/QTLs with different resistance spectra into the elite cultivars are the alternative ways to achieve durable and broad-spectrum blast resistance (6 - 10). Therefore the continuous search for new resistance sources of the blast is important for sustainable rice production.

Ramkumar and coworkers (7) demonstrated that Amano Bavo and Boha Tulasi Joha (two landraces) have novel alleles of *Pi54* and offer higher level of resistance. Wang and coworkers (8) reported the high level of panicle and leaf blast

resistance in *japonica* landrace Jiangnanwan. Upon characterizing, RIL population developed from Jiangnanwan identified and fine mapped *Pi-jnw1* gene responsible for panicle blast resistance. It is well established from earlier studies that rice landraces are a good source of identification and mining of novel blast R-genes/QTLs.

India is known for having rich rice diversity and particularly the North Eastern part of India is one of the hotspots for rice biodiversity in the world. Such landraces are worthy candidates for a detailed examination of the blast resistant genes (11). Present study carried out with motivation to identify and characterize novel source of leaf and neck blast resistance. For this work, we selected Akhanaphou (7) which is one of the unique landraces of North-East India, showing high-level of resistance to both leaf and neck blast. Genetic characterization of Akhanaphou and its population for inheritance of leaf as well as neck blast resistance at two different locations revealed the presence of multiple genes. Gene profiling was employed for determining the known blast R-genes. Based on multivariate tests like phenotyping and agronomic evaluation and gene profiling, best RIL lines were selected which can be used for introgression of blast resistance during varietal development program.

Material and Methods

Plant material : Akhanaphou (*indica*) is a popular landrace of Manipur possessing a high level of resistance to leaf and neck blast. One hundred and three RILs (Recombinant Inbred Lines) (Akhanaphou X Leimaphou) were developed by SSD (Single Seed Descent) method at NEH-RC (North East Hilly-region Research Center), Manipur up to F_8 generation and seeds were received through personal communication. Leimaphou (*indica*) is a commercially important cultivar of rice from Manipur which is popular for its cooking quality and high yield but showing high susceptibility for leaf and neck blast. RIL population was maintained and forwarded at IIRR (Indian Institute of Rice Research) for the next two successive generations by using SSD method. An F_2 population was also developed

using same donor and recurrent parent of RILs *i.e.* Akhanaphou and Leimaphou respectively.

Phenotyping of Akhanaphou, RILs and F_2 s for blast resistance

: Akhanaphou was extensively screened for leaf blast as well as neck blast resistance as done by Rama Devi and coworkers (12). Screening for leaf blast resistance was done at two locations, IIRR, Rajendranagar, Hyderabad and at NEH-RC, Manipur. However, screening for neck blast was done only at one location *i.e.* NEH-RC, Manipur. Screening for the leaf blast resistance was carried out on UBN (Uniform Blast Nursery) at IIRR, Rajendranagar for the three seasons (Nov-2013, Nov-2014, and Sept-2015) with two replications. At NEH-RC, Manipur, Akhanaphou was screened under field condition for both leaf and neck blast resistance in two successive seasons (Aug-2014 and Aug-2015) with two replications.

At IIRR, Rajendranagar, the entire nursery bed was surrounded from all sides by two rows of HR12 to function as a spreader source for the pathogen. About 30-40 ml of the spore suspension (NLR-1 isolate) of the blast pathogen (approximately 10^5 spores per ml mixed with Tween-20 @ 0.2%) was sprayed on 15-day old seedlings using a glass atomizer. The inoculum was also provided by placing pieces of infected leaves over the test material. High humidity (95%) was maintained using sprinklers. The observation on disease reaction was recorded when the susceptible check was severely infected by the blast. For F_2 s, individual plants in each line were scored based on 0-9 scale (13). For RILs, ten plants from each line were scored and the average score was used for further QTL analysis.

Screening for leaf and neck blast was done in the field conditions, under natural disease pressure and also augmented with artificial inoculums. For leaf blast screening, modified UBN conditions were maintained and pathogen inoculums was augmented with a spray of leaf blast infected leaves and a daily spray of water for maintaining high humidity. For neck blast screening, individual plants were syringe

inoculated with a spore suspension (a mixture of pathogen's pure cultures). Phenotyping for leaf blast was done based on 0-9 scale (13).

Field resistance of Akhanaphou for leaf and neck blast was also checked across different parts of the country in AICRP (All India Coordinated Research Project) on rice during Kharif-2012. In the AICRP on rice trials, Akhanaphou was checked for its reaction to the leaf blast at 23 centers whereas; the neck blast resistance was checked at six centers.

The RIL population and F_2 populations were also screened for the leaf blast resistance at IIRR, Rajendranagar during Feb-2012 and Sep-2015 respectively whereas, for leaf and neck blast resistance at NEH-RC, Manipur during Kharif-2014, Kharif-2015 with two replications.

Study of inheritance of blast resistance : Chi-square test for goodness of fit was applied to study the inheritance of blast resistance in Akhanaphou. Obtained Resistance: Susceptible ratio in F_2 population was used to test fitness for Mendelian 3:1 monogenic ratio and also other ratios such as dihybrid ratio, trihybrid ratio, and ratios of epistatic interactions.

Genomic DNA isolation and Gene profiling study : Genomic DNA of individual RILs, Akhanaphou and Leimaphou were isolated using modified CTAB (Cetyltrimethylammonium bromide) method (14). The quality of isolated DNA was checked using 0.8% agarose gel electrophoretically and quantified using the Nanodrop (Thermo Fisher, USA). Gene profiling study was conducted for Akhanaphou and Leimaphou as done by Rama Devi and coworkers (12). The SSR (Simple Sequence Repeats) markers linked to nine important blast resistant genes viz., *Pi54*, *Pi9*, *Pib*, *Pi20*, *Pita-2*, *Pitp*, *Pik-s*, *Pi33* and *Pi38* were used to know whether the Akhanaphou and Leimaphou contain any of these genes by comparing the marker allele data with positive and negative controls (Supplementary Table 1). Further, their segregation was also checked across RIL population.

Agro-morphological evaluation of the RILs :

During Kharif-2014, RIL population was grown along with donor and recurrent parents. Observations were recorded for the following agro-morphological parameters (i) days to 50 % flowering, (ii) plant type, (iii) average plant height, (iv) number of tillers per plant, (v) number of productive tillers per plant, (vi) panicle exertion and (vii) seed type

Identification of the best RILs : Based on phenotyping for the blast resistance, evaluation of agronomic traits, gene profiling analysis and presence of QTL (15); RIL population was evaluated for identification of good RIL lines for the blast resistance.

Results

Characterization of Akhanaphou for the blast resistance :

Akhanaphou showed a high level of resistance to leaf blast (score-2) at IIRR, Rajendranagar, and NEH-RC, Manipur, whereas for neck blast, it showed resistance reaction (score-1). Leimaphou showed a highly leaf blast susceptible reaction (8-9 score) at both locations whereas; for neck blast it recorded '8' score. During 2012-AICRP on rice screening, Akhanaphou showed an average score of '3.1' for leaf blast and '2.7' for neck blast (Table 1).

Genetics of blast resistance : Out of 196 F_2 plants screened for leaf blast resistance at Rajendranagar, 171 plants showed resistance reaction while the remaining 25 plants showed susceptible reaction. While screening for the leaf blast resistance at Manipur, out of 80 F_2 plants, 25 plants found to be resistant and 55 plants found to be susceptible. In case of neck blast resistance out of 80 plants screened, only 27 plants recorded resistance and 53 plants recorded susceptible reaction.

Obtained Resistance: Susceptible ratios of F_2 population, for leaf and neck blast resistance screened at Rajendranagar and Manipur did not fit into any Mendelian ratios (Table 2). So, it is concluded that the blast resistance of Akhanaphou is governed by polygenes rather than a single gene. The graph plotted for the frequency

distribution of disease severity of the leaf blast and neck blast at two locations showed normal distribution which support proposed hypothesis.

Gene profiling analysis : Gene profiling analysis revealed the presence of *Pi38* and *Pitp* genes in Akhanaphou. Since, it showed similar marker alleles as positive control (Tadukan) in the case of *Pi38* with two linked flanking markers *i.e.* RM206 and RM21. Similarly, Akhanaphou also showed similar marker allele as a positive control (Tetep) with RM246 indicating the presence of *Pitp*. In contrary, Leimaphou showed the presence of allele similar to the negative control in case of *Pi38* and *Pitp* genes (Supplementary Table 1 and Fig. 1).

Segregation of *Pi38* and *Pitp* were observed among RILs, there was a good segregation among RILs for these two markers. Out of 103 RILs, 15 RILs were positive for *Pi38* genes, 10 RILs were positive for *Pitp* gene; whereas, 3 RILs were positive for both the genes *Pi38* and *Pitp*. The total of 81 RILs did not show the presence of any of these genes. Details of the analysis are given in Table 3.

Phenotyping reaction of RILs : At IIRR, Rajendranagar, 60 RILs showed resistance reaction with a 0-4 score and 41 showed a susceptible reaction with a 5-9 score. At Manipur 34 RILs recorded a resistance reaction with a 0-4 score and 69 RILs recorded a susceptible reaction with a 5-9 score for leaf blast disease. In case of neck blast screening 34 RILs showed a resistance reaction with 0-3 score whereas, 69 RILs recorded a susceptible reaction with a 0-3 score.

Identification of best RILs : Out of 103 RILs, only 22 RILs found to contains one or two blast R-genes. Among 22 RILs, 15 and 10 RILs found to contain *Pi38* and *Pitp* gene respectively. Only three RILs found to contain both the blast R-genes (Table 3). Disease reaction pattern of RILs were decided based on phenotyping at three different environments namely 1) screening for leaf blast at IIRR, Rajendranagar, Hyderabad, 2) screening for leaf blast at NEH-RC, Manipur and 3) screening for neck blast at NEH-RC, Manipur. RILs showing leaf blast resistance at any one environment were

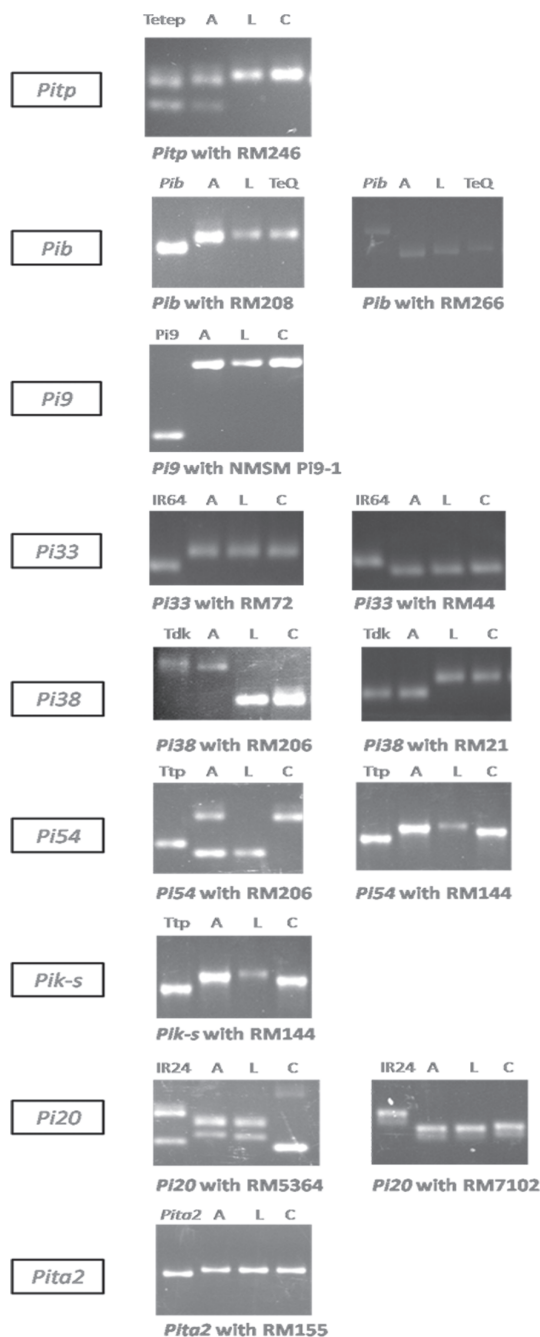


Fig. 1. Gene profiling of Akhanaphou with linked SSR markers. A-Akhanaphou, L-Leimaphou, C-Co-39, Tdk-Tadukan, Ttp-Tetep, TeQ- Te-Qing, *Pib*- IRBLb-IT13[CO], *Pita2*- IRBLta2-Pi, *Pi9*- IRBL9-W[LT].

Table 1-1. Nine important blast resistant genes and related information such as chromosomal location, linked markers, their distance (cM) from respective R-gene, positive control and negative control.

Sr. No.	Blast	Chromosome resistant gene	Linked location	Positive markers	Negative control	Akhanaphou control	Leimaphou
1	<i>Pitp</i>	1	RM246	Tetep	Co-39*	+	-
2	<i>Pib</i>	2	RM208RM266	IRBLb-IT13[CO]	Te-Qing	-	-
3	<i>Pi9</i>	6	NMSMPi9-1	IRBL9-W[LT]	Co-39*	-	-
4	<i>Pi33</i>	8	RM72RM44	IR64	Azucena	-	-
5	<i>Pi38</i>	11	RM206RM21	Tadukan	Co-39	++	-
6	<i>Pi54</i>	11	RM206RM144	Tetep	Co-39*	-	-
7	<i>Pik-s</i>	11	RM144	Tetep	Co-39*	-	-
8	<i>Pi20</i>	12	RM1337 RM5364 RM7102	IRBL20-IR24	Co-39*	-	-
9	<i>Pita-2</i>	12	RM55	IRBLta2-Pi	Co-39*	-	-

*As standard negative control given for blast R-genes were not available with us, Co-39 is considered as negative control for these blast R-genes in the gene profiling study. The rice blast resistance gene scored as the presence (+) and absence (-) of amplicon

Table 1. Characterization of Akhanaphou for the blast resistance

Sr. No.	Phenotyping for the blast	Recorded score for Akhanaphou	Recorded score for Leimaphou	Recorded score for C101LAC	Recorded score for C101A51	Recorded score for HR12
I. Phenotyping for the leaf blast resistance at Rajendranagar						
1	Feb-2012	1	9	5	5	9
2	Nov-2014	2	8	2	2	9
3	Sept-2015	3	8	3	2	9
II. Phenotyping for the leaf blast resistance at NEH-RC, Manipur						
1	Aug-2014	3	9	4	3	9
2	Aug-2015	2	8	3	4	9
III. Phenotyping for the neck blast resistance at NEH-RC, Manipur						
1	Aug-2014	1	7	3	3	9
2	Aug-2015	1	7	3	4	9
IV. Phenotyping for the leaf blast resistance in the ACRIP trials						
1	2012	3.1	-	6.1	7.2	8.0
V. Phenotyping for the neck blast resistance in the ACRIP trials						
1	2012	2.7	-	7.1	8.2	8.2

- data not available

C101LAC & C101A51-positive controls

HR12-negative control

Table 2. Chi-square table for F₂ (Akhanaphou X Leimaphou) populations screened for the leaf blast resistance at IIRR, Rajendranagar, Hyderabad and screened for leaf and neck blast at NEH-ICAR, Research Center, Lamphelpat, Manipur

Blast type and location	Phenotyping for leaf blast at Rajendranagar	Phenotyping for leaf blast at Manipur	Phenotyping for neck blast at Manipur
Resistant	171	25	27
Susceptible	25	55	53
Total	196	80	80
Chi-square value for monohybrid ratio	15.67	81.66	72.60
Chi-square value for dihybrid ratio	256.00	177.82	172.40

Table value for monohybrid ratio: 3.84

Table value for dihybrid ratio: 7.81

Table 3. Segregation of *Pi38* and *Pitp* gene among RILs (Akhanaphou X Leimaphou)

RILs positive for	Number of RILs	RILs
<i>Pi38</i>	15	RIL: 2, 3, 12, 18, 24, 27, 50, 58, 62, 68, 71, 91, 96, 100, 102
<i>Pitp</i>	10	RIL: 13, 20, 34, 44, 46, 50, 59, 69, 71, 91
<i>Pi38 + Pitp</i>	3	RIL: 50, 71, 91

considered as resistant to leaf blast disease. Among the 15 RILs which contain the *Pi38*, five RILs viz., RIL: 2, 3, 27, 91 and 96 showed leaf blast resistance whereas, out of 10 RILs which contain the *Pitp*, three RILs showed leaf blast resistance namely, RIL: 13, 34 and 91. Interestingly, nine RILs viz., RIL: 13, 18, 20, 27, 34, 44, 91, 100 and 102 containing either *Pi38* or *Pitp* showed neck blast resistance. Based on all these parameters along with another study results (15), 3 RILs namely RIL: 13, 34 and 91 were considered as best for blast resistance (Table 4).

Discussion

Blast disease is a devastating disease of rice, threatening the global rice production particularly from tropical and subtropical rice growing regions of the world. Though, many methods and practices are available for control of

blast disease in the field, resistance breeding is the most economic, effective and feasible method for control of blast disease. Deployment of resistant genes and QTL is one of the important approaches of resistance breeding since a lot of genetic variation for the resistance exists among the rice germplasm. In the changing climatic scenario, the neck blast has become a serious threat and endemic in many rice growing areas. Hence, the identification of genes or QTL for both leaf and neck blast resistance is a continuing a challenging part in rice improvement program. Among the 100 blast R-genes identified so far, only one gene *i.e.* *Pb1*, identified from Modan (Indonesian) rice variety, confers resistance specifically for neck blast (16).

Landraces are one of the important components of germplasm of any crop. Landraces

Table 4. Comparison of Akhanaphou, Leimaphou and Three good donor RILs for blast resistance along with their details

RIL No.	Akhanaphou	Leimaphou	13	34	91
Screening of RILs for presence of Pi genes					
<i>Pi38</i>	+	-	-	-	+
<i>PitP</i>	+	-	+	+	+
Distribution of QTLs among RILs					
<i>qLNBL-5</i>	+	-	+	+	+
<i>qLNBL-7</i>	+	-	-	+	-
Evaluation of RILs for agronomic traits					
Flowering days	104	92	84	96	103
Plant type	Erect	Spreading	Erect	Erect	Erect
Dwarf/Tall/Medium	Tall	Dwarf	Dwarf	Medium	Tall
Panicle emergence	Well exerted	Partly exerted	Partly exerted	Partly exerted	Well exerted
Grain type	Medium bold	Long bold	Medium bold	Medium bold	Long bold
Average productive tillers	5	7	4	4	4
Average plant height	133	78	52	91	134
Phenotyping of RILs for leaf blast at Rajendranagar					
Disease reaction	Resistant	Susceptible	Resistant	Resistant	Resistant
Phenotyping of RILs for leaf blast at NEH-RC, Manipur					
Disease reaction	Resistant	Susceptible	Resistant	Resistant	Resistant
Phenotyping of RILs for neck blast at NEH-RC, Manipur					
Disease reaction	Resistant	Susceptible	Resistant	Resistant	Resistant

are “balanced populations in equilibrium with both the environment and pathogens, and are genetically dynamic” (17). The North Eastern part of India is known for rich biodiversity including rice and also one of the hot spots of rice blast disease particularly for neck blast with existence of high genetic diversity of *M. oryzae* (18, 19). In North Eastern India, wide genetic variation and high pathogen pressure of blast pathogen contributes to the evolution of many novel gene(s). Among several landraces, Akhanaphou is one of the unique landraces from Manipur having a high level of resistance to leaf and neck blast, whose genetic base for resistance is not known.

In the extensive and rigorous phenotyping, Akhanaphou proved resistant against leaf and neck blast. Interestingly it showed a high resistant reaction to neck blast with 1 score during both of the seasons. There was no change in disease reaction showed by Akhanaphou during UBN and field evaluation for leaf blast; though the pathogen

pressure at Manipur was very high. After confirming high level of blast resistance of Akhanaphou we had gone for inheritance study in F₂ population. In inheritance study, based on chi-square test and from graphs showing normal frequency distribution of disease severity, it was confirmed that the trait of leaf and neck blast resistance of Akhanaphou is under polygenic control. To date approximately 350 QTL resistances to leaf blast have been mapped for blast resistance in rice which provide evidence for polygenic control of blast resistance in many rice germplasm (2, 20 - 23).

After confirming polygenic inheritance of blast resistance, gene profiling study was done to know the presence of major blast R-genes in Akhanaphou. For this study, nine blast R-genes which are being used more often in blast resistance breeding programs in India were selected (24). Though gene specific and functional markers are available for some of the blast R-gene, we did not use them in gene profiling

because they are allele specific. Different alleles of the same gene can be present in a population, which cannot be identified with gene specific and functional markers. Gene profiling is a rapid method to know the presence of known blast R-genes using tightly linked markers. Moreover, it is difficult and time-consuming process to conduct allelic tests for all the known blast R-genes. Similar approach was followed earlier for identification of alleles or better performing alleles from the diverse germplasm through PCR-based approach (12, 18, 25, 26, 27, 28, 29). Gene profiling of ten major rice blast resistance genes has been determined in 192 rice germplasm accessions using SSR markers by Singh and coworkers (27). Rama Devi and coworkers checked the allelic status of seven important blast R-genes in the 326 introgression lines derived from six different wild species using gene-based markers (12). Gene profiling revealed that Akhanaphou contain *Pi38* and *Pitp* blast R-genes. As both of these genes were identified for leaf blast and genetics study revealed polygenic nature of blast resistance, we hypothesized that, there may be some novel genes or QTLs which contribute to true blast resistance in Akhanaphou.

We developed RIL population by crossing Akhanaphou with Leimaphou, an elite variety with good agronomic traits such as good yield and famous for cooking quality. RIL population is stabilized population and achieves significant homozygosity, for almost all of the loci after 6-7 generations. Akhanaphou is a landrace and many undesirable traits are associated with it such as low yield, tallness, grain shattering nature etc. Direct use of Akhanaphou in rice breeding program as donor will cause more linkage drag which is highly undesirable. Use of RILs showing blast resistance rather than Akhanaphou will reduce linkage drag in crossing program. RHLs (Recombinant Heterogeneous Lines) developed by the crossing of two donor RILs will also act as valuable and useful breeding material for blast resistance breeding. Identification of good RILs showing blast resistance along with good agronomic traits will act as good candidates for

direct varietal release. In order to shortlist good donors, two type of analysis was done. In the first analysis, RILs containing either *Pi38* or *Pitp* or both genes were checked for their disease reaction. Interestingly nine RILs viz., RIL: 13, 18, 20, 27, 34, 44, 91, 100 and 102 which contain either *Pi38* or *Pitp* showed neck blast resistance. These results help to infer that *Pi38* and *Pitp* may also contribute to neck blast resistance of Akhanaphou. Surprisingly, RILs which do not contain either *Pi38* or *Pitp* but still showed blast resistance were also identified which includes 16 RILs showing leaf blast resistance and 42 RILs showing neck blast resistance whereas, 8 RILs showing resistance to both leaf and neck blast. These results are in supports of our hypothesis that, leaf and neck blast resistance in Akhanaphou is under the polygenic control. RILs which do not contain either *Pi38* or *Pitp* but still showing leaf or/and neck blast resistance will be more informative and helpful in novel QTL mapping approach. Moreover, use of RIL population rather than F_2 s will also advantageous to identify minor effect QTLs. The results obtained in our recent studies are in support of polygenic nature of blast resistance of Akhanaphou. The mapping studies conducted in Akhanaphou has leads to identification of two novel QTLs i.e. *qLNBL-5* and *qLNBL-7*; for leaf and neck blast resistance on chromosomes 5 and 7 respectively (15).

In conclusion, Akhanaphou found to be a reliable resource for leaf and neck blast resistance. Extensive phenotypic analysis (at two different locations with artificial and field screening as well as screening at the diverse location through AICRP on rice) revealed the broad spectrum nature of resistance in Akhanaphou. Akhanaphou contains two major blast R-genes i.e. *Pi38* and *Pitp*. The identified stable breeding lines (RIL: 13, 34 & 91) which contains either or both of the genes and having good agronomic traits can be explored in rice improvement program. They can even used for direct varietal release after multi-location trials. The breeding lines which do not have major blast R-genes but yet showing resistance can be explored for identification of novel QTLs. Thus the

identified unique landrace Akhanaphou and its population can be further exploited for deciphering the complete blast resistance mechanism.

References

1. Kiyosawa, S. (1967). The inheritance of resistance of the Zenith type varieties of rice to the blast fungus. *Japanese J Breeding*, 17: 99-107.
2. Ashkani, S., Yusop, M. R., Shabanimofrad, M., Azadi, A., Ghasemzadeh, A., Azizi, P. and Latif, M. A. (2015). Allele mining strategies: principles and utilization for blast resistance genes in rice (*Oryza sativa* L.). *Current Issues of Mol Biol*, 17: 57-74.
3. Hulbert, S. H., Webb, C. A., Smith, S. M. and Sun, Q. (2001). Resistance gene complexes: Evolution and utilization. *Ann Rev in Phytopathol*, 39: 285–312.
4. Gayatonde, V., Mahadevu, P., Prasanna Kumar, M. K. and Vennela, P. R. (2016). Interaction of AVR-R gene and rice blast resistance. *The Bioscan* 11: 1867-1864.
5. Arunakumari, K., Durgarani, C. V., Satturu, V., Sarikonda, K. R., Chittoor, P. D. R., Vutukuri, B., Laha, G. S., Nelli, A. P. K., Gattu, S., Jamal, M. and Prasadbabu, A. (2016). Marker-Assisted Pyramiding of Genes Conferring Resistance Against Bacterial Blight and Blast Diseases into Indian Rice Variety MTU1010. *Rice Science*, 23(6): 306-316.
6. Xiao, N., Wu, Y., Pan, C., Yu, L., Chen, Y., Liu, G., Li, Y., Zhang, X., Wang, Z., Dai Z., and Liang, C. (2016). Improving of rice blast resistances in japonica by pyramiding major R-genes. *Frontiers in Plant Science*, 7.
7. Ramkumar, G., Madhav, M. S., Devi, S. R., Umakanth, B., Pandey, M. K., Prasad, M. S., Sundaram, R. M., Viraktamath, B. C. and Babu, V. R. (2016). Identification and validation of novel alleles of rice blast resistant gene *Pi54*, and analysis of their nucleotide diversity in landraces and wild *Oryza* species. *Euphytica*, 209: 725-737.
8. Wang, R., Fang, N., Guan, C., He, W., Bao, Y. and Zhang, H., (2016). Characterization and fine mapping of a blast resistant gene *pi-jnw1* from the japonica rice landrace Jiangnanwan. *PloS one*, 11(12).
9. Chaipanya, C., Telebanco-Yanoria, M. J., Quime, B., Longya, A., Korinsak, S., Korinsak, S., Toojinda, T., Vanavichit, A. Jantasuriyarat, C., and Zhou, B. (2017). Dissection of broad-spectrum resistance of the Thai rice variety Jao Hom Nin conferred by two resistance genes against rice blast. *Rice*, 10(1): 18.
10. Nagaoka, I., Sasahara, H., Tabuchi, H., Shigemune, A., Matsushita, K., Maeda, H., Goto, A., Fukuoka, S., Ando, T. and Miura, K. (2017). Quantitative trait loci analysis of blast resistance in *Oryza sativa* L. 'Hokuriku 193'. *Breeding science*, 67(2): 159-164.
11. Das, B., Sengupta, S., Parida, S. K., Roy, B., Ghosh, M., Prasad M. and Ghose, T. K. (2013). Genetic diversity and population structure of rice landraces from Eastern and the North Eastern States of India. *BMC genet*, 14: 71-72.
12. Rama Devi, S. J. S., Singh, K., Umakanth, B., Vishalakshi, B., Renuka, P., Sudhakar, K. V., Prasad, M. S., Viraktamath, B., Babu, V. R. and Madhav, M. S. (2015). Development and identification of novel rice blast resistant sources and their characterization using molecular markers. *Rice Sci*, 22: 300-308.
13. IRRI. (1996). Standard Evaluation System for Rice. 4th ed. International rice research institute, Los Banos, Philippines.
14. Saghai-Maroo, M. A., Soliman, K. M., Jorgensen, R. A. and Allard, R. W. (1984). Ribosomal DNA spacer-length polymorphisms in barley: Mendelian inheritance, chromosomal location, and population dynamics. *PNAS*, 81(24): 8014-8018.

15. Aglawe, S. B., Umakanth, B., Rama Devi, S. J. S., Vishalakshi, B., Badana, V. P., Sharma, S. K., Sharma, P. K., Kumar, S., Prasad, M. S. and Madhav, M. S. (2017). Identification of novel QTLs conferring field resistance for rice leaf and neck blast from an unique landrace of India. *Gene Reports*, 7: 35-42.
16. Hayashi, N., Inoue, H., Kato, T., Funao, T., Shirota, M., Shimizu, T., Kanamori, H., Yamane, H., Hayano Saito, Y., Matsumoto, T. and Yano, M. (2010). Durable panicle blast-resistance gene *Pb1* encodes an atypical CC-NBS-LRR protein and was generated by acquiring a promoter through local genome duplication. *The Plant J*, 64: 498–510.
17. Harlan, J. R. (1975). *Crops and Man*. Madison, Wisconsin: American Society of Agronomy and Crop Science Society of America.
18. Imam, J., Alam, S., Mandal, N. P., Variar, M. and Shukla, P. (2014). Molecular screening for identification of blast resistance genes in North East and Eastern Indian rice germplasm (*Oryza sativa* L.) with PCR-based markers. *Euphytica*, 196: 199–211.
19. Anupam, A., Imam, J., Quatadah, S. M., Siddaiah, A., Das, S. P., Variar, M. and Mandal, N. P. (2017). Genetic diversity analysis of rice germplasm in tripura state of northeast India using drought and blast linked markers. *Rice Science*, 24(1): 10-20.
20. Zhang, Y., Yang, J., Shan, Z., Chen, S., Qiao, W., Zhu, X., Xie, Q., Zhu, H., Zhang, Z., Zeng, R., Ding, X. (2012). Substitution mapping of QTLs for blast resistance with SSSLs in rice (*Oryza sativa* L.). *Euphytica*, 184: 141–150.
21. Ashkani, S., Rafii, M. Y., Rahim, H. A. and Latif, M. A. (2013). Genetic dissection of rice blast resistance by QTL mapping approach using an F₃ population. *Mol Biol Reporter*, 40: 2503–2515.
22. Jiang, H., Yan, B., Duan, T., Li, Y., Gao, G., Zhang, Q., Xiao, J., Xu, C., Jiang, G. and He, Y. (2015). Mapping and evaluating quantitative trait loci for blast resistance under natural infection conditions using an advanced backcross population in rice. *Euphytica*, 204:121–133.
23. Liu, Y., Qi, X., Gealy, D. R., Olsen, K. M., Caicedo, A. L. and Jia, Y. (2015). QTL Analysis for resistance to blast disease in U.S. weedy rice. *Mol Plant-Microbe Interactions*, 28: 834–844.
24. Prasad, M.S., Madhav, M.S., Laha, S., Ladhakshmi, D., Krishnaveni, D., Satendrakumar, M., Balachandran, S. M., Sundaram, R. M., Arunakanthi, B., Madhanmohan, K., Ratnamadhavi, K., Kumar, V. and Viraktamath, B. C. (2011). *Rice Blast Disease and Its Management*. Directorate of Rice Research, Hyderabad, India.
25. Ingole, K. D., Prashanthi, S. K. and Krishnaraj, P. U. (2014). Mining for major blast resistance genes in rice landraces of Karnataka. *Indian J Genet and Plant Breeding*, 74: 378–383.
26. Khan, M. A. I., Sen, P. P., Bhuiyan, R., Kabir, E., Chowdhury, A. K., Fukuta, Y., Ali, A. and Latif, M. A. (2014). Phenotypic screening and molecular analysis of blast resistance in fragrant rice for marker assisted selection. *Comptes rendus boil*, 337: 318–324.
27. Singh, A. K., Singh, P. K., Arya, M., Singh, N. K. and Singh, U. S. (2015). Molecular screening of blast resistance genes in rice using SSR markers. *Plant Pathol J*, 31: 12–24.
28. Mahesh, H. B., Shirke, M. D., Singh, S., Rajamani, A., Hittalmani, S., Wang, G. L. and Gowda, M. (2016). Indica rice genome assembly, annotation and mining of blast disease resistance genes. *BMC genomics*, 17(1): 242.
29. Yadav, M. K., Aravindan, S., Ngangkham, U., Shubudhi, H. N., Bag, M. K., Adak, T., Munda, S., Samantaray, S. and Jena, M. (2017). Use of molecular markers in identification and characterization of resistance to rice blast in India. *PLoS*

Phytochemical screening, antioxidant and antimicrobial efficacy of *Protorhus longifolia* (Bernh. Ex C. krauss) Engl. (Anacardiaceae) seed extracts

Nonsikelolo Yvonne Mhlongo¹, Krishna Suresh Babu Naidu², Reddy Kandappa Himakar¹, Sershen³, Abdelkrim Cheriti⁴ and Patrick Govender^{1*}

¹. Dept. of Biochemistry, School of Life Sciences, Westville, University of KwaZulu-Natal, Durban-4000 South Africa. Email: mhlongony@gmail.com

². Department of Biomedical and Clinical Technology, Durban University of Technology, Durban-4000, South Africa. Email: Sureshk@dut.ac.za.

³. Dept. of Applied Biology, School of Life Sciences, Westville, University of KwaZulu-Natal, Durban, South Africa. Email: naidoose@ukzn.ac.za

⁴. Phytochemistry & Organic synthesis Laboratory, University of Bechar, 08000, Bechar, Algeria
Email: Karimcheriti@yahoo.com; Phone / Fax (Works): +213 49 81 52 44

*For Correspondence - patrickgovender.ukzn@gmail.com

Abstract

The objective of this study was to elucidate the phytochemical, antioxidant and antimicrobial activities of *Protorhus longifolia* seed extracts *in vitro*. The phytochemical analysis revealed the presence of flavonoids, glycosides and sterols predominately in the methanol and ethanol extracts. Antioxidant activities were evaluated *in vitro* by DPPH-radical scavenging, H₂O₂ and ABTS⁺ assays. Methanol extract had the highest DPPH scavenging activity (95% at 200 µg/ml), while hexane extract had the lowest DPPH scavenging activity (16% at 25 µg/ml). Aqueous extract showed high percentage of scavenging activity in ABTS⁺ radical system compared to other assays. Amongst all the extracts, methanol extract showed significant inhibitory effect against *Staphylococcus aureus* (inhibition zone diameter 16mm) while different seed extracts showed no activity against *Enterococcus faecalis*. While in the case of fungal strains, only methanol extract showed antifungal activity against *Candida albicans* ATCC 10231 (< 9 mm) and *Candida albicans* (< 7 mm). The study indicates that

methanol extract of seeds of *P. longifolia* exhibit strong antioxidant and antimicrobial activity and would be potential sources of antioxidant and antimicrobial agents of natural origin and could be used as potential alternative for treating various diseases.

Keywords: Antibacterial; Antifungal; Flavonoids; Methanol extract; Phytochemical; *P. longifolia* seed extract

Introduction

Natural products, such as plants extract, either as pure compounds or as standardized extracts, provide unlimited opportunities for new drug discoveries because of the unmatched availability of chemical diversity (1). According to World Health organization (WHO), more than 80% of world's populations of Asia, Africa and Latin America rely on traditional medicine for their primary health care needs (2). Nevertheless, of all the c.250 000 species of higher plants on earth, only a fraction has been examined for all aspects of their potential therapeutic medicinal value (3). The study of plants continues principally for the

discovery of novel secondary metabolites. Around 80% of product were of plant origin and there sales exceeded US \$64 billion in 2003

Plants based bioactive molecules that can be used as medicine with wide spectrum of activities can be derived from any part of the plant like leaves, bark, flowers, roots, fruits, seeds etc. (4, 5). This therapeutic property is attributed by variety of chemical substances synthesized by plants as secondary metabolites which include alkaloids, saponins, tannins, flavonoids, glycosides, and anthraquinones (6). Furthermore, the use of traditional medicine and medicinal plants in most developing countries remains more affordable than western medicine and also easily accessible by the poor communities (7). In South Africa in particular, many rural ethnic groups rely on traditional indigenous plant knowledge to treat various diseases in both humans and livestock (8, 9). In the order of 15% of the 24 000 taxa recorded in southern Africa are used in traditional medicines (10) and an estimated 500 plant species are traded in informal medicinal plant markets (11).

Protorhus longifolia (Benrh.) Engl. (Red beech) of Anacardiaceae family is a medium to large mostly dioecious tall tree native to South Africa and Swaziland. The bark of *P. longifolia* has been traditionally used to cure various diseases such as heart water and diarrhea in cows (12), hemiplegic paralysis, heart burn, bleeding from the stomach and in the management of blood clotting related diseases (13). The leaves extracts of *P. longifolia* have been reported to possess antimicrobial activity (14, 15) and 10.2-18% tanning material from the bark (16).

Given the alarming incidence of antibiotic resistance in bacteria of medical significance, and paucity of biological activity from seed of *P. longifolia*, the present study was taken to explore phytochemical, antioxidant and antimicrobial activity using different in vitro approaches.

Materials and Methods

Chemicals: Hexane (HE), Ethyl acetate (EA), Chloroform (CH), Methanol (MetOH), Ethanol

(EtOH), DPPH (2,2-diphenyl-1-picrylhydrazyl), Hydrogen Peroxide (H₂O₂) and ABTS™ (2,2'-azino-bis) was purchased from Sigma-Aldrich Chemical Co. (St Louis, MO, USA). All the chemicals used including the solvents, were of analytical grade.

Collection and preparation of plant material:

Seeds of *Protorhus longifolia* were collected from Westville campus, University of KwaZulu-Natal (GPS co-ordinates -29.817897, 30.942771). Seeds (100 g) were air-dried and powdered. The dry powder of seeds (100 mg) was individually extracted with hexane (HE), ethyl acetate (EA), chloroform (CH), methanol (MetOH), ethanol (EtOH) and water (H₂O) by the cold percolation method (17). Samples were vigorously mixed using a vortex [Lasec SA (Pty) Ltd.] and left to stand for 24 hours at room temperature. The supernant was collected and allowed to completely evaporate using rotary vacuum evaporator (40°C). The extracts were diluted in 10% DMSO for the bioassay to remove other solvents which would possible affect the testing compounds.

Preliminary phytochemical screening:

The preliminary phytochemical screening of aqueous, methanol, ethanol, hexane, ethyl acetate and chloroform seed extracts of *P. longifolia* was subjected to different chemical tests for the detection of different phytoconstituents using standard procedures (18-24). The qualitative phytochemical analysis was performed to identify the presence of alkaloids, flavonoids, glycosides, tannins, saponins, steroids and phenolic compounds from the seed extracts of *P. longifolia*.

In vitro methods

Disc diffusion method: Disc diffusion method for antimicrobial susceptibility testing was carried out according to the standard method by Bauer et al. (25) to assess the presence of antibacterial activities of the plant extracts. A bacterial culture (which has been adjusted to 0.5 McFarland standard) was used to lawn Mueller-Hinton agar plates using evenly using a sterile swab. The plates were dried for 15 minutes and then used for sensitivity test. The discs which had been impregnated with series of plant extracts were

placed on Mueller-Hinton agar surface. Each test plate comprises of six discs, one positive control, which is a standard commercial antibiotic disc, one negative control and four treated discs. Sterile filter paper discs (10 mm in diameter, Whatmann) were aseptically transferred on agar surfaces and immediately impregnated with 2 μ l (400 μ g) of prepared plant extracts and incubated for 24-48 h at 37 °C. Likewise, Vancomycin (30 μ g) and Amoxicillin (25 μ g) were used as positive control. After the incubation, the plates were examined for inhibition zone. After the incubation, the plates were examined for inhibition zone. The inhibition zone were then measured using calipers and recorded. The test were repeated three times to ensure reliability.

Evaluation of minimum inhibitory concentrations (MICs)

Antibacterial activity: Minimum inhibitory concentration, defined as the lowest concentration of an antimicrobial agent that inhibits the growth of a microorganism after overnight incubation was determined by monitoring the growth of bacteria in a microplate reader (Synergy HT, BioTek Instruments) at 630 nm by micro dilution method as per NCCLS guidelines (26). The bacterial test cultures used in this study were *Escherichia coli* (ATCC 35218), *Klebsiella pneumoniae* (ATCC 700603), *Staphylococcus aureus* (ATCC 43300), *Enterococcus faecalis* (ATCC 5129) and *Pseudomonas aeruginosa* (ATCC 27853). A serial two fold dilutions of crude extracts were made over the range of 200-1.25 μ g/ml to make up in sterile 96-well plates (27). The wells were then inoculated with diluted overnight broth culture initially adjusted to a cell density of 1.5×10^8 (0.5 McFarland standards) and incubated at 35°C for 24 hours. Neomycin (Sigma) served as a positive control. MIC was recorded as the lowest concentration at which no growth was observed. All experiments were carried out in triplicates.

Antifungal activity: MIC values were determined using standard broth microdilution method according to M27-A2 (for yeast) as per CLSI guidelines (28). Briefly, yeast strains *Candida albicans* (ATCC-90028); *Candida krusei* (ATCC-

6258); *Candida parapsilosis* (ATCC-22019) were grown aerobically overnight at 35°C on Sabouraud dextrose agar (Merck) plates. Yeasts were harvested and suspended in 1% sterile saline and the turbidity of the supernatants measured spectrophotometrically at 625 nm with an absorbance of 0.08-0.1 equivalents to the No. 0.5 McFarland standard following the NCCLS M27-A2 guidelines. The working suspension was diluted 1:20 in a mixture containing RPMI 1640 medium and 0.165 m morpholine-propanesulfonic acid (MOPS, Sigma-Aldrich) buffered to pH 7.0. The working suspension was further diluted with the medium (1:50) to obtain the final test inoculums ($1-5 \times 10^3$ CFU ml⁻¹). The microtitre plates were allowed to thaw and equilibrate to room temperature under aseptic conditions which contains different concentrations of testing compounds. 100 μ l aliquots of working inoculum suspensions were dispensed into each well and the plates incubated in an aerobic environment at 35 °C for 24 h. After incubation, 20 μ l of 3-(4,5-dimethylthiazol-2-yl)-5-(3-carboxymethoxyphenyl)-2-(4-18sulfophenyl)-2H-terazolium salt (MTS, Promega Corporation, Madison, USA) was added directly to each well, incubated at 37 °C for 4 h and the absorbance recorded at 490 nm on a 96-well plate reader (Mindray MR-96A). Amphotericin-B was used as standard drug for the comparison of antifungal activity. MIC was recorded as the lowest concentration at which no growth was observed.

Study of antioxidant properties

DPPH free radical scavenging activity: The DPPH radical scavenging capacity of different extracts was measured according to Barku et al. (29), with minor modifications. Extract solutions were prepared by dissolving 0.05g of dry extract in 50ml of methanol. An aliquot of 2ml of 0.004% DPPH solution in methanol and 1ml of seed extract in methanol at various concentrations (25, 50, 75, 100 and 200 μ g/ml) were mixed and incubated at 25°C for 30 min and absorbance of the test mixture was read at 517 nm using a spectrophotometer (UV min 1240, Shimadzu) against a DPPH control containing only 1 ml of methanol in place of the extract. All experiments were performed in

triplicates and the results were averaged. Ascorbic acid was used as a standard (30). The DPPH radical scavenging activity was calculated by the formula given below

$$\% \text{ Radical Scavenging activity} = \left(\frac{A_{\text{blank}} - A_{\text{sample}}}{A_{\text{blank}}} \right) \times 100$$

Where A_{blank} and A_{sample} represent absorption of the blank and tested extract samples respectively.

H_2O_2 scavenging activity: The H_2O_2 scavenging capacity of different extracts was evaluated according to Ruch et al. (31) with minor modifications. A 4 mM solution of H_2O_2 was prepared in phosphate buffered saline (PBS; pH 7.4) at 20°C. Different extract solutions were prepared 100% methanol and then added to H_2O_2 at a final concentrations (25, 50, 75, 100 and 200 $\mu\text{g/ml}$). H_2O_2 A_{230} was determined 10 min later using a spectrophotometer (UV min 1240, Shimadzu) against a blank containing PBS without H_2O_2 .

The % of inhibition was calculated by the following equation:

$$\% \text{ Scavenged } [H_2O_2] = (A_c - A_s) / A_c \times 100$$

Where A_c is the absorbance of the control and A_s is the absorbance of the test samples respectively.

ABTS⁺ radical scavenging activity: The ABTS⁺ scavenging activities of the seed extracts were determined according to the method of Re et al. (32) with minor modification. Briefly, ABTS⁺ (2 mM) was prepared by dissolving in 50 ml of phosphate buffered saline (PBS; pH 7.4). ABTS⁺ was produced by reacting 50 ml of stock solution with 200 μL of 70 mM potassium persulfate ($K_2S_2O_8$) water solution. The mixture was allowed to stand in the dark at room temperature for 15–16h before use. For the evaluation of antioxidant activity, the ABTS⁺ solution was diluted with PBS to obtain the absorbency of 0.70 (\pm 0.02) at 734 nm. Different concentrations (25, 50, 75 and 100 $\mu\text{g/ml}$) of the extracts were prepared and mixed with 1 ml of ABTS solution. The absorbance was read at room temperature after 10 min at 734 nm. PBS solution was used as a blank sample.

The % of inhibition was calculated by the following expression

$$\text{ABTS scavenging activity (\%)} = (A_0 - A_1) / A_0 \times 100$$

Where A_0 is the absorbance of the control, and A_1 is the absorbance of the test samples respectively.

Results

Preliminary phytochemical screening: The results of phytochemical screening and qualitative estimation of different extracts of *P. longifolia* studied show that the seeds were rich in flavonoids, glycosides and sterols (Table 1). The seed extracts lacked alkaloids, saponins, phenols and tannins which is worth noting. Particularly, chloroform, methanol and ethanol seed extracts of *P. longifolia* were good sources of different classes of phytochemicals. This indicates that these solvents are effective to isolate active biological compounds due to their high polarity.

Antimicrobial activity: The powdered *P. longifolia* seeds were evaluated for both antibacterial and antifungal activity using hexane, ethyl acetate, chloroform, methanol, ethanol and water using the disc diffusion method in concurrence with the minimum inhibitory concentration (MIC). The results based on the disc diffusion method are presented in Table 2. All crude extracts were found to exhibit antibacterial activity at a concentration of 400 $\mu\text{g/ml}$, while minimal antifungal activity was observed for different extracts as shown in Table 3. Methanolic and ethanolic extracts displayed high activity against *S. aureus* (>13 mm), *E. coli* (>11 mm), *P. aeruginosa* (>14 mm) and *K. pneumoniae* (>10mm) as presented in Table 2. Antifungal activity was noted maximum for only methanolic extract against *C. albicans* (<7mm) and *C. albicans* 10321 (<9mm).

The minimum inhibitory concentration (MIC) assay was used to quantify the antibacterial activity of *P. longifolia* seed extracts. An advantage in using the method is that both polar and non-polar compounds can be tested found within the crude extracts. The most potent extract was methanol which had MIC values of 62.5 $\mu\text{g/ml}$

Table 1. Qualitative phytochemical analysis of various seed extracts of *P. longifolia*

Phytochemical Test	Hexane	Ethyl acetate	Chloroform	Methanol	Ethanol	Water
Alkaloids	-	-	-	-	-	-
Flavonoids	-	-	-	+	+	-
Glycosides	+	-	+	+	+	-
Saponins	-	-	-	-	-	-
Sterols	-	-	+	+	+	-
Phenols	-	-	+	+	+	+
Tannins	-	-	-	-	-	-

Note: "+" indicates the presence and "-" absence.

Table 2. Antibacterial activity of extracts of *Protorus longifolia* seeds extract by disc diffusion method (400 µg/disc concentration) and zone of inhibition (mm ± SD)

Test organisms	HE	EA	CH	MetOH	EtOH	H ₂ O	Neomycin* (PC)
<i>S. aureus</i>	10 ± 0.47	10 ± 0.47	9 ± 0.47	16 ± 0.47	13 ± 0.47	8 ± 0.94	7
<i>E. coli</i>	7 ± 0.47	7 ± 0.47	7 ± 0.47	13 ± 0.82	11 ± 0.94	8 ± 0.47	15
<i>P. aeruginosa</i>	9 ± 1.41	11 ± 0.82	12 ± 0.47	15 ± 0.47	14 ± 0.47	9 ± 0.47	14
<i>K. pneumoniae</i>	8 ± 0.94	7 ± 0.82	7 ± 0.47	13 ± 0.47	10 ± 0.94	9 ± 0.82	15
<i>E. faecalis</i>	NA	NA	NA	NA	NA	NA	8

HE = Hexane; EA = Ethyl acetate; CH = Chloroform; MetOH = Methanol; EtOH = Ethanol; H₂O = Water; 'NA'=No activity
 *PC- Positive control (50 µg/ml)

Table 3. Antifungal activity of extracts of *Protorus longifolia* seeds by disc diffusion method (400 µg/disc concentration) and zone of inhibition (mm)

Test organisms	HE	EA	CH	MetOH	EtOH	H ₂ O	Amphotericin-B* (PC)
<i>C. albicans</i>	NA	NA	NA	7	NA	NA	12
<i>C. albicans 10231</i>	NA	NA	NA	9	NA	NA	11
<i>C. krusei</i>	NA	NA	NA	NA	NA	NA	9
<i>C. parapsilosis</i>	NA	NA	NA	NA	NA	NA	10

HE = Hexane; EA = Ethyl acetate; CH = Chloroform; MetOH = Methanol; EtOH = Ethanol; H₂O = Water; 'NA' indicates = no activity; *PC = Positive control (20 µg/ml)

against *P. aeruginosa* and was the same as the positive control (Table 4). This antibacterial effect could have resulted from the bioactive composition of phytochemicals present in the plant. Phytochemicals are known to exhibit antimicrobial activity through different mechanisms (33). Flavonoids disrupt microbial cell wall by forming complex with extracellular soluble proteins in the bacteria (34,35). Predominately, flavonoid rich plants possess a broad spectrum of antimicrobial activity (34)

Antioxidant properties: The free radical scavenging activity of *P. longifolia* was studied by its ability to reduce the DPPH, a stable free radical. The DPPH inhibition of various seed extracts are shown in Fig. 1. Percentage scavenging activity of different solvent extracts increased with increase in concentrations. Methanol, ethanol and water extracts exhibited more effective scavenging activity than other solvent extracts. Methanol extract had the highest DPPH scavenging activity (95% at 200 µg/ml), while hexane extract had the lowest DPPH scavenging activity (16% at 25 µg/ml) as compared to the standard control (96% at 200 µg/ml). The reduction in the number of DPPH molecule can be correlated with the available number of hydroxyl groups. Hence the significant scavenging activity may be due to the presence of hydroxyl groups present in the extracts (35).

In the H₂O₂ scavenging assay, all crude extracts quenched the H₂O₂ radical at different concentrations (Fig. 2). Water extract had the highest H₂O₂ scavenging ability (90% at 200 µg/ml), where we can consider it nearly fully inhibiting, while hexane extract had the lowest H₂O₂ scavenging activity (22% at 25 µg/ml). Water extract was more effective as it exhibited the same activity as the standard control (90% at 200 µg/ml). However, the reducing power of various extracts increased with increasing dose.

In ABTS assay, aqueous extract had the highest ABTS⁺ scavenging activity (96% at 200 µg/ml), while hexane had the lowest ABTS⁺ scavenging activity (17% at 25 µg/ml) as shown

in Fig. 3. This wide range of antioxidant activity may be attributed to the wide variety of bioactive compounds like phenolics, flavonoids, tannins etc. present in the plant. In all antioxidant assays evaluated, the extracts showed efficient activity as compared to standard ascorbic acid.

Discussion

Ethno-pharmaceutical studies and alternative medicine have become increasingly valuable in the recent years and medicinal plants

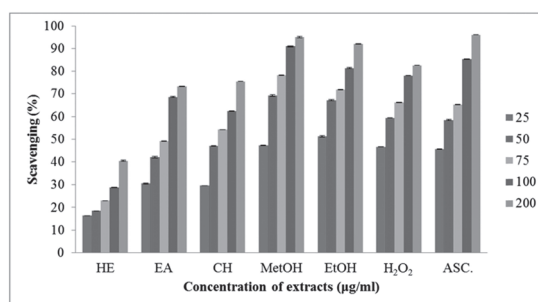


Fig. 1. DPPH radical scavenging activity of different concentrations of *P. longifolia* seed extracts and ascorbic acid.

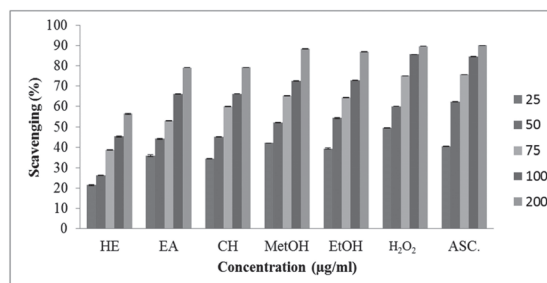


Fig. 2. H₂O₂ scavenging activity of different concentrations of crude extracts and ascorbic acid.

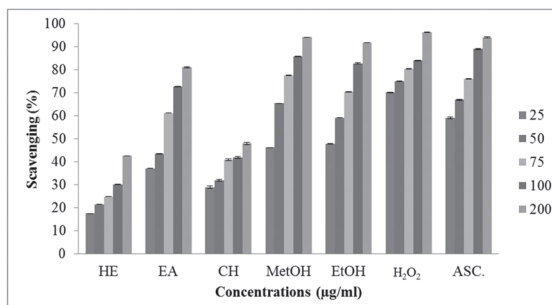


Fig. 3. ABTS⁺ scavenging activity of different concentrations of crude extracts and ascorbic acid

Table 4. In vitro antibacterial activity of *P. longifolia* extracts (MIC in µg/ml)

Test organisms	HE	EA	CH	MetOH	EtOH	H ₂ O	PC*
<i>S. aureus</i>	200	200	200	100	200	200	128
<i>E. coli</i>	200	100	-	150	100	200	62.5
<i>P. aeruginosa</i>	150	100	150	62.5	100	150	62.5
<i>K. pneumoniae</i>	150	100	200	100	>100	150	62.5
<i>E. faecalis</i>	NT	NT	NT	NT	NT	NT	100

S. aureus: *Staphylococcus aureus*; *E. coli*: *Escherichia coli*; *P.aeruginosa*: *Pseudomonas aeruginosa*; *K. pneumoniae*: *Klebsiella pneumoniae*; *E. faecalis*: *Enterococcus faecalis*.

HE = Hexane; EA = Ethyl acetate; CH = Chloroform; MetOH = Methanol; EtOH = Ethanol; H₂O = Water; '-' indicates = no activity

*PC = Positive Control (Neomycin) - 20 µg/ml and NT=Not tested.

are now part of the health care system. The medicinal plant conservation programs and their sustained supply are part of global health strategy (36).

The present findings of phytochemical content were in agreement with another study carried out by other researchers Moosa et al. (37, 38) who carried out in vitro evaluation of antihyperlipidemic potential of triterpenes from stem bark of *Protorhus longifolia* commonly used by Zulu traditional healers to manage blood clotting related diseases. Presence of flavonoids, glycosides and phenols in methanolic extract may be responsible for its free radical scavenging activity. It is not surprising that there are differences in the antimicrobial effects of plant groups, due to phytochemical properties and differences among species. The investigated plant seeds did not show presence of alkaloids; however, negative results do not mean absence of bioactive constituents. Active compound may be present in insufficient quantities in the crude extracts to show activity with the dose levels employed (39, 40). Lack of activity can thus only be proven by using large doses (41). Alternatively, if the active principle is present in high enough quantities, there could be other constituents exerting antagonistic effects or negating the positive effects of the bioactive agents (42).

The methanolic extract of seeds of *P. longifolia* displayed highest antibacterial activity against the majority of pathogens tested. This indicates that the extracts possess substances such as flavonoids, glycosides, and tannins which have been linked with the healing properties of plants (43). The relatively high antibacterial activity of methanol extract and ethanol extract could imply that the methanol and ethanol solvents extracted more bioactive compounds and accordingly contributed to a great degree of inhibition. Water is mostly used by traditional healers in preparing extracts however, plant extracts derived from methanol and ethanol have also been found to be active against bacteria from this study. *S. aureus* (Gram positive) was more susceptible to the extracts than Gram negative pathogens tested as shown in Table 4. Antimicrobial studies have shown that Gram negative bacteria show a higher resistance to plant extracts than Gram positive bacteria (44). This may be as a result of the variation in the cell wall structure of Gram positive and Gram negative. More especially, Gram negative bacteria have an outer membrane that is composed of high density lipopolysaccharides that serves as a barrier to many environmental substances including antibiotics (45). Alternatively, the passage of the active compound through the Gram negative cell wall may be inhibited. It is thought that observed

differences may result from the doses used in this study. In addition, microorganisms show variable sensitivity to chemical substances related to different resistance levels between strains (46).

DPPH is a stable free radical at room temperature and accepts an electron or hydrogen radical to become a stable diamagnetic molecule (47). The reduction in the number of DPPH molecules can be correlated with the number of available hydroxyl groups. We can infer that, the high antioxidant activities of the methanolic, ethanolic and water extracts may be probably due to the presence of compounds with hydroxyl group.

Hydrogen peroxide is a weak oxidizing agent that has an ability to directly inactivate enzymes by oxidation of essential thiol (-SH) groups (48). It can cross cell membranes rapidly, and once inside the cell, H_2O_2 probably reacts with Fe^{2+} , and possibly Cu^{2+} ions to form hydroxyl radical which may be the origin of many of its toxic effects (49). It is therefore biologically advantageous for cells to control the amount of hydrogen peroxide that is allowed to accumulate. The methanol extract, chloroform extract, water extract and ethanol extract scavenged H_2O_2 with increasing concentrations and this may be attributed to the presence of phenolics, which could donate electrons thereby neutralizing it into water.

ABTS⁺ assay can be used as a guide that reflects the antioxidant activity of different extracts. ABTS is a fairly stable free radical which involves the generation of ABTS⁺ mono-cation without involvement of intermediary cation. High antioxidant activity of *P. longifolia* seeds maybe due to bioactive compounds present in the plant extracts such as flavonoids, which was evident in both the methanolic and ethanolic extracts. Flavonoids are responsible for the antioxidant properties of the medicinal plants. Biological effects of flavonoids are linked to their potential cytotoxicity and their capacity to interact with enzymes through protein complexation. Furthermore, flavonoids act as scavengers of free radicals such as reactive oxygen species (ROS),

and also prevent their formation by chelating metals. Furthermore, flavonoids contain broad spectrum of biological activity like antimicrobial properties (50, 51).

Conclusion

The seed extracts of *P. longifolia* is a potentially a good source of antimicrobial agent and demonstrate the importance in medicine and in assisting primary health care in this part of the world. Preliminary phytochemical analysis during the present study also ascertains the presence of some potential group of bioactive substances, but the nature of active phytochemical responsible for antibacterial activity cannot be ascertained. Amongst various solvents investigated to access the extraction effectiveness, methanol extract showed remarkable activity. Further studies are necessary to isolate and characterize the active components of the extracts and also to elucidate their antimicrobial mechanisms of action and to further validate pharmacological evaluation.

Acknowledgements:

This work was financially supported by the National Research Foundation (NRF) of South Africa.

Conflict of Interest: Authors declare no conflict of interest.

References:

1. Sasidharan, S., Chen, Y., Saravanan, D., Sundram, K.M and Yoga Latha L. (2011). Extraction, Isolation and characterization of bioactive compounds from plants' extracts. *African Journal of Traditional, Complementary, and Alternative Medicines* 8:1-10
2. AFRO, W. (2010). African Traditional Medicine day. *The African Health Monitor* 31 August Special Issue
3. Wagner, H., Hikino, H. and Farnsworth NR. (2012). *Economic and Medicinal Plant Research*. Academic Press.
4. Nwankwo, I., Ukaegbu-Obi, K., Mushtaq, A., Pervez, S. and Hussain S, et al. (2014).

- Preliminary phytochemical screening and antibacterial activity of two Nigerian medicinal plants (*Ficus asperifolia* and *Terminalis catappa*). *Journal of Medicinal Plant and Herbal Therapy Research* 2: 1-5
5. Parekh, J. and Chanda S. (2007). Antibacterial and phytochemical studies on twelve species of Indian medicinal plants. *African Journal of Biomedical Research* 10:175-181
 6. Rios, J. and Recio M. (2005). Medicinal plants and antimicrobial activity. *Journal of Ethnopharmacology* 100:80-4
 7. Hoareau, L. and DaSilva E. J. (1999). Medicinal plants: a re-emerging health aid. *Electronic Journal of Biotechnology* 2:3-4
 8. Masika, P. and Afolayan A. (2002). Antimicrobial activity of some plants used for the treatment of livestock disease in the Eastern Cape, South Africa. *Journal of Ethnopharmacology* 83:129-34
 9. McGaw, L. and Eloff J. (2008). Ethnoveterinary use of southern African plants and scientific evaluation of their medicinal properties. *Journal of Ethnopharmacology* 119:559-74
 10. Van Wyk, B. E. (2008). A broad review of commercially important southern African medicinal plants. *Journal of Ethnopharmacology* 119:342-55
 11. McGaw, L., Jäger, A., Grace, O., Fennel, C. and Van Staden J. (2005). Medicinal plants. In *Ethics in Agriculture—An African Perspective*:67-83: Springer. Number of 67-83 pp.
 12. Dold, A.P.C. M.L. (2001). Traditional veterinary medicine in the Alice district of the Eastern Cape Province, South Africa. *South African Journal of Science* 97:375-9
 13. Moosa Lazarus, G.G., Gwala, P.E., Oyedeji, A.O. and Opoku A.R. (2011). In Vitro Anti-platelet Aggregation, Antioxidant and Cytotoxic Activity of Extracts of Some Zulu Medicinal Plants. *Journal of Natural Products* 4: 136-146
 14. Suleiman, M.M., Bagla, V., Naidoo, V. and Eloff J. N. (2010). Evaluation of selected South African plant species for antioxidant, antiplatelet, and cytotoxic activity. *Pharmaceutical Biology* 48:643-50
 15. Suleimana, M.M., McGaw, L.J., Naidoo, V. and Eloff J.N. (2010). Detection of antimicrobial compounds by bioautography of different extracts of leaves of selected South African tree species. *African Journal of Traditional, Complementary and Alternative Medicines : AJTCAM / African Networks on Ethnomedicines* 7:64-78
 16. Mosa, R.A., Naidoo, J.J., Nkomo, F.S., Mazibuko, S.E., Muller, C.J. and Opoku A. R. (2014). In vitro antihyperlipidemic potential of triterpenes from stem bark of *Protorhus longifolia*. *Planta Medica* 80:1685-91
 17. Chanda, S., Dudhatra, S. and Kaneria M. (2010). Antioxidative and antibacterial effects of seeds and fruit rind of nutraceutical plants belonging to the Fabaceae family. *Food & Function* 1:308-15
 18. Mallikharjuna, P., Rajanna, L., Seetharam, Y. and Sharanabasappa, G. (2007). Phytochemical studies of *Strychnos potatorum* L.f.-A medicinal plant. *Journal of Chemistry* 4:510-8
 19. Savithamma, N., Rao, M.L. and Suhrulatha, D. (2011). Screening of medicinal plants for secondary metabolites. *Middle-East Journal of Scientific Research* 8:579-84
 20. Farnsworth, N. R. (1966). Biological and phytochemical screening of plants. *Journal of Pharmaceutical Sciences* 55:225-76
 21. Kumar, A., Ilavarasan, R., Jayachandran, T., Decaraman, M. and Aravindhan, P. et al. (2009). Phytochemicals investigation on a tropical plant, *Syzygium cumini* from Kattuppalayam, Erode district, Tamil Nadu,

- South India. *Pakistan Journal of Nutrition* 8:83-5
22. Treare, G. and Evans, W. Pharmacognosy 17th edn, Bahive Tinal, London, 1985: 149
23. Thite, S., Chavan, Y., Aparadh, V. and Kore, B. (2013). Preliminary phytochemical screening of some medicinal plants. *International Journal of Pharmaceutical, Chemical and Biological Sciences* 3: 87-90
24. Paris, R. and Moyses, H. (1969). *Precis de matiere medicinale*. Paris: Masson, 1969.
25. Bauer, A.W., Kirby, W.M., Sherris, J.C. and Turck, M. (1966). Antibiotic susceptibility testing by a standardized single disk method. *American Journal of Clinical Pathology* 45:493-6
26. Villanova, P. (2000). Methods for Dilution Antimicrobial Susceptibility Tests for Bacteria, which Grows Aerobically. NCCLS:5th ed., Approved Standard M7-A5
27. Annamalai, A., Christina, V.L.P., Sudha, D., Kalpana, M and Lakshmi, P.T.V. (2013). Green synthesis, characterization and antimicrobial activity of AuNPs using *Euphorbia hirta* L. leaf extract. *Colloids and Surfaces B-Biointerfaces* 108:60-5
28. NCCLS. (2002). Clinical and Laboratory Standards Institute. Reference method for broth dilution antifungal susceptibility testing of yeasts, approved standard M27-A2. Villanova, PA.: CLSI Document. Clinical and Laboratory Standards Institute
29. Barku, V.Y.A., Boahen, Y.O., Ansah, E.O., Dayie, N.T.K.D. and Mansah, F.E. (2013). In-Vitro assessment of antioxidant and antimicrobial activities of methanol extracts of six wound healing medicinal plants. *Journal of Natural Sciences Research* 3:74-80
30. Ramnik, S., Narinder, S., Saini, B. and Rao, H.S. (2008). In vitro antioxidant activity of pet ether extract of black pepper. *Indian Journal of Pharmacology* 40:147
31. Ruch, R.J., Cheng, S.J., Klaunig, J.E. (1989). Prevention of cytotoxicity and inhibition of intercellular communication by antioxidant catechins isolated from Chinese green tea. *Carcinogenesis* 10:1003-8
32. Re, R., Pellegrini, N., Proteggente, A., Pannala, A., Yang, M. and Rice-Evans, C. (1999). Antioxidant activity applying an improved ABTS radical cation decolorization assay. *Free Radical Biology and Medicine* 26:1231-7
33. Owoyele, B.V., Oyewole, A.L., Alimi, M.L., Sanni, S.A. and Oyeleke, S.A. (2015). Anti-inflammatory and antipyretic properties of *Corchorus olitorius* aqueous root extract in Wistar rats. *Journal of Basic and Clinical Physiology and Pharmacology* 26: 363-368
34. Pourcel, L., Routaboul, J.M., Cheynier, V., Lepiniec, L. and Debeaujon, I. (2007). Flavonoid oxidation in plants: from biochemical properties to physiological functions. *Trends in Plant Science* 12:29-36
35. Singh, G. and Kumar, P. (2014). Antibacterial activity of flavonoids of *Withania somnifera* L. *International Journal of Green Pharmacy* 8:114-118.
36. Rauha, J.P., Remes, S., Heinonen, M., Hopia, A., Kähkönen, M. et al. 2000. Antimicrobial effects of Finnish plant extracts containing flavonoids and other phenolic compounds. *International Journal of Food Microbiology* 56:3-12
37. Goveas, S.W. and Abraham, A. (2013). Evaluation of antimicrobial and antioxidant activity of stem and leaf extracts of *Coscinium fenestratum*. *Asian Journal of Pharmaceutical and Clinical Research* 6
38. Ibrahim, M.M., Al Sahli, A.A.A., Alaraidh, I.A., Al-Homaidan, A.A., Mostafa, E.M. and El-Gaaly, G.A. (2015). Assessment of antioxidant activities in roots of Miswak (*Salvadora persica*) plants grown at two

- different locations in Saudi Arabia. *Saudi Journal of Biological Sciences* 22:168-75
39. Taylor, J., Rabe, T., McGaw, L., Jäger, A. and Van Staden, J. (2001). Towards the scientific validation of traditional medicinal plants. *Plant Growth Regulation* 34:23-37
40. Farnsworth, N.R. (1993). Ethnopharmacology and future drug development: the North American experience. *Journal of Ethnopharmacology* 38:137-43
41. Wall, M., Wani, M., Brown, D., Fullas, F., Olwald J. et al. (1996). Effect of tannins on screening of plant extracts for enzyme inhibitory activity and techniques for their removal. *Phytomedicine* 3:281-5
42. Lindsey, K., Jäger, A.K., Raidoo, D.M. and Van Staden, J. (1998). Screening of plants used by Southern African traditional healers in the treatment of dysmenorrhoea for prostaglandin-synthesis inhibitors and uterine relaxing activity. *Journal of Ethnopharmacology* 64:9-14
43. Whitehead, S.R., Jeffrey, C.S., Leonard, M.D., Dodson, C.D., Dyer, L.A. and Bowers, M.D. (2013). Patterns of secondary metabolite allocation to fruits and seeds in *Piper reticulatum*. *Journal of Chemical Ecology* 39:1373-84
44. Palombo, E.A. and Semple, S.J. (2001). Antibacterial activity of traditional Australian medicinal plants. *Journal of Ethnopharmacology* 77:151-7
45. Kujumgiev, A., Tsvetkova, I., Serkedjieva, Y., Bankova, V., Christov, R. and Popov, S. (1999). Antibacterial, antifungal and antiviral activity of propolis of different geographic origin. *Journal of Ethnopharmacology* 64:235-40
46. Çetin, E and Gürler, N. 1989. Antibiotic susceptibility tests of bacteria. *Kükem Dergisi* 2:97-105
47. Soares, A.A., de Souza, C.G.M., Daniel, F.M., Ferrari, G.P, da Costa, S.M.G. and Peralta, R.M. (2009). Antioxidant activity and total phenolic content of *Agaricus brasiliensis* (*Agaricus blazei* Murril) in two stages of maturity. *Food Chemistry* 112:775-81
48. Bhaskar, H. and Balakrishnan, N. (2009). In vitro antioxidant property of Laticiferous plant species from western ghats Tamilnadu, India. *International Journal of Health Research* 2:163-170
49. Miller, M., Sadowska-Krowicka, H., Chotinaruemol, S., Kakkis, J.L. and Clark, D.A. (1993). Amelioration of chronic ileitis by nitric oxide synthase inhibition. *Journal of Pharmacology and Experimental Therapeutics* 264:11-6
50. Williams, R.J., Spencer, J.P. and Rice-Evans, C. (2004). Flavonoids: antioxidants or signalling molecules? *Free Radical Biology and Medicine* 36:838-49
51. Heim, K.E., Tagliaferro, A.R. and Bobilya, D.J. (2002). Flavonoid antioxidants: chemistry, metabolism and structure-activity relationships. *The Journal of Nutritional Biochemistry* 13:572-8

Determination of adipocyte cell size by H & E stained adipose tissue and collagenase digested isolated adipocytes

Devaligoda Gamage Kalpani Yashodara Perera^{1*}, Hemantha Senanayake²,
Tharanga Thoradeniya¹

¹Department of Biochemistry and Molecular Biology, Faculty of medicine,
University of Colombo, Sri Lanka.

²Department of Obstetrics & Gynaecology, Faculty of Medicine, University of Colombo, Sri Lanka.

*For Correspondence : kalpaniperera2013@gmail.com

Abstract

The aim is to compare the two methods H & E stained adipocytes and collagenase digested isolated adipocytes, and determine if collagenase digested isolated adipocytes analysis is an accurate method for cell size estimation. The adipose tissue samples (superficial subcutaneous adipose tissue; sSAT, deep subcutaneous adipose tissue; dSAT and visceral adipose tissue; VAT) were collected from three pregnant women undergoing caesarian section. The adipocyte size was determined in collagenase digested isolated adipocytes and H & E Stained adipocytes by ImageJ software and the two methods were compared. There were no significant difference in the two methods and was strongly correlated ($r=0.99$, $P<0.01$). The bias was observed between the collagenase digested isolated adipocytes and H & E stained adipose tissue since 97.48% of the total adipocytes was within the limit of agreement. In conclusion the collagenase digested isolated adipocytes can be used as an accurate and less cumbersome method for the cell size determination.

Key words : Adipose tissue, H & E stained, isolated adipocytes, method comparison

Abbreviations

sSAT: superficial subcutaneous adipose tissue, dSAT: deep subcutaneous adipose tissue,

VAT: visceral adipose tissue, H & E: Hemotaxylin and Eosin.

Introduction

Adipose tissue is known to be a highly metabolically active tissue, which is important for regulation of energy intake and expenditure, lipid metabolism and creates systemic inflammation (5, 7, 13). Adipocyte size is known as an indicator of the adipose tissue expansion during weight gain, obesity and also during the process of pregnancy (17). The AT expansion takes place in two phases. The first phase is hypertrophy, wherein the adipocytes increase in size. Secondly, hyperplasia takes place where precursor cells known as preadipocytes are formed (2, 12, 20). Determination of adipocyte size is essential for metabolic studies, to determine endocrine functions and to detect the changes in adipose tissue morphology (4, 8, 19).

The adipocyte size measurement have been commonly done on stained tissue (4, 12) as well as collagenase digested isolated adipocytes (3,21)although drawbacks are observed in both methods. The collagenase digested isolated adipocytes must be determined immediately after Isolation, if the cell suspension is stored it causes changed in the cell morphology (3) such as distortion in larger isolated adipocytes (4). Furthermore, since the isolated adipocytes are

unfixed and floating the same adipocyte may be captured more than once (4). The histological slide preparation has the ability to minimize the morphological changes and the cells overlapping when compared with collagenase digested isolated adipocytes (11). The main drawback of histological slide preparation is the need of well-trained personals. Moreover, histological sample preparation is more time consuming (19) compared to collagenase digested cell isolation which is a less expensive and a faster method (21). Thick histological preparations (19) and prolonged storage in 10% formalin may cause the shrinkage of the adipocytes (3).

Our objective was to compare the two methods H & E stained adipocytes and collagenase digested isolated adipocytes, and determine if collagenase digested isolated adipocytes analysis is an accurate method for cell size estimation.

Materials and methods

Adipose tissue collection : The adipose tissue samples were collected from three pregnant women undergoing caesarian section at De Soysa maternity hospital. The study procedure was approved by the Ethics Review Committee of the Faculty of Medicine, Colombo. Permission was granted by the director of the De Soysa maternity hospital.

The adipose tissue samples were collected under surgical conditions with sterile equipment. The samples were collected from pregnant women while performing lower segment caesarian section and after the delivery of the child. The samples of the adipose tissue (superficial subcutaneous adipose tissue; sSAT, deep subcutaneous adipose tissue; dSAT and visceral adipose tissue; VAT) were collected from the lower quadrant 10-12cm from the umbilicus in the hypogastric region. The VAT was collected below the rectus fascia. The sSAT was collected just below the skin and the dSAT was collected from just above the rectus fascia. All the samples were collected in phosphate buffered saline (PBS) and transferred into the laboratory within 30 minutes.

Determination of adipocyte size in collagenase digested isolated adipocytes

The isolation of the adipocytes was done by the method described by Rodbell (1964). Before the isolation blood vessels were removed from the adipose tissue using a forceps and a scalpel. For the adipocyte isolation 100mg of adipose tissue was suspended in 1ml of Krebs-Ringer bicarbonate buffer (137 NaCl, 5 KCl, 4.2 NaHCO₃, 1.3 CaCl₂, 0.5 MgCl₂, 0.5 KH₂PO₄, 0.5 MgSO₄, 20 HEPES (pH 7.4) and 1% BSA) and to this 5 mM glucose and 1 mg/ml collagenase (SIGMA catalogue no.C0130) was added. The digestion was carried out at 37 °C (water bath) with constant shaking for 45 minutes. Cells were filtered through a cloth mesh and washed three times with Krebs-Ringer bicarbonate buffer. The suspension is centrifuged for 1 minute at 400 x g. The fat cells floated in the surface, while the stromal-vascular cells (capillary, endothelial, mast, macrophage, and epithelial cells) were sedimented. The pellet was removed and the fat cells were resuspended in 1ml of Krebs-Ringer bicarbonate buffer containing glucose and it is centrifuged for 1 minute at 400 x g. This procedure was repeated three times. By the end of this centrifugation process the stromal-vascular cells were absent and the fat cells were found floating in the surface of the tubes. About 30µl of adipocytes cell suspension was placed on a glass slide and the area was covered with a cover slip. The cell image was captured using the 10x objective of the Olimpus 1x70 fluorescent inverted microscope. Successive images (50 images) were taken while assuring that the images were not captured previously.

Determination of cell viability in the collagenase digested isolated adipocytes

The cell viability was measured in adipocyte suspension by trypan blue staining. The cell viability was assayed just after the cell isolation and after 3 hours. A drop of trypan blue was mixed with 100µl of cell suspension and left for 1-2 minutes for absorption. The suspension was loaded to the hemocytometer and the total cell number and the stained cell number was counted.

The percent of cell viability was detected by the following equation;

$$\text{Percent viability} = \frac{\text{Total cells counted} - \text{stained cells}}{\text{Total cells counted}}$$

Determination of adipocyte size in in stained adipose tissue : The adipose tissue was fixed in 10% formalin and stained using the H & E stain (18). Firstly the samples are paraffin embedded using cassettes. The sample is cut into 5 μ m thin tissue and then the slides are prepared. For the staining the following steps are followed deparafinization, dehydration, staining with Harri's Hematoxylin solution followed by washing and dehydration and counter staining by eosin Y solution. After the slides were prepared 10 successive images were captured using the 10x objective of the Olimpus 1x70 fluorescent inverted microscope.

Determination of adipocyte size using ImageJ software : After the capturing of the images the ImageJ software (<http://imagej.nih.gov/ij/>) was used for the quantification the adipocyte cell size. ImageJ is a free software which can be used for manual counting of cell number and size.

Before the ImageJ was used to determine the cell size the software was calibrated using an image captured from the same microscope with a known scale. After the calibration the image of the adipocytes were opened in the software and converted to a grey scale image. The background noise of the image was removed to improve the clarity of the image. A threshold image was prepared to identify the membrane material and the empty space in black and white. The unwanted particles were removed and the specific adipocytes were chosen to determine the adipocyte size. Finally, the adipocyte size was measured using the cell surface area (μm^2) using the criterion's mentioned below. Cells having an area below 150 μm^2 were excluded since they may include stromal vascular cells and cells having an area more than 50,000 μm^2 were also excluded because they might be distorted, the shape factor of the adipocytes was placed between 0.35-1 (In this 1 represent a perfect circle while 0 represents

a straight line), adipocytes touching the border of the image were excluded and larger adipocytes which were shrunken were excluded. For the analysis 150 adipocytes was used (14, 15, 23).

Statistical analysis : To compare the two methods H & E stained adipose tissue and collagenase digested isolated adipocytes several statistical tests were performed. Student's paired t-test was performed to observe the difference in the two methods. The spearman's correlation and scatter plots were used to assess the association and the linear relationship of the methods. The Bland-Altman plots (1) were used to assess the existence of bias between the two methods. For this the difference between the methods (Bias=isolated adipocyte size-stained adipocyte size) were plotted on the y axis against the average of the method on the x axis. All the statistical analysis were performed using SPSS (Statistical Package for Social Sciences) version 18.0 statistical software (SPSS Inc., Chicago, IL, USA) and Microsoft Excel 2010 was utilized.

Comparison of adipocyte size in pregnant women : Apart from the method comparison the cell surface area (μm^2) of the adipocytes was compared in two groups of pregnant women (3 normal weight pregnant women and 3 overweight pregnant women) utilizing the isolated adipocytes methodology. The cell size of the two groups was compared utilizing student's t-test and Spearman's coefficient.

Results

To compare the size of collagenase digested isolated adipocytes and H & E stained adipose tissue a total of 9 adipose tissue depots were used with a total of 1350 adipocytes. Images captured of the adipocytes from the florescent inverted microscope of one pregnant woman is presented in the figure 1. There was no significant difference in the paired t-test values of the mean adipocyte cell area (Table 1). The spearman's correlation (Table 1) of the different AT depots provides evidence that the two independent parameters have a strong linear relationship.

Scatter plots depicted in figure 2 describe the variability of the paired measurement through the ranges of measure. Bland Altman plot assessed the agreement, displaying the mean difference between the H & E stained AT and collagenase digested isolated adipocytes (Figure3). Most of the values (97.48% of the total adipocytes) were within the 95 % limits of agreement (Table 1). The adipocytes with larger size have a tendency to become overestimated in all AT depots.

The cell viability was calculated as described. The percentage viability of the adipocytes at both time points (immediately and 3 hours after isolation) was found to be 100%.

The adipocyte size was compared in two groups of pregnant women (3 normal weight pregnant women and 3 overweight pregnant women) (Table2). When the adipocyte size was considered the adipocyte size was significantly higher in the sSAT of overweight pregnant women (4720.6±370.2) than the normal weight pregnant women (2630.9±324.9)(P=0.006). Furthermore, dSAT of overweight pregnant women (4336.2±699.4) was also significantly higher when compared to normal weight pregnant women(2013.3±562.1)(P=0.03).

Discussion

This study demonstrated that the isolated adipocytes can be used as a cost effective

simpler and accurate method for the cell size determination. The two methods were strongly correlated in all adipose tissue depots. As analyzed by Bland-Altman plot,97.48% values were within the limit of agreement, therefore the two methods were found to be bias. In a similar study performed to compare the adipocyte size in collagenase digested isolated adipocytes, stained adipocytes and Osmium fixed adipocytes,the techniques were found to be strongly intercorrelated (10). They have found that

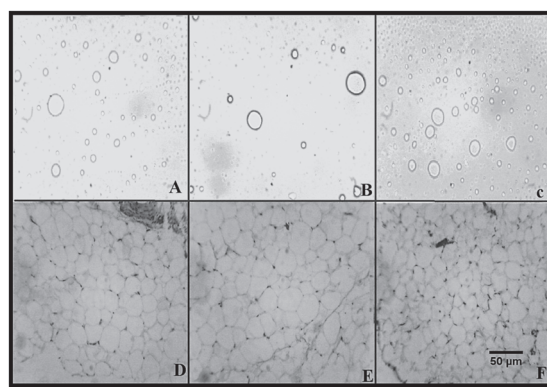


Figure 1 Collagenase digested isolated adipocytes of (A) superficial subcutaneous adipose tissue, (B) deep subcutaneous adipose tissue and (C) visceral adipose tissue. H & E stained adipose tissue of (D) superficial subcutaneous adipose tissue, (E) deep subcutaneous adipose tissue and (F) visceral adipose tissue of one pregnant woman.

Table 1: Comparison of the two methods. sSAT: superficial subcutaneous adipose tissue, dSAT: deep subcutaneous adipose tissue, VAT: visceral adipose tissue.

	Size of adipocytes (Mean ± SD) μm ²		Student's paired t test	Spearman's correlation		Bland Altman		
	H & E stained adipocytes	Isolated adipocytes		r	p value	Mean	Limit of agreement	Percentage of agreement
sSAT	3843.46±5286	3140.93±6172	0.337	0.97	0.01	3846.44	-867.53 to 8560.41	99.7 %
dSAT	3020.43±1957	2426.16±5420	0.615	0.99	0.01	594.14	-8819.15 to 10000	98.67%
VAT	3189.86±2515	2140.5±5095	0.794	0.99	0.01	1049.37	-5141.96 to 5000	99.1%
Total			0.582	0.99		1829.98		99.15%

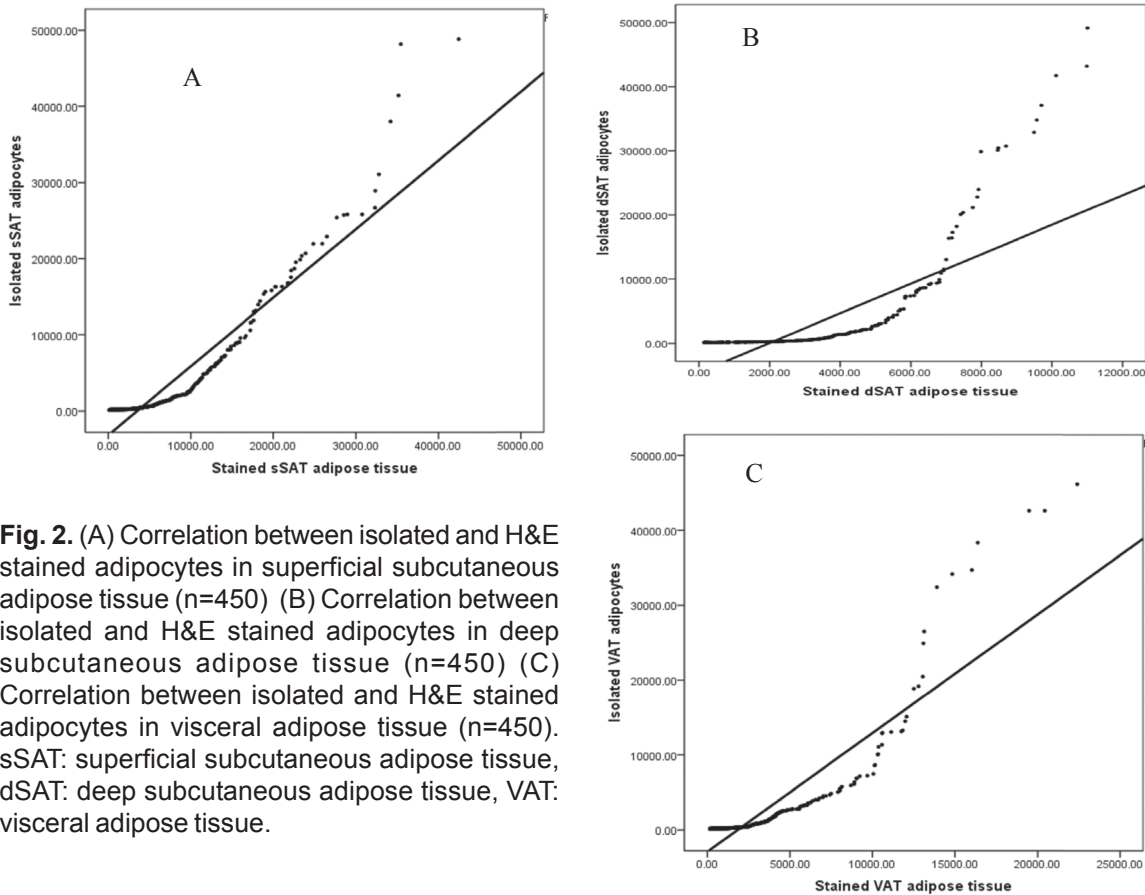


Fig. 2. (A) Correlation between isolated and H&E stained adipocytes in superficial subcutaneous adipose tissue (n=450) (B) Correlation between isolated and H&E stained adipocytes in deep subcutaneous adipose tissue (n=450) (C) Correlation between isolated and H&E stained adipocytes in visceral adipose tissue (n=450). sSAT: superficial subcutaneous adipose tissue, dSAT: deep subcutaneous adipose tissue, VAT: visceral adipose tissue.

Osmium fixed adipocytes have a strong association with cardio metabolic risk factors, however this is an expensive technique and also it was stated by them that Osmium fixed adipocytes are larger due to the space filled by osmium during fixation.

Isolation of adipocytes can be performed using basic laboratory equipment and is less time consuming (10, 21), while histological sample preparation is more time consuming (19) and require skilled personnel.

The demerits caused by collagenase digested isolated adipocytes were addressed in our study as follows. We excluded larger cells and the cells between the size of 150-50,000 μm^2 taken for our calculation. This exclusion of cells also results in exclusion of adipocytes which had

lost the actual shape and sized during the isolation process. In ImageJ analysis, the distorted cells were excluded. Since previous studies showed that, some larger collagenase digested isolated adipocytes tend to be distorted due to collagenase treatment and these changes in the morphology may affect the results (4). Moreover in the present study the images of adipocytes were captured as soon as they were isolated and a cover slip was placed over the cell suspension. Prolonged storage of the collagenase digested isolated adipocytes suspension cause changes in the morphology in the adipocytes(3) and the collagenase digested isolated adipocytes are unfixed therefore they may be floating and the same adipocyte may be captured more than once (4). In our study the cell viability was assessed and the cells were found to be viable throughout

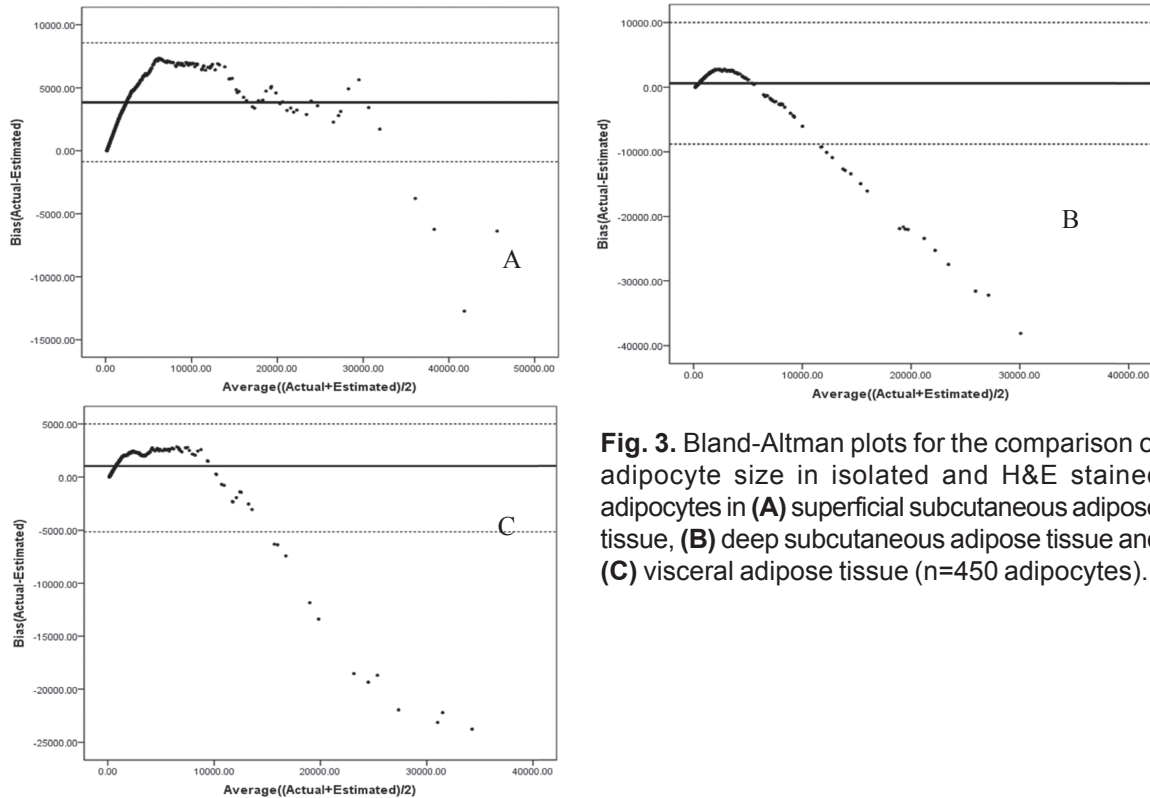


Fig. 3. Bland-Altman plots for the comparison of adipocyte size in isolated and H&E stained adipocytes in (A) superficial subcutaneous adipose tissue, (B) deep subcutaneous adipose tissue and (C) visceral adipose tissue (n=450 adipocytes).

Table 2: Characteristics of pregnant women of the two groups

Pregnant women groups	Age (years)	Parity	Weight at first antenatal visit (Kg)	Height (cm)	Weight before delivery (Kg)	BMI at delivery (Kg/m ²)	Weight gained pregnancy (Kg)	Weight of baby (Kg)	
Normal weight group (Mean±SE)	34±3		52.8±4.7	154.7±3.1	22.0±1.2	26.3±6.2	26.6±2.1	10.1±3.1	2.6±0.1
Participant 1	40	1	53	152	22.94	68	29.43	15.0	2.90
Participant 2	31	-	61	161	23.55	72	27.79	11.0**	2.35
Participant 3	31	1	44.5	151	19.58	51.5	22.59	4.3**	2.74
Overweight group (Mean±SE)	33.7±1.8		62.7±1.8	148.7±2.9	28.4±0.4	73.3±1.2	33.29±0.8	10.7±0.9	2.6±0.1
Participant 1	36	-	65	150	28.88	74	32.89	9.0	2.75
Participant 2	30	2	59	143	28.70	71	34.80	12.3*	2.81
Participant 3	35	2	64	153	27.52	75	32.19	11.0	2.36

Body mass index(BMI) cutoff values: Normal weight (18.5-25 Kg/m²) and Overweight (>25 Kg/m²) (WHO, 2006)

*Individuals who gained more than the recommended weight gain

**Individuals who gained below the recommended weight gain (Recommended weight gain during pregnancy: Normal weight (11.2-15.9Kg) and Overweight (6.8-11.2Kg)

the experiment. Therefore, we could predict minimal morphological changes during the study procedures. However, the histological slide preparation has the ability to minimize the morphological changes and the cells overlapping when compared with isolated cells (11).

The H & E stained slides also have several drawbacks. Thick histological preparations (19) and prolonged storage in 10% formalin may cause the shrinkage of the adipocytes (3). For the present study thin (5µm) adipose tissue histological preparations and only stored the samples for 1-2 months. The 10% formalin was also replaced every 2 weeks.

In addition, the clinical significance of adipocyte size measurement has been discussed extensively and has shown to have a positive correlation with serum insulin levels and triacylglycerol levels (9, 22). Moreover, the studies of Fang *et al.*, (2015) have found an association between adipocyte size distribution and type 2 diabetes mellitus. Hence, adipocyte size measurement and the adipocyte distribution can be utilized as a measure of the extent and the tendency for chronic disease risk such as obesity, diabetics and CVD.

In the two groups studied, the adipocyte size was significantly higher in sSAT when compared to VAT in overweight pregnant women but not in normal weight women. Furthermore, the sSAT and dSAT size was significantly higher in overweight when compared to normal weight pregnant women. These findings imply the varied contribution of different adipose tissue depots in disease risk among overweight women and highlight the importance of further metabolic studies which may shed light on innovative intervention strategies in chronic disease prevention.

Conclusion

In conclusion, the collagenase digested isolated adipocytes can be used as an accurate and less cumbersome method for the cell size determination. However, the technique has demerits and merits which have to be realized by the researcher and necessary precautions needs be taken as relevant to the study of interest.

Acknowledgement

University grant AP/3/2/2016/SG/14 and MSc vote Department of Biochemistry and Molecular Biology, Faculty of medicine, University of Colombo. The authors acknowledge the contribution of the Dr. Gihan, surgeons, and nurses of De Soysa maternity hospital. The authors also thank the study participants.

References

1. Altman D.G. and Bland J.M. (1983). Measurement in Medicine: the Analysis of Method Comparison Studies. *The Statistician*, 32: 307-317.
2. Bjørndal B., Burri L., Staalesen V., Skorve J. and Berge R.K. (2011). Different Adipose depots: Their role in the development of metabolic syndrome and Mitochondrial response to Hypolipidemic agents. *Journal of Obesity*, 1–15.
3. Bjørnheden T., Jakubowicz B. and Levin M. (2004). Computerized determination of Adipocyte size. *Obesity Research*, 12: 95–105.
4. Chen H. and Farese R. (2002). Determination of adipocyte size by computer image analysis. *Journal of lipid research*, 43: 986–9.
5. Costa S.S., Blotta R.M., Meurer L. and Edelweiss M.I.A. (2011). Adipocyte morphometric evaluation and angiogenesis in the omentum transposed to the breast: A preliminary study. *Clinics*, 66: 307–312.
6. Fang L., Guo F., Zhou L., Stahl R. and Grams J. (2015). The cell size and distribution of adipocytes from subcutaneous and visceral fat is associated with type 2 diabetes mellitus in humans. *Adipocyte*, 4:273-279.
7. Frayn K.N., Karpe F., Fielding B.A., Macdonald I.A. and Coppack S.W. (2003). Integrative physiology of human adipose tissue. *International Journal of Obesity*, 27:875–888.
8. Kenéz, Á., Kulcsár, A., Kluge, F., Benbelkacem, I., Hansen, K., Locher, L.,

- Meyer, U., Rehage, J., Dänicke, S. and Huber, K. (2015). Changes of Adipose tissue morphology and composition during late pregnancy and early Lactation in dairy cows. *PLOS ONE*, 10:1-11
9. Krotkiewski M., Sjostrom L., Bjorntorp P. and Smith U. (1975). Regional adipose tissue cellularity in relation to metabolism in young and middle-aged women. *Metabolism*, 24:703–710.
10. Laforest S., Michaud A., Paris G., Pelletier M., Vidal H., Gélouën A. and Tchernof A. (2016). Comparative Analysis of Three Human Adipocyte Size Measurement Methods and Their Relevance for Cardiometabolic Risk. *Obesity*, 00: 1-10.
11. Maroni B., Haesemeyer R., Wilson L. and DiGirolamo M. (1990). Electronic determination of size and number in isolated unfixed adipocyte populations. *Journal of lipid research*, 3: 1703–1709.
12. Meena, V.P., Seenu, V., Sharma, M.C., Mallick, S.R., Bhalla, A.S., Gupta, N., Mohan, A., Guleria, R., Pandey, R.M., Luthra, K. and Vikram, N.K. (2014). Relationship of Adipocyte size with Adiposity and metabolic risk factors in Asian Indians. *PLoS ONE*, 9:1-7
13. Nascimento C.M.O., Ribeiro E.B. and Oyama L.M. (2009). Metabolism and secretory function of white adipose tissue: Effect of dietary fat. *Anais da Academia Brasileira de Ciências*, 81: 453–466.
14. Osman, O.S., Selway, J.L., Kępczyńska, M.A., Stocker, C.J., O'Dowd, J.F., Cawthorne, M.A., Arch, J.R., Jassim, S. and Langlands, K. (2013). A novel automated image analysis method for accurate adipocyte quantification. *Adipocyte*, 2: 160–164.
15. Parlee S., Lentz S., Mori H. and MacDougald O. (2014). Quantifying size and number of adipocytes in adipose tissue. *Methods in enzymology*, 537: 93–122.
16. Rodbell M. (1964). Metabolism of isolated fat cells. I. effects of hormones on glucose metabolism and lipolysis. *The Journal of biological chemistry*, 239: 375–80.
17. Rojas-Rodriguez, R., Lifshitz, L.M., Bellve, K.D., Min, S.Y., Pires, J., Leung, K., Boeras, C., Sert, A., Draper, J.T., Corvera, S. and Moore Simas, T.A. (2015). Human adipose tissue expansion in pregnancy is impaired in gestational diabetes mellitus. *Diabetologia*, 58: 2106–2114.
18. Sheehan D.C. and Hrapchak B.B. (1987) *Theory and Practice of Histotechnology: Battelle.*
19. Sjöström L., Björntorp P. and Vrána J. (1971). Microscopic fat cell size measurements on frozen-cut adipose tissue in comparison with automatic determinations of osmium-fixed fat cells. *Journal of lipid research*, 12: 521–30.
20. Sniderman A.D., Bhopal R., Prabhakaran D., Sarrafzadegan N. and Tchernof A. (2007). Why might south Asians be so susceptible to central obesity and its atherogenic consequences? The adipose tissue overflow hypothesis. *International Journal of Epidemiology*, 36: 220–225.
21. Tchoukalova Y.D. (2003). A quick, reliable, and automated method for fat cell sizing. *The Journal of Lipid Research*, 44: 1795–1801.
22. Tchoukalova Y. D., Koutsari C., Karpayak M.V., Votruba S.B., Wendland E. and Jensen M.D. (2008) Subcutaneous adipocyte size and body fat distribution. *American journal of clinical nutrition*, 87:56–63.
23. Zeidler-Erdely, P.C., Antonini, J.M., Meighan, T.G., Young, S.-H., Eye, T.J., Hammer, M.A. and Erdely, A. (2016). Comparison of cell counting methods in rodent pulmonary toxicity studies: Automated and manual protocols and considerations for experimental design. *Inhalation Toxicology*, 28: 410–420.

Spectroscopic studies, Antioxidant and Anticancer attributes of diffusible eumelanin produced by marine *Streptomyces rochei*

Satheesh Periyasamy¹, Shalini Devi.S², Preethi Kathirvel¹

¹ Department of Microbial Biotechnology, Bharathiar University, Coimbatore, India.

² Department of microbiology, Bhavans Vivekananda college, Hyderabad, India

* For Correspondence - satheesh.grd@gmail.com

Abstract

The diffusible melanin pigment from marine *Streptomyces rochei* isolated from Vishakhapatnam coast was characterized using UV Spectrophotometer, GC-MS, NMR, EPR Spectroscopy, CHNS elemental analysis, Ramon Spectroscopy and found to be a pure form of eumelanin. Anticancer activity of the melanin pigment from *Streptomyces rochei* was studied by MTT assay using MFB4 cell lines with an IC₅₀ value of 26 µg/mL, in comparison the standard 5-fluorouracil exhibited an IC₅₀ value of 16.5 µg/mL and the DNA damage was also assessed by alkaline single-cell gel electrophoresis (COMET assay). The antioxidant activity was assessed by DPPH assay and the percentage of inhibition at 100 µg/mL concentration of melanin was found to be 71.53 which was higher than that for 5-fluorouracil at 63.32 and ascorbic acid at 51.43. The potential for commercial exploitation of this melanin for its biotechnological role is enormous and the *Streptomyces rochei* strain can be a credible source of melanin and can serve as cost effective substitute for the currently marketed products.

Key Words: Eumelanin, Spectroscopy, MTT, DPPH, COMET

Introduction

Melanin is arguably the most prevalent naturally occurring pigment in nature but the studies on melanin does not provide us an unambiguous prediction about its structure till date (1). The various potential applications of

melanin apart from its usual structural and functional role in animals, plants, insects fungi and bacteria has intrigued the researchers to pursue the study on melanin (2). There is a widespread understanding among the scientific community that melanin exists as a complex mix comprising of eumelanin and pheomelanin in higher order organisms and bacteria in general produce pure eumelanin (3). The complex chemical nature and occurrence of different forms of melanin in varying proportions have complicated the issue.

Synthetic and sepia melanin are the most widely available sources for commercial use. Despite the successful attempts made by a number of researchers to increase the yield of melanin, there are not many alternatives in the market which are well characterized. Bacterial melanins reported from various sources like *Klebsiella* (4), *Streptomyces* (5), *Brevundimonas* (6), *Bacillus* (7) etc were reported to be pure form of eumelanin.

Melanins are extremely beneficial other than the widely known property of UV absorption. They can act as redox polymers, radical scavengers, ion chelating agent, semiconductor, photoacoustics, anticancer, antioxidant, antivenin agents and as biopolymers that exhibit high tensile strength etc (8)

Due to its diverse applications not restricted to any particular field, makes study of melanin a demand of the hour. Animal sources of melanin will be usually contaminated with proteins, while

plant sources produce large quantities of melanin which are too complicated to separate from the other phenolics produced by the plant (9). Besides plant melanins are subject to batch variations. Most purified melanin without any batch variations can be obtained from bacterial sources (10).

A marine *Streptomyces rochei* capable of producing alkali soluble melanin was isolated from the marine source by our team. This study was aimed to further characterize this melanin by different spectroscopy techniques and elemental analysis. Anticancer and antioxidant properties were studied by MTT and DPPH assays respectively.

Materials and Methods:

Collection of marine sediments: A total of 18 marine soil samples and 6 marine water samples were collected from Vishakhapatnam and Chennai coasts at different depths up to 10 meters using core sampler. The sediment samples were brown to black in colour and of sandy texture. They were maintained at ambient temperature with sea water and brought to the laboratory in sterile polypropylene bags for isolation of marine actinomycetes (11).

Isolation of Marine Actinomycetes: The soil and water samples were air dried thoroughly for 3 days, pre heated at 55°C for 2 hrs and serial diluted till 10^{-6} with sterile sea water (11). Diluted samples were plated on starch casein agar, pH 7.0 ± 0.1 , supplemented with streptomycin 30 µg/L and nystatin 50 µg/L (12) to prevent bacterial and fungal growth. The plates were incubated at 30°C for 21 days, the actinomycetes colonies were identified by their characteristic chalky, powdery/leathery appearance and subcultured (13).

Screening of Actinomycetes for melanin production: Potent melanin producing actinomycetes isolates were screened for the production of diffusible melanin pigment by inoculating pure cultures on International Streptomyces Project-7 (ISP 7) medium (L-Asparagine 1.0 g, L-Tyrosine 0.5 g, Dipotassium phosphate 0.5 g, Magnesium sulphate $7H_2O$ 0.5

g, Sodium chloride 0.5 g, Ferrous sulphate $7H_2O$ 1.36 mg, Copper chloride $2H_2O$ 0.027 mg, Cobalt chloride, $6H_2O$ 0.040 mg, Sodium molybdate, $2H_2O$ 0.025 mg, Zinc chloride 0.020 mg, Boric acid 2.85 mg, Manganese chloride $4H_2O$ 1.8 mg, Sodium tartarate 1.77 mg, distilled water 1 L, agar 20 g; pH 7.3) and incubated at 30°C for 7 days. The colonies which showed promising level of blackish brown diffusible pigments around them were identified.

16s rRNA sequencing and phylogenetic analysis:

The actinomycetes isolate (VZ/T4/W1) was inoculated in ISP 7 broth and incubated 30°C for 7 days. DNA was isolated from the culture broth (14), 16S rDNA gene was PCR amplified with F and R primers and the amplicon was electrophoresed in a 1% Agarose gel. The amplicon concentration was verified in a Nanodrop ND 2000 and Sequencing of amplicon was performed with universal forward and reverse primers in ABI 3730xl cycle sequencer. The sequence analysis was carried out using bioinformatics tool BLAST of NCBI, based on maximum identity score first few sequences were selected and aligned using multiple sequence alignment software ClustalW and the Dendrogram was constructed (4).

Production and Purification of Melanin: The isolate was inoculated into ISP7 broth supplemented with 5 g/L of tyrosine and 20 mL/L of Glycerol. The culture flasks were incubated in an orbital shaker at 150 RPM at 30°C for 15 days. Culture broth was centrifuged at 10000 RPM for 15 min at 25°C and the supernatant containing the melanin pigment was collected. Hydrochloric acid (6N) was gradually added to the supernatant until the pH of the solution reaches 3.0 and allowed to stand for 6 hrs (5). The precipitate observed was centrifuged at 15000 RPM for 15 min at RT and the pellet obtained was suspended in pepsin (10 µg/mL). This mixture was incubated at 37°C for 6 hrs and centrifuged at 5000 RPM for 10 min (repeated thrice). The pellet fractions were pooled and heated at 95°C for 60 min, cooled down to room temperature and dried in a centrifugal vacuum concentrator until completely dry and weighed.

UV Spectrophotometry: The purified melanin pigment was analysed by diluting it with 0.1 N NaOH to different concentrations (4). The initial concentration of 1 mg/mL was diluted to 1:1, 1:2, 1:3 and 1:4. 1:4 dilution was further diluted 1:1 and 1:2 and all dilutions were scanned from 180 to 900 nm wavelengths using 0.1 N NaOH as the blank.

Gas Chromatography-Mass Spectrometry: The freeze dried melanin sample was dissolved and concentration made up to 1 mg/mL with DMSO. The GC Chromatograph with mass spectrometer (Shimadzu QP2010) was injected with 1 μ L of the sample and separation was carried out on a 30m x 0.32 mm i.d., film thickness 0.5 μ m ZB-5MS column (5% diphenyl 95% dimethyl polysiloxane). The column flow was maintained with 99.999% Helium at a flow rate of 1.5 mL/min. The column oven temperature was maintained at 50°C for 1 min and increased to 150°C at a rate of 10°C, held for 1 min and increased further at a rate of 8°C to 300°C and held for 5 min. The mass spectrometer was operated in EI mode (70 eV) with ion source temperature 210°C and interface temperature 250°C. Mass spectra was recorded from 40 to 1000 m/z (16)

EPR Spectroscopy: Electron paramagnetic resonance (EPR) spectroscopy at X-band (9.3 GHz) was used for identification of type of melanin biopolymers in biological samples. EPR spectra were recorded by JEOL spectrometer in the range of microwave power of 0.3, 0.7 and 1 mW. Lineshape and the parameters (amplitude, integral intensity, linewidth, g-factor) were analysed (15).

NMR Spectroscopy: The ¹H NMR spectrum for the purified melanin from *Streptomyces rochei* dissolved in DMSO and analyzed by Bruker AVANCE III 600 spectrometer (17).

Raman Spectroscopy: The Raman Spectra were recorded using dilor DZ-24 spectrometer in the frequency range of 10cm⁻¹-3500cm⁻¹ (23).

CHNS elemental analysis: The Carbon, Hydrogen, Nitrogen and sulphur analysis were performed using Flash 1112 series CHNS analyser from Thermo Finningan.

Maintenance of Cell Line: The HFB4, Skin Cancer cell lines were purchased from NCCS, Pune. The cells were maintained in RPMI supplemented with 10% FBS and the antibiotics penicillin/streptomycin (0.5 mL⁻¹), in atmosphere of 5% CO₂/95% air at 37° C. For the MTT assay, HFB4, Skin Cancer cells were plated in 96 well plate at 5.0 X 10³ cells were per well in culture medium and incubated overnight at 37°C.

Cell Viability: Cell viability was evaluated by the MTT Assay with three independent triplicate experiments of six concentrations of compounds (5, 10, 25, 50, 75 and 100 μ g). After 24 hrs of incubation, each treatment was withdrawn and MTT solution (0.5 mg / mL⁻¹) was added to each well and plates were incubated at 37°C for 3 hrs (19). At the end of incubation time, precipitates are formed as a result of the reduction of the MTT salt to chromophore formazan crystals by the cells with metabolically active mitochondria. The optical density of solubilized crystals in DMSO was measured at 560 nm on a microplate reader (20).

ABTS radical scavenging activity: ABTS radical-scavenging activity of the Sample was determined according to Re et al (21). The ABTS.+cation radical was produced by the reaction between 5 mL of 14 mM ABTS solution and 5 mL of 4.9 mM potassium per sulfate (K₂S₂O₈) solution, stored in the dark at room temperature for 16 h. Before use, this solution was diluted with ethanol to get an absorbance of 0.700 \pm 0.020 at 734 nm. The Sample at various concentrations with 1mL of ABTS solution and its absorbance was recorded at 734 nm (22). Ethanol blanks were run in each assay, and all measurements were done after at least 6 min. Similarly, the reaction mixture of standard group was obtained by mixing 950 μ L of ABTS. + Solution and 50 μ L of BHT. As for the antiradical activity, ABTS scavenging ability was expressed as IC₅₀ in μ g/mL (22).

The inhibition percentage of ABTS radical was calculated using the following formula:

$$\text{ABTS scavenging activity (\%)} = (A_0 - A_1) / A_0 \times 100$$

Where A₀ is the absorbance of the control, and A₁ is the absorbance of the sample.

COMET Assay: DNA damage was estimated by alkaline single-cell gel electrophoresis (comet assay), a layer of 1% normal melting point agarose was prepared on microscope slides. The untreated control and POEet-treated cells (50 μ L) were mixed with 200 μ L of 0.5% low melting point agarose and were pipetted onto the precoated slides. Slides were immersed in cold lysis solution at pH 10 (2.5 M NaCl, 100 mM Na₂EDTA, 10 mM Tris pH 10, 1% Triton X-100, 10% DMSO) and incubated at 4°C for 60 min. To allow denaturation of DNA, the slides were placed in alkaline electrophoresis buffer at pH 13 for 25 min. Subsequently, slides were transferred to an electrophoresis tank with fresh alkaline electrophoresis buffer. Electrophoresis was performed at field strength of 1.33 V/cm for 25 min at 4°C. Slides were neutralized in 0.4 M Tris (pH 7.5) for 5 min and stained with 20 μ g/mL EtBr. For the visualization of DNA damage, observations were made using a 40 x objective in an epifluorescent microscope equipped with an excitation filter of 510–560 nm and a barrier filter of 590 nm (23).

Results and Discussion

A total of 36 Actinomycetes were isolated from marine soil samples and 3 from marine water samples. Out of these 39 isolates, only 7 isolates produced diffusible pigment on SCA agar which included brown black pigments production by 5 isolates, pink pigment by 1 isolate and yellow from 1 isolate. All these colonies were elevated, convex and powdery in nature. Similar morphological characteristics were reported in earlier publications which described streptomycetes spp (13). The actinomycetes which were producing highest amount of diffusible pigment designated as VZ/T4/W1 (Figure 1) was selected for further study and characterized. The morphological and biochemical characteristics of these isolates were presented in table 1.

16S rRNA gene has become an important tool in bacterial identification, since it provides information about the phylogenetic placement of species (26). The 16S rRNA gene has been widely used for phylogenetic and diversity studies for

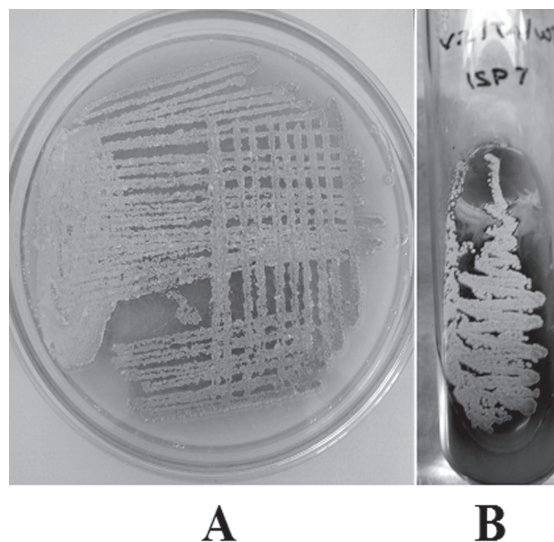


Fig. 1: *Streptomyces rochei* on SCA agar (A) and ISP 7 agar (B)

several reasons (26). It consists of conserved and variable regions which allow the development of primers and probes with variable levels of specificity. The conserved regions carry information about phylogenies at the higher taxonomic levels, since they have evolved slowly and are highly similar among the different taxa, whereas the variable regions have undergone more mutations during evolution, and are more useful for classification at the intraspecies level (6).

The 16S rRNA genes (rDNA) isolated from *Streptomyces* Isolate VZ/T4/W1 was amplified by using universal primers 27f (5'-AGA GTT TGA TCM TGG CTC AG-3'; positions 8 to 27; (26) and 1525r (5'-AAG GAG GTG WTC CAR CC-3'; (12) and the BLAST search was performed in Genbank using the two 16s rRNA sequences of 1270 bp and 1183 bp and submitted in Genbank with accession number MF927509. The phylogenetic tree was constructed via the bootstrap test of neighbor-joining algorithm method based on the 16S rRNA gene sequences of the isolate and respective related organisms (26, 27). The Isolate (VZ/T4/W1) shows significant similarity with *Streptomyces rochei* (99%) based on nucleotide homology and phylogenetic analysis (Figure 2).

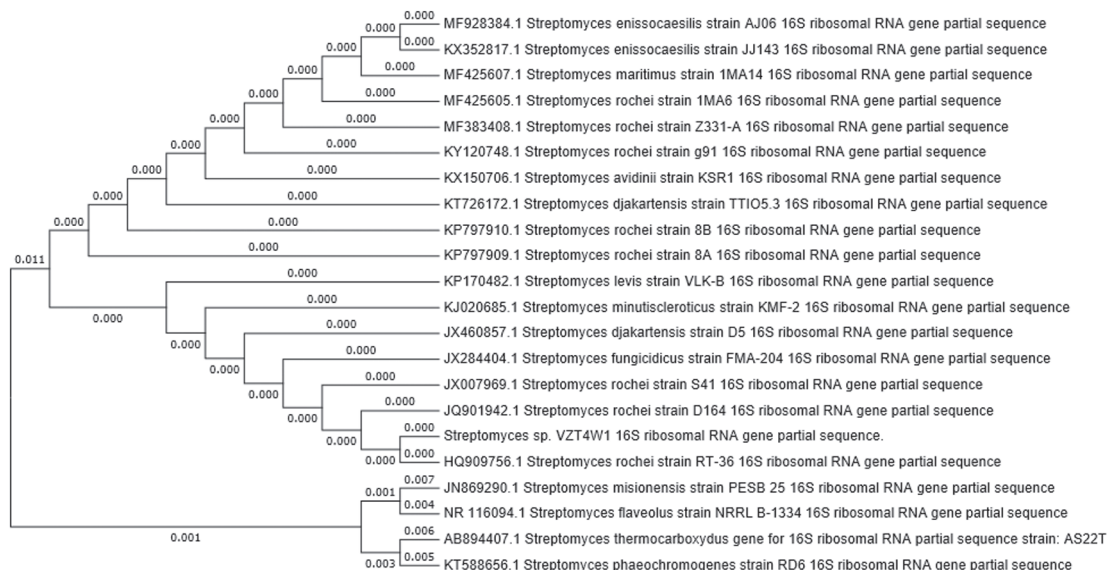


Fig. 2: Evolutionary relationships of taxa for Streptomyces isolate VZ/T4/W1

The pigment production in ISP 7 media was carried in ISP 7 broth for 15 days, pigment was extracted and purified with the yield of the dried pigments at 430 mg/L which was higher than the reported value of 179 mg/L for *Streptomyces glaucescens* NEAE-H (27).

The UV spectra obtained for the various concentrations of melanin pigment were proportional to their concentrations and exhibited a progressive decrease of absorbance with the increase in their wavelengths (Figure 3). There was a linear negative slope when the optical density was plotted against wavelength from the region 400 to 600 nm. This phenomenon is typical of melanin and were also used to identify melanin (4).

EPR spectroscopy is typically carried out to analyse the presence of free radicals in the melanin pigment. Homogeneous broadening of EPR lines is observed for the melanin pigment from *S. rochei* and the linewidth increases corresponding to the increase in microwave power (15). The comparison of spectras arising from DPPH, synthetic melanin and melanin from *S. rochei* are presented (Figure 4) EPR spectra of

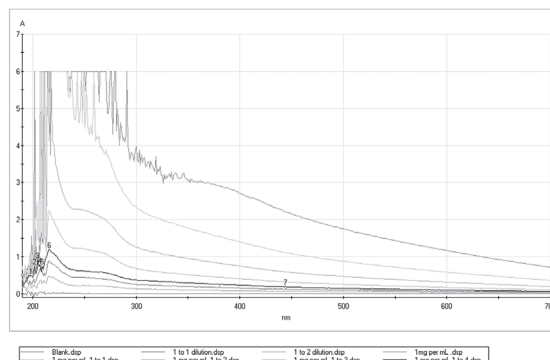


Fig. 3: UV spectroscopy of melanin pigment at different concentrations

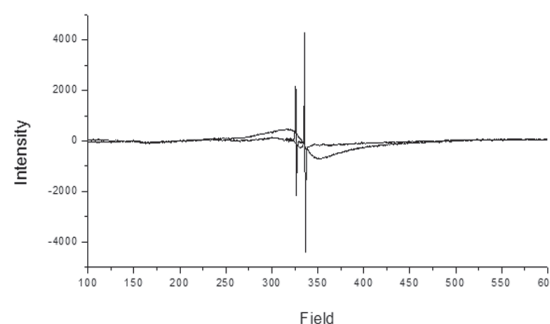


Fig. 4: EPR spectra of melanin pigment from *S. rochei*

melanin from *S.rochei* yielded and Synthetic melanin yielded a single and clean EPR spectra showing that they are a pure form of eumelanin. (15).

Proton NMR of the melanin pigment (Figure 5) showed resonances at 2.92, 3.0, 3.5 and 3.9 PPM of the aliphatic region. Aromatic region also showed resonances at 7.3, 7.8 and 8.3 PPM. There were also small cluster of resonances at 1 to 2.5 PPM arising from residual protein. The spectra has significant resonances from both aromatic and aliphatic region (17). This is similar to the Structural Characteristics of melanin pigment from *Lachnum singerianum* (17).

Raman spectroscopy of the melanin pigment from *S.rochei* (Figure 6) shows two major bands at 1330 and 1590 cm^{-1} specific for eumelanin (18).

There were several reports published on the chromatographic separation and analysis of melanin degradation products by HPLC and ion chromatography (28, 29). In chemical degradation methods, all the markers of melanin subunits are of completely different structure as compared to parent monomers of intact pigment. To obtain these markers, prolonged heating of the biopolymer with the effective oxidants or reductants in strong alkaline or acid media is required. Such a harsh procedure may produce artifactual alterations of the pigment framework, which undoubtedly affects the structure and the yield of the final degradation products (16). Hence, the melanin pigment was solubilized in DMSO and directly analysed by GC-MS.

The Total Ion chromatogram of melanin showed major peaks at 1.143, 1.417, 2.008, 4.201 and 29.709. The mass spectra of all the peaks were analysed and compared with the literatures and identified. DHI and DHICA monomers, markers of eumelanin with molecular mass of 179 (Figure 8) and 152 (Figure 7) were identified at retention time of 2.008 and 1.417 respectively (30).

The CHNS elemental analysis revealed that there is no presence of sulphur in the sample with 2.3% nitrogen, 58.5% Carbon and 6.8 %

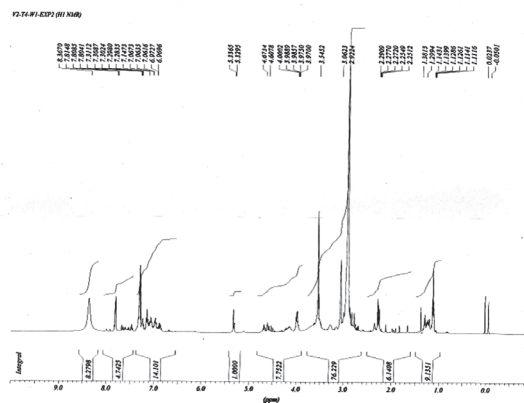


Fig. 5: NMR spectra of melanin pigment from *S. rochei*

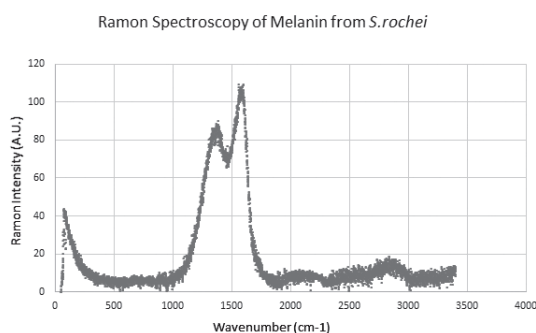


Fig. 6: Raman spectra of melanin pigment from *S. rochei*

Hydrogen (Figure 12) which is a typical characteristic of eumelanin (5).

The MTT assay of the melanin pigment was performed with 5-fluorouracil as standard on HFB4 skin cancer cell line shows the pigment has potent anticancer activity (Figure 9). The IC_{50} for the sample was at 26 $\mu\text{g}/\text{mL}$ (Table 3) the standard 5-Fluoro Uracil was 16.5 $\mu\text{g}/\text{mL}$ (Table 2). The percentage viability of the cells at 100 $\mu\text{g}/\text{mL}$ was 32.26 for the sample which is comparable to that of 5-fluorouracil at 25.14 (19, 20).

The ABTS radical scavenging activity to assess the antioxidant property of the melanin sample 62.73, 5-fluorouracil 44.15, ascorbic acid

<< Target >>

Line#:4 RTime:1.417(Scan#:51) MassPeaks:53
RawMode:Averaged 1.408-1.425(50-52) BasePeak:121.05(49850)
BG Mode:Calc. from Peak

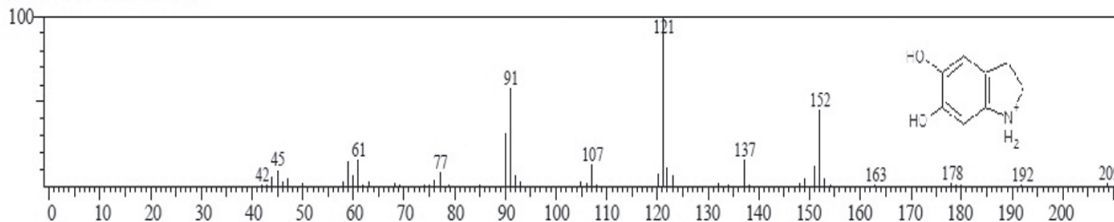


Fig. 7: GC-MS spectra for the peak at RT 1.417 min

<< Target >>

Line#:4 RTime:1.417(Scan#:51) MassPeaks:53
RawMode:Averaged 1.408-1.425(50-52) BasePeak:121.05(49850)
BG Mode:Calc. from Peak

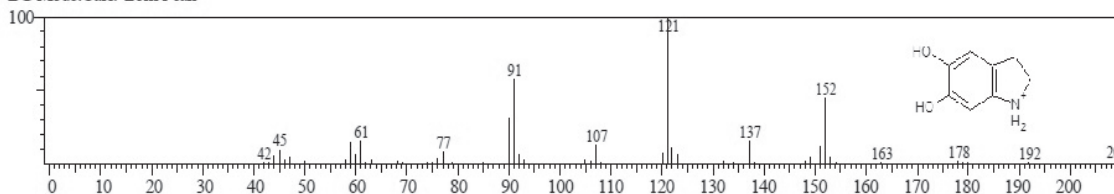


Fig. 8: GC-MS spectra for the peak at RT 2.008 min

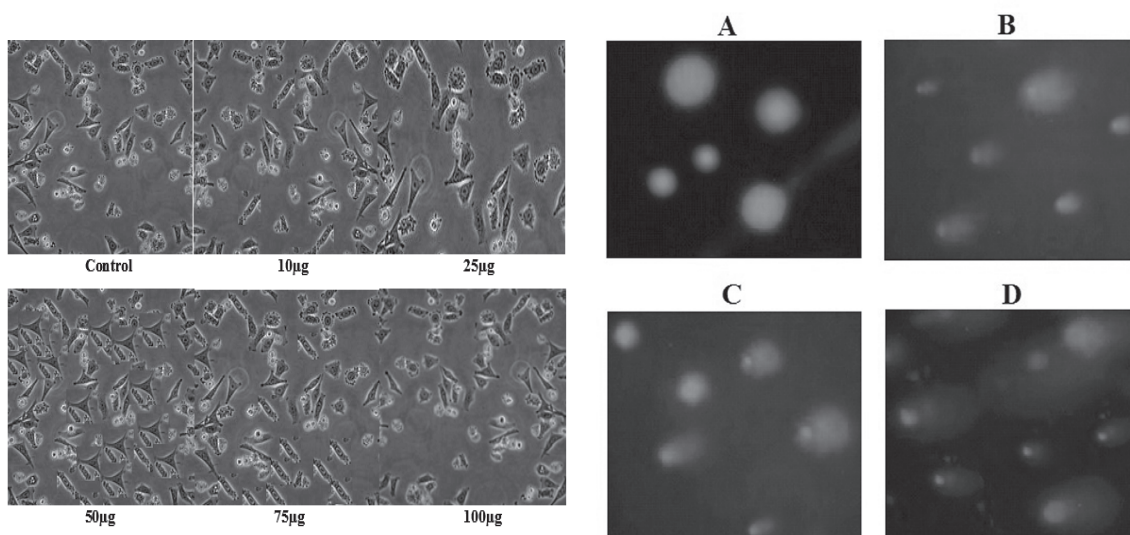


Fig. 9: Cytotoxic properties of melanin on HFB4, Skin Cancer cell line.

Figures 10 and 11: Morphological assessment of apoptosis by COMET assay

Table 1: Morphological and Biochemical characteristics of Streptomyces isolate VZ/T4/W1

	Characteristic	Streptomyces Isolate VZ/T4/W1
Morphological	Gram's Staining Spore chain morphology Spore mass colour Spore surface Aerial Mycelium Substrate Mycelium Diffusible pigment production	+ Spiral White Smooth White Brown +
Melanin Production	Starch casein agar ISP 7 Tyrosine agar medium Peptone-yeast extract iron agar Basal salts medium	+ + + + -
Biochemical reactions	Nitrate reduction H ₂ S production Urea Hydrolysis Citrate utilization	- - + -
Hydrolytic enzyme activity	Protease Amylase Lipase Phosphatase Pectinase Ligninase Cellulase Aryl sulphatase Chitinase	+ - + + + + - - +
Utilization of carbon source	L-Arabinose Rhamnose D+Galactose D-Mannose Sucrose Trehalose Ribose	+ + + + + + +

18.67 (Table 4). The percentage of inhibition at 100 µg/mL concentration of the melanin, 5- Fluoro Uracil and Ascorbic acid were 71.53, 63.32 and 51.43 respectively. The results exhibited that the melanin pigment possess good antioxidant activity (21).

The Untreated Control Cells show largely non-fragmented DNA whereas Sample Cells Showed fragmented DNA which appear as a Comet during Single-Cell Gel Electrophoresis (Figure 10). There was no change observed in

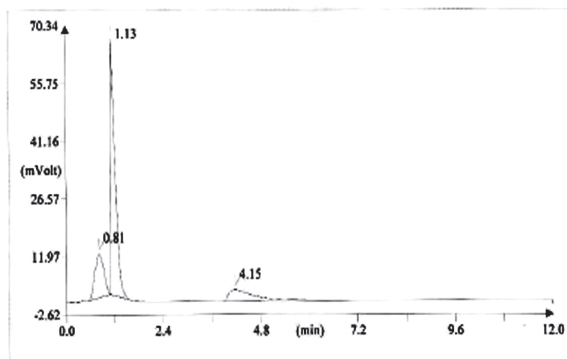


Fig. 12: CHNS profile of melanin from *S. rochei*

levels of DNA damage in the Untreated Control Cells (23).

The comet lengths were analyzed using the CASP software. Sample (50 And 100 $\mu\text{g}/\text{mL}$) treatment significantly ($P < 0.05$) expanded tail length, percentage of DNA, OTM, and TM (Figure 11). Similar results were observed with the Positive Control, TAM at 5 $\mu\text{g}/\text{mL}$ (23).

These results are consistent with the earlier reports on bacterial melanins and the anticancer and antioxidant potential of the *Streptomyces rochei* melanin are encouraging for the further studies.

Table 2 : Cytotoxic Properties of 5- Fluoro Uracil on HFB4, Skin Cancer cell line

Conc ($\mu\text{g}/\text{mL}$)	Absorbance at 570 nm			Average	Average-Blank	% Viability	IC ₅₀ ($\mu\text{g}/\text{mL}$)
100	0.321	0.323	0.324	0.322	0.314	25.14	16.501
75	0.411	0.412	0.414	0.412	0.404	32.345	
50	0.498	0.5	0.501	0.499	0.491	39.311	
25	0.586	0.587	0.589	0.587	0.579	46.357	
10	0.642	0.644	0.645	0.643	0.635	50.84	
5	0.701	0.703	0.705	0.703	0.695	55.644	
Untreated	1.257	1.258	1.257	1.257	1.249	100	
Blank	0.008	0.009	0.008	0.008			

Table 3: Cytotoxic Properties of melanin on HFB4, Skin Cancer cell line.

Conc ($\mu\text{g}/\text{mL}$)	Absorbance at 570 nm			Average	Average-Blank	% Viability	IC ₅₀ ($\mu\text{g}/\text{mL}$)
100	0.41	0.412	0.413	0.411	0.403	32.265	26
75	0.486	0.488	0.489	0.487	0.479	38.35	
50	0.534	0.535	0.537	0.535	0.527	42.193	
25	0.611	0.612	0.614	0.612	0.604	48.358	
10	0.682	0.683	0.685	0.683	0.675	54.043	
5	0.725	0.726	0.728	0.726	0.718	57.486	
Untreated	1.257	1.258	1.257	1.257	1.249	100	
Blank	0.008	0.009	0.008	0.008			

Table 4: ABTS Radical Scavenging Activity of melanin pigment, 5-fluoro uracil and Ascorbic acid

S.No	Sample	Conc (µg/mL)	% of Inhibition	IC ₅₀ Value (µg/mL)
1	Melanin pigment	5	34.94 ± 1.56	62.73 ± 3.63
		10	50.30 ± 0.89	
		25	52.39 ± 1.65	
		50	62.13 ± 1.88	
		75	67.41 ± 0.56	
		100	71.53 ± 1.55	
2	5-Fluoro Uracil	5	21.37 ± 1.56	44.15 ± 3.48
		10	46.69 ± 1.95	
		25	50.38 ± 0.23	
		50	55.24 ± 1.48	
		75	62.94 ± 0.48	
		100	63.32 ± 0.89	
3	Ascorbic acid	5	34.675 ± 0.96	18.67 ± 2.78
		10	40.546 ± 0.58	
		25	45.907 ± 0.77	
		50	49.864 ± 1.65	
		75	50.8 ± 0.94	
		100	51.438 ± 1.55	

Conclusion:

The spectroscopic studies of the pigment revealed that properties of melanin from *Streptomyces rochei* are similar to that of pure eumelanin. The pigment showed considerable anticancer and antioxidant activities when compared with the standards like 5-fluorouracil and ascorbic acid. The potential for commercial exploitation of this melanin for its biotechnological role is enormous and the *Streptomyces rochei* strain can be a credible source of melanin and can serve as cost effective substitute for the currently marketed products.

References:

1. F. Solano (2014). Melanins: Skin Pigments and Much More—Types, Structural Models, Biological Functions, and Formation Routes. *New Journal of Science* Volume, Article ID 498276, 28 pages.
2. Joshua D. Nosanchuk, Ruth E. Stark and Arturo Casadevall (2015). Fungal Melanin: What do We Know about Structure?. *Front Microbiol*, 6: 1463.
3. Enochs WS1, Nilges MJ, Swartz HM (1993). A standardized test for the identification and characterization of melanins using electron paramagnetic resonance (EPR) spectroscopy. *Pigment Cell Res.*, Mar; 6(2):91-9.
4. Sajjan, Shrishailnath S., Anjaneya O, Guruprasad B. Kulkarni, Anand S. Nayak, Suresh B. Mashetty, and T. B. Karegoudar (2013). Properties and Functions of Melanin Pigment from *Klebsiella* sp. GSK. *Korean J. Microbiol. Biotechnol*, 41(1): 60–69.
5. Deepthi, A. & Rosamma, P (2014). Actinomycete isolates from Arabian Sea and Bay of Bengal: biochemical, molecular and functional characterization: Thesis, Cochin University of Science and Technology, Cochin, Kerala 682022, India.
6. Shripad N. Surwase, Shekhar B. Jadhav, Swapnil S. Phugare, and Jyoti P. Jadhav

- (2013). Optimization of melanin production by *Brevundimonas* sp. SGJ using response surface methodology. 3 Biotech, 3: 187–194.
- (7). Justyna M. Drewnowska, Monika Zambrzycka, Beata Kalska-Szostko, Krzysztof Fiedoruk, Izabela Swiecicka (2015). Melanin-Like Pigment Synthesis by Soil Bacillus weihenstephanensis Isolates from Northeastern Poland, PLoS ONE, 10:4.
- (8). D. N. Madhusudhan, Bi Bi Zainab Mazhari, Syed G. Dastager and Dayanand Agsar (2014). Production and Cytotoxicity of Extracellular Insoluble and Droplets of Soluble Melanin by *Streptomyces lusitanus* DMZ-3. BioMed Research International, 2014:11 pages.
- (9). Kurian Noble K, Sarita G. Bhat (2015). Melanins from marine bacteria Characterization production and applications: Thesis, Cochin University of Science and Technology, Cochin, Kerala 682022, India.
- (10). Korumilli Tarangini, Susmita Mishra (2014). Production of melanin by soil microbial isolate on fruit waste extract: two step optimization of key parameters. Biotechnology Reports, 4: 139-146.
- (11). Y.S.Y.V. Jagan mohan, B. Sirisha, R. Haritha, T. Ramana (2013). Selective screening, Isolation and Characterization of Antimicrobial Agents from Marine Actinomycetes. International Journal of Pharmacy and Pharmaceutical Sciences 5:443-449
- (12). Kamil Isik, Talha Gencbay, Fadime Özdemir-Kocak and Elif Cil (2014). Molecular identification of different actinomycetes isolated from East Black Sea region plateau soil by 16S rDNA gene sequencing. African Journal of Microbiology Research, 8: 878-887.
- (13). Subramani Ramesh, Mahalingam Rajesh, Narayanasamy Mathivanan (2009). Characterization of a thermostable alkaline protease produced by marine *Streptomyces fungicidicus* MML1614. Bioprocess Biosyst Eng, 32: 791–800.
- (14). Chao Xin, Jia-hua Ma, Cheng-jia Tan, Zhou Yang, Feng Ye, Chan Long, Shuang Ye, and Da-bin Hou (2014). Preparation of melanin from *Catharsius molossus* L. and preliminary study on its chemical structure. Journal of Bioscience and Bioengineering, 119: 446-454.
- (15). Pilawa, B., Buszman, E., Latocha, M., Wilczok.T (1996). EPR studies of melanin from *Cladosporium cladosporioides*. Polish journal of medical physics and engineering, 2: 59-65
- (16). Anna Dzierzega, Lecznara Slawomir, Kurkiewicz Krystyna, Stepiena Ewa, Chodurekb Tadeusz, Wilczokc Thomas, Arzbergerd, Peter Riederere, Manfred Gerlachf (2004). GC/MS analysis of thermally degraded neuromelanin from the human substantia nigra, Journal of the American Society for Mass Spectrometry, 15:20-926.
- (17). Ming Ye, Xiao Chen, Guang Wei Li, Geng Yi Guo, Liu Yang (2011). Structural Characteristics of Pheomelanin-Like Pigment from *Lachnum singerianum* Advanced Materials Research, 284-286: 1742-1745.
- (18). Ismael Galvan, Alberto Jorge, Fransisco Solano, Kazumasa Wakamatsu (2013). Vibrational characterization of pheomelanin and trichochrome F by Ramon spectroscopy Spectrochimica Acta Part A: Molecular and Biomolecular spectroscopy, 110: 55-59.
- (19). Alet van Tonder, Annie M Joubert, and A Duncan Cromarty (2015). Limitations of the 3-(4,5-dimethylthiazol-2-yl)-2,5-diphenyl-2H-tetrazolium bromide (MTT) assay when

- compared to three commonly used cell enumeration assays. BMC Res. Notes, 8: 47.
- (20). Jessica M. Posimo, Ajay S. Unnithan, Amanda M. Gleixner, Hailey J. Choi, Yiran Jiang, Sree H. Pulugulla and Rehana K (2014). Leak Viability Assays for Cells in Culture. J Vis Exp, 83: 50645.
- (21). Re R, Pellegrini N, Proteggente A, Pannala A, Yang M, Rice-Evans (1999). Antioxidant activity applying an improved ABTS radical cation decolorization assay. Free Radic Biol Med. 26:1231-7.
- (22). Nishaa.S, Vishnupriya.M, Sasikumar.J.M, Hephzibah P Christabel, Gopala krishnan.V.K (2012). Antioxidant activity of ethanolic extract of *Maranta arundinacea* tuberous rhizomes. Asian J Pharm Clin Res, 5: 85-88.
- (23). Chiarelli-Neto O, Ferreira AS, Martins WK, Pavani C, Severino D, Faião-Flores F, et al. (2014) Melanin Photosensitization and the Effect of Visible Light on Epithelial Cells. PLoS ONE 9:11.
- (24). Daniil Olennikov, L. M. Tankhaeva, A. V. Rokhin, S. V. Agafonova. Physicochemical properties and antioxidant activity of melanin fractions from *Inonotus obliquus sclerotia*. Chemistry of Natural Compounds, 48: 3.
- (25). Tarangini Korumilli and Mishra Susmita (2013). Production, Characterization and Analysis of Melanin from Isolated Marine Pseudomonas sp. using Vegetable waste. Research Journal of Engineering Sciences, 2: 40-46.
- (26). Gascuel O. BIONJ (1997). An improved version of the NJ algorithm based on a simple model of sequence data. Mol Biol Evol, 14:685–695.
- (27). Noura El-Ahmady El-Naggar & Sara M. El-Ewasy (2017). Bioproduction, characterization, anticancer and antioxidant activities of extracellular melanin pigment produced by newly isolated microbial cell factories *Streptomyces glaucescens* NEAE-H Nature Scientific reports, 7:42129.
- (28). Akihiko Takasaki¹, Dzj Eneta Nezirevic, Kerstin A Rstrand, Kazumasa Wakamatsu, Shosuke Ito And Bertil Ka Gedal (2003). HPLC Analysis of Pheomelanin Degradation Products in Human Urine, Pigment Cell Res 16: 480–486.
- (29). Kazumasa Wakamatsu And Shosuke Ito (2002). Advanced Chemical Methods in Melanin Determination, Pigment Cell Res 15: 174–183.
- (30). P Di Donato, A (2003). Napolitano 1,4-Benzothiazines as Key Intermediates in the Biosynthesis of Red Hair Pigment Pheomelanins. Pigment Cell Res, 16: 532-539.

Optimization of process parameters for Poly Hydroxy Butyrate Production from Isolated *Acinetobacter nosocomialis* RR20 through Submerged Fermentation

A. Ranganadha Reddy^a, T.C. Venkateswarulu^{a*}, P. Sudhakar^c, S. Krupanidhi^a,
K. Vidya Prabhakar^{b*}

^{a & a*} Department of Biotechnology Vignan's Foundation for Science, Technology & Research, Valdamudi-522 213, India

^{b*} Department of Biotechnology Vikrama Simhapuri University SPSR Nellore-524003, India

^c Department of Biotechnology Acharya Nagarjuna University Guntur-522510, India

*For Correspondence - kodalividya^aprabhakar@gmail.com and venki^b_biotech327@yahoo.com

Abstract

Poly Hydroxy Butyrate member of polyhydroxyalkanoates family and is generally used as an alternative to polypropylene based plastic. Production of Poly Hydroxy Butyrate, biodegradable polymer from industrial wastes has several advantages such as recycle of waste and the production of high valuable products. It has been isolated from various sources till date. In this study, different strains of isolated bacteria were evaluated for their PHB productivity, but *Acinetobacter nosocomialis* RR20 strain resulted highest production. Therefore, optimization of process parameters was determined in batch fermentation mode using one-parameter -at a-time approach for enhanced production of PHB. The influence of physical and chemical variables namely incubation temperature, incubation time, inoculums size, pH, carbon source, nitrogen source and mineral salts were studied for improving the production of PHB. Maximum PHB was found 4.17 g/L at optimized conditions of incubation period 48 h, temperature 37 °C, pH 7.0, inoculums size of 4%, 30g/L molasses, 3g/L Ammonium sulphate and MgSO₄ 0.3g/L.

Key words: PHB, *A.nosocomialis* RR20, Shake flask culture, Process variables

Introduction

In our day-to-day life polypropylene based synthetic polymers have become an

integral part. The compounds produced from fossil resources like polyvinylchloride, polyhomopropylene, polyethylene and others include desirable properties like durability and resistance to degradation. The non-biodegradable plastics pose serious threat to the surroundings by accumulating in the global environment at a rate of 25 million tons per year (1). Poly-3-hydroxybutyrate (PHB) is the most predominant member of the family of PHAs (2,3). PHB is a biodegradable polymer and serves as a source for biodegradable plastics. Poly-3-hydroxybutyrate (PHB) is similar compound like Polyhydroxyalkanoate (PHA), emerged recently as an alternative for synthetic plastics as its structural properties are similar to polypropylene (4-6) and yet it is completely biodegradable (7-9). PHA's are widely used in the manufacturing of surgical pins, sutures, staples, wound dressing, stimulation of bone growth, replacement of bones, blood vessel replacements, and packaging industry (includes films, bags etc)(10-12). Polyhydroxybutyrate (PHB) is a biodegradable polymer synthesized and accumulated in cells as intracellular granules (inclusion bodies) by a diverse group of bacteria (13-15) because of nutritional limitation or excess carbon in the growth media and they are biodegraded by the bacteria itself. In previous studies many researchers reported the production of PHB from different bacterial species such as *Bacillus* sp., *Pseudomonas* sp., *Methylobacterium* sp.,

Ralstonia sp., *Alcaligenes* sp., through the submerged fermentation (16-20). However, no reports were found on the production of PHB from *Acinetobacter* species for higher yields. PHB production is influenced by various physical and chemical factors like bacterial strain type, pH, incubation period, temperature, inoculum size, agitation speed, carbon, nitrogen and mineral salts. Many researchers were reported the production of PHB from various bacterial species present in sewage sludge (21). However, there are very few reports are found on production of PHB from *Acinetobacter* species and hence, we aimed to produce the high PHB production through optimization study.

MATERIALS AND METHODS

Microorganism: The bacterial isolate *Acinetobacter nosocomialis* RR20 (KY913802) was isolated from sewage effluent, outskirts of Guntur, India. The bacterial isolate with distinct characteristic feature was maintained as pure culture on nutrient agar slants and stored at 4 °C.

Inoculum preparation and shake flask fermentation: The Basal culture medium comprised of 10 g/L of yeast extract, 10 g/L of polypeptone, 5 g/L of beef extract, 5 g/L NaCl and pH7.2 was used for inoculum preparation. The fermentation medium (MSM), comprised of 2.0 g/L $(\text{NH}_4)_2\text{SO}_4$, 2.0 g/L KH_2PO_4 , 0.6 g/L Na_2HPO_4 , 0.2 g/L $\text{MgSO}_4 \cdot 7\text{H}_2\text{O}$, 20 mg/L CaCl_2 , 10 mL/L trace metal solution; 0.1 g/L yeast extract was used (22-23). The trace metal solution consisted of: 1.3 mg/L $\text{ZnSO}_4 \cdot 7\text{H}_2\text{O}$, 0.2 mg/L $\text{FeSO}_4 \cdot 7\text{H}_2\text{O}$, 0.6 mg/L $(\text{NH}_4)_6\text{Mo}_7\text{O}_{24} \cdot 4\text{H}_2\text{O}$ and 0.6 mg/L H_3BO_3 solution and pH7.0. The shake flask fermentation was carried out with 100ml of fermentation medium in 250mL conical flask.

Effect of culture conditions on PHB production

Inoculum size: The effect of inoculum size on PolyHydroxy Butyrate production was studied by changing the percent of inoculum (1-6%, v/v) to production medium.

Incubation time: The effect of incubation time on PolyHydroxy Butyrate production was

determined by incubating the bacterial isolate at 37°C in broth medium at different time intervals.

Temperature: Optimum temperature for PolyHydroxy Butyrate production was determined by incubating inoculated culture medium at different temperatures 25°C, 30°C, 37°C, 40°C and 45°C for 48h.

pH : The most suitable pH for PolyHydroxy Butyrate production was optimized by using broth medium and determined by adjusting pH (5-9) of medium using 1N NaOH and 1N HCl. The inoculated culture flasks were kept for incubation for a period of 48h.

Carbon source: The effect of different carbon sources on Poly Hydroxy Butyrate production were investigated by using different carbon sources like glucose, fructose, maltose, starch and cane molasses for 48h.

Nitrogen sources: The effect of different nitrogen sources on Poly Hydroxy Butyrate production were investigated by using different nitrogen sources like ammonium sulphate (AS), ammonium chloride (AC), Ammonium nitrate (AN), Ammonium persulfate (APS) and urea (U).

Mineral salts: The effect of different mineral salts on Poly Hydroxy Butyrate production were investigated by using different inorganic salts like MgSO_4 , CaCl_2 , ZnSO_4 , KCl and FeSO_4 in the concentration range of 0.1g/L and further the MgSO_4 concentration was varied from 0.2g/L to 0.4g/L. All flasks were incubated for 48h in the liquid medium.

Extraction of PHB and assay: The cells were harvested by centrifuging the culture at 4°C (3000 g) for 10 min; the bacterial culture 10 mL sample was collected and centrifuged for 15min at 10,000 rpm and lyophilized and then, cell pellet was treated with 4% of sodium hypochlorite at 37°C for 1 h. The cell pellet was collected by centrifugation, later washed with phosphate buffer saline, water, acetone and ethanol respectively. Finally, the extracted biopolymer was dissolved in hot chloroform and kept for complete

evaporation (24). Dry weight of PHB estimated as g/L and the residual biomass estimated as difference between cell dry weight and dry weight of PHB (25-27). PHB assay was carried out by the method of Law and Slepecky (28).

Results and Discussion

Effect of incubation time on biopolymer production:

The changes in PolyHydroxyButyrate production were observed during incubation periods from 12 to 96 h. This represents the change in state of population number from lag phase to death phase. The maximum biopolymer production of 3.23 g/l was found after 48 hours of incubation beyond this the production declined due to depletion of nutrients (Fig.1). Shilpi Khanna and Ashok K. Srivastava reported that the highest biopolymer production was found at 48 h of incubation time through fermentation in shake flasks with a *Ralstonia eutropha* NRRL B14690 strain (29). Similarly, Gowdhaman et al (30) observed the PolyHydroxy Butyrate production with 48 hours of incubation period in submerged fermentation process by using *Bacillus cereus* BB613. Findings of Khaled Mohamed Aboshanab et al (31) also show that the optimum incubation period for PHB production by *Acinetobacter baumannii* isolate p39 was 48 h. Joseph Selvin et al reported that the highest PolyHydroxy Butyrate production was found at 48 h of incubation period under solid state fermentation by using *Bacillus megaterium* MSBN04(32). Nisha et al reported the maximum PHB production of 2.2 g/L at 48h of incubation period under submerged fermentation by using *Bacillus sphaericus* NCIM 5149(33).

Effect of temperature on biopolymer production:

The submerged fermentation process showed that the biopolymer production increases with an increase in incubation temperature up to 37 °C and then slows down at elevated temperature. Thus, 37°C was found optimum temperature for Poly Hydroxy Butyrate production by *A. nosocomialis* strain RR20 (Fig.2). Guo-Qiang Chen et al (34) stated that PHB production

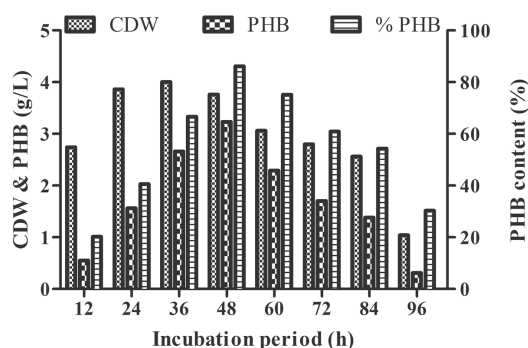


Fig. 1. Effect of incubation period on PHB production

was increased by *Bacillus* sp. JMa5 strain when the cultivation temperature was maintained at 37 °C. Tokiwa and Ugwu reported that at higher temperature (>40°C) PHB content decreased due to PHB depolymerase enzyme activity which is in conformity with present findings [35]. Aboshanab et al (36) reported that maximum PHB production was obtained with *Azomonas macrocytogenes* isolate P173 at 37°C. Aslim et al. (37) and Hamieh et al. (38), who reported that optimum incubation temperature for PHB production by *Bacillus subtilis*, *Bacillus pumilis* and *Bacillus thuringiensis* was 37 °C. Paolo Visca et al (39) reported the optimal growth of *Acinetobacter nosocomialis* as 37 °C.

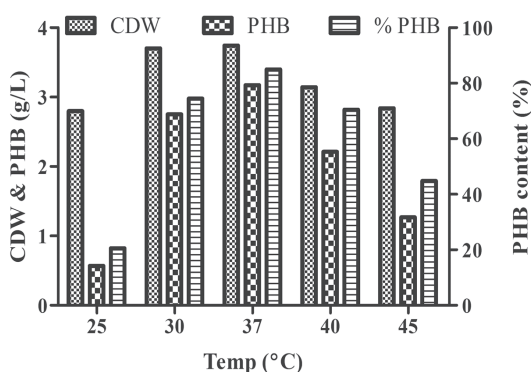


Fig. 2. Effect of Temperature on PHB production

Effect of pH on biopolymer production:

Biopolymer production gradually increased with changes in the pH of the medium from 5.0 to 7.0 and the activity slowly decreased with an increase in pH. The maximum biopolymer production was found 3.27 g/L at pH 7.0 (Fig.3). The biopolymer Poly Hydroxy Butyrate production was high at pH 7.0 through cultivation of *B. cereus* RBL6 and *P. pseudoalcaligenes* RBL7 (40). Gowdhaman et al (30) reported the maximum polyhydroxybutyrate production at pH 7 through submerged fermentation using the strain *Bacillus cereus* BB613. Abhishek Dutt Tripathi et al (41) proved that PHB production was higher at pH 6.54 through submerged fermentation using the strain *Alkaligenes* sp Aggarwal et al (42) reported that the pH 7.0 is the optimum for the production of poly hydroxyl butyrate through the submerged fermentation from *Bacillus subtilis* NG220. Reddy et al reported the highest PHB production at pH 7 through submerged fermentation using the strain *Bacillus* sp 88D(43).

Effect of inoculum size on biopolymer production:

Inoculum size of bacterial isolate has an important effect on the production of biopolymer quantity. Maximum biopolymer production of 3.21 g/L was observed with an inoculum size of 4%, and minimum with 1% inoculum, respectively (Fig.4). Sindhu et al (44) observed the highest PHB production by *Comamonas* sp.at 5.5% v/v inoculums which was

isolated from a Milma dairy effluent sample. Ali Raza et al found the highest PolyHydroxy Butyrate production when the fermentation medium was inoculated with 1% (v/v) of inoculums (45). Poorna chandrika et al (26) reported that the higher PHB production was achieved with 2% inoculum of *Acinetobacter junii* BP25. Pinaki Dey and Vivek Rangarajan found the highest production of Poly Hydroxy Butyrate when the fermentation medium was inoculated with 5%(v/v) of 24h grown inoculums(46). Aboshanab et al (36) reported that maximum PHB production was obtained with *Azomonas macrocytogenes* isolate P173 at 5% v/v inoculums.

Effect of carbon source on biopolymer production:

The effect of different carbon sources on growth and PHB production of *A. nosocomialis* RR20

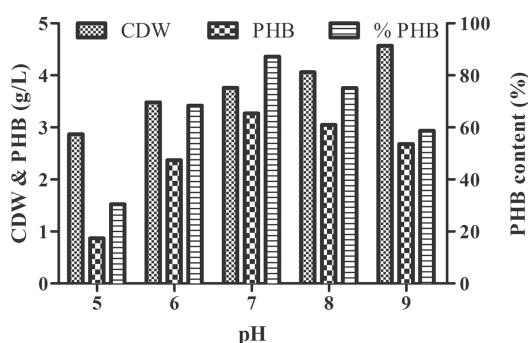


Fig. 3 Effect of pH on PHB production

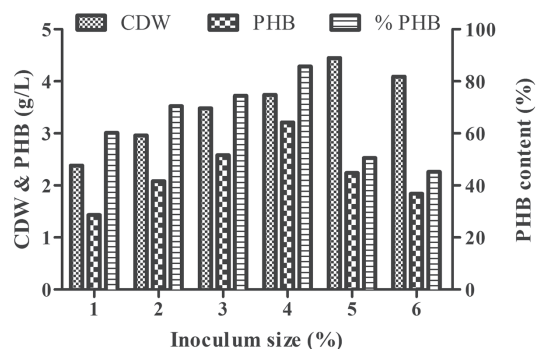


Fig. 4. Effect of Inoculums size on PHB production

supplemented with different carbon sources (i.e., glucose, fructose, maltose, starch and sugar cane molasses at 10 g/L. Inoculums were prepared as described above. The flasks were incubated at 37°C. Biomass and PHB were estimated in the culture broth after 48 h (Fig.5a). Further, the optimization was done by varying the concentration of molasses from 10 to 50 g/L. Maximum PHB production of 3.84g/L is obtained with 30g/L cane molasses as carbon source by using *Acinetobacter nosocomialis* RR20 (Fig.5b).

Limpon Bora (47) reported that highest polyhydroxybutyrate production of 1.38 g/L was obtained with *Bacillus megaterium* in the production medium with glucose as the carbon source. Singh et al reported highest PHB production of 2.3 g/L was obtained with *Vibrio harveyi* MCCB 284 in the production medium with glycerol as the carbon source (48). Gouda et al (49) reported that maximum production of PHB was obtained with *Bacillus megaterium* strain with 2% molasses as carbon source in fermentation medium.

Effect of nitrogen source on biopolymer production

These experiments were done in MSM containing cane molasses (30 g/L) as carbon source and different nitrogen sources (1 g/L) (i.e., ammonium sulphate, urea ammonium chloride, ammonium nitrate and ammonium persulfate). The flasks were incubated at 37°C. Biomass and PHB were estimated in cell broth after 48 h. (Fig. 6a). Further, the production of PHB was enhanced with the supplementation of varied concentrations of ammonium sulphate and found the highest production of PHB 4.0g/L by using *Acinetobacter nosocomialis* RR20 (Fig.6b). Khanna and

Srivastava reported that highest PHB accumulation of 3.84 g/L was obtained with *Ralstonia eutropha* NRRL B14690 after 60 h in the production medium with urea as the nitrogen source (50). Deepthi et al (51) reported that maximum production of PHB was obtained with *Bacillus firmus* NII 0830 with 4g/L ammonium sulphate as nitrogen source in fermentation medium. Jin Wang and Han-Qing Yu (52) reported that highest PHB production of 0.34 g/g was obtained with *Ralstonia eutropha* ATCC 17699 with 3.2 g/L ammonium sulphate as nitrogen source in fermentation medium. Neeraj K. Aggarwal(42) reported highest production of PHB with (1%w/v) ammonium sulphate as nitrogen source in the fermentation medium by using *Bacillus subtilis* NG220. Pinaki Dey and Vivek Rangarajan (46) reported highest production of PHB with 2g/L ammonium sulphate as nitrogen source in the fermentation medium by using *Cupriavidus necator* (MTCC 1472).

Effect of mineral salts on biopolymer production

The effect of different mineral salts on production of PHB was studied by supplementing the medium with salt concentration of 0.1g/L and found the

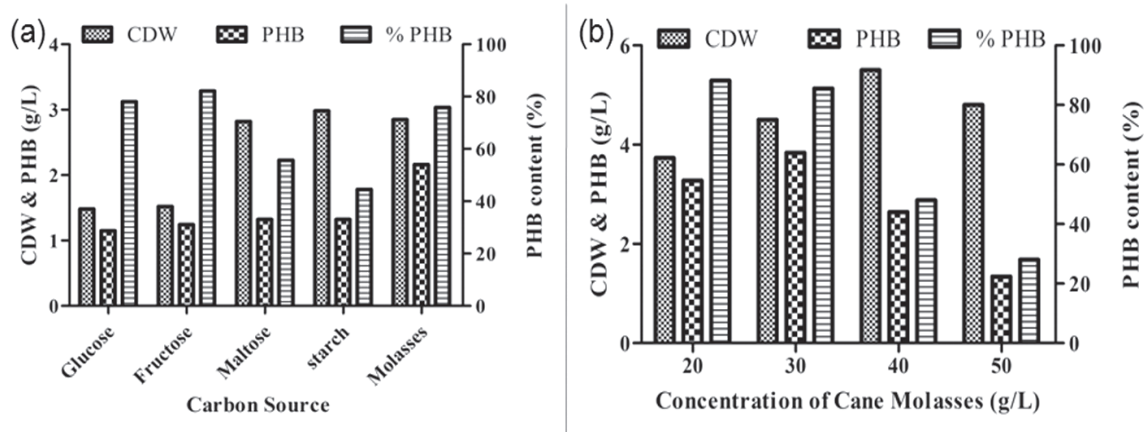


Fig. 5a. Effect of different carbon sources on PHB production; 5b Effect of different cane molasses concentration on PHB production

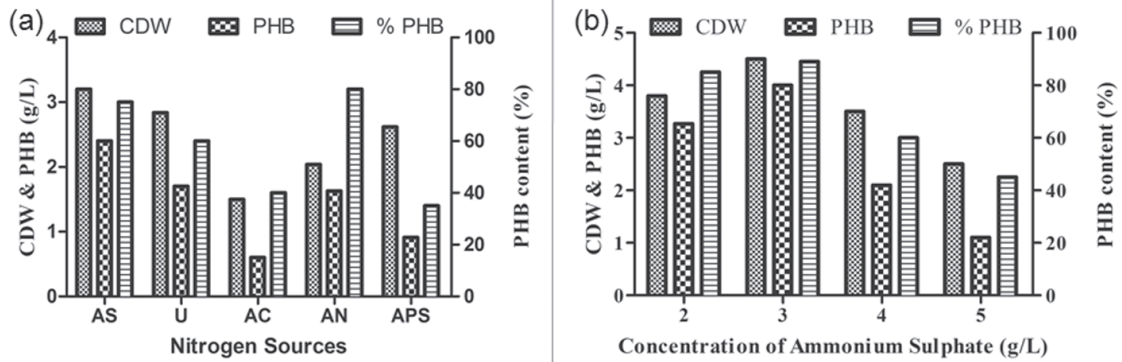


Fig. 6a Effect of different Nitrogen sources on PHB production; **6b** Effect of different Ammonium sulphate concentration on PHB production

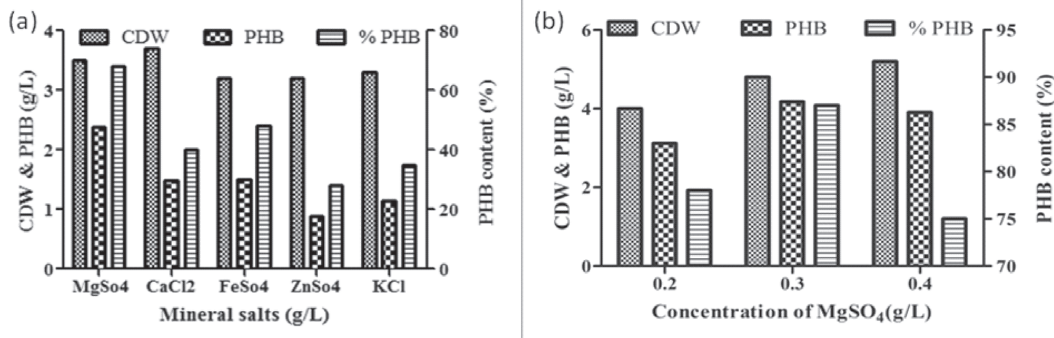


Figure 7a Effect of different mineral salts on PHB production; **7b** Effect of different MgSO₄ concentration on PHB production

highest production with MgSO₄ (Fig.7a). Further the MgSO₄ concentration was varied and found the significant improvement in the production of PHB (4.17 g/L) as shown in Fig.7b. The influence as Mg²⁺ ions on the composition of and production PHA were reported earlier (53, 54). Considering all the above factors, the isolate *Acinetobacter nosocomialis* RR20 could be designated as a potential prospect for industrial production of PHB. Based on the statistical analysis, various process parameters such as the incubation time, temperature, inoculums size, pH, carbon source, nitrogen source, and mineral salts were identified to have significant impact on the growth and PHB production.

Conclusion

The maximum PolyHydroxy Butyrate production was found 4.17 g/L at optimum conditions of incubation time 48 h, 37 °C, 4% (v/v) inoculums size, pH 7, 30g/L cane molasses, 3g/L ammonium sulphate and 0.3 g/L MgSO₄. Based on these findings, it is concluded that for the production of PolyHydroxy Butyrate, *A. nosocomialis* RR20 strain will be used as the promising alternative for commercial production of PHB.

Acknowledgments: The authors thankful to the Vignan's Foundation For Science, Technology and Science, Vadlamudi-522213 for providing necessary facilities to carry out this work.

References

1. Joa, O., Cavalheiro, M., Almeida, C.M.D.D., Christian, G., Fonseca, M.M.R. (2009) Poly (3hydroxybutyrate) production by *Cupriavidus necator* using waste glycerol. *Process Biochem.*, 44: 509-515.
2. Kwang-Min Lee, David F. G. (2005) Formulation and process modeling of biopolymer (polyhydroxyalkanoates: PHAs) production from industrial wastes by novel crossed experimental design. *Process Biochem.*, 40:229-246.
3. Ramsay, B. A., Lomaliza, K., Chavarie, C., Dubé, B., Bataille, P., Ramsay, J. A. (1990) Production of poly-(β -hydroxybutyric-Co- β -Hydroxyvaleric) acids. *Appl. Environ. Microbiol.*, 56: 2093-2098.
4. Sathiyarayanan, G., Kiran, G.S., Selvin, J., Saibaba, G. (2013) A statistical approach for optimization of polyhydroxybutyrate production by marine *Bacillus subtilis* MSBN17. *Int. J. Biol. Macromolec.*, 59: 170-177.
5. Sindhu, R., Silviya, N., Binod, P., Pandey, A. (2013) Pentose rich hydrolysate from acid pretreated rice straw as a carbon source for the production of poly-3-hydroxybutyrate. *Biochem. Eng. J.*, 78: 67-72.
6. Arun, A., Arthi, R., Shanmugabalaj, V., Eyini, M. (2009) Microbial production of poly-b-hydroxybutyrate by marine microbes isolated from various marine environments. *Bioresour. Technol.*, 100:2320-2323.
7. Yousuf, R.G., Winterburn, J.B. (2016) Date seed characterisation, substrate extraction and process modelling for the production of polyhydroxybutyrate by *Cupriavidus necator*. *Bioresour. Technol.*, 222: 242-251.
8. Mergaert, J., Anderson, C., Wouters, A., Swings, J., Kersters, K. (1992) Biodegradation of polyhydroxyalkanoates. *FEMS Microbiol. Rev.*, 103:317-321.
9. Abhishek, D.T., Suresh, K.S., Ravipratap, S. (2013) Statistical optimization of physical process variables for bio-plastic (PHB) production by *Alcaligenes sp.* *Biomass Bioenergy.*, 55:243-250.
10. Enrico, G., Murray, M.Y. (1999) Yusuf, C., Fermentation optimization for the production of poly (b-hydroxybutyric acid) microbial thermoplastic. *Enzyme Microb. Technol.*, 25:132-141.
11. Singh, A.K., Sharma, L., Mallick, N., Jyoti, N. (2017) Progress and challenges in producing polyhydroxyalkanoate biopolymers from cyanobacteria. *J Appl Phycol.* 29: 1213-1232.
12. Ansari, S., Fatma, T. (2016) Cyanobacterial Polyhydroxybutyrate (PHB): Screening, Optimization and Characterization. *PLoS ONE.*, 11: e0158168.
13. Venkateswar Reddy, M., Mawatari, Y., Onodera, R., Nakamura, Y., Yajima, Y., Chang, Y.C. (2017) Polyhydroxyalkanoates production from synthetic waste using *Pseudomonas pseudoflava*: Polyhydroxyalkanoate synthase enzyme activity analysis from *P. pseudoflava* and *P. palleronii*. *Bioresour. Technol.* 234: 99-105.
14. Shilpi, K., Ashok, K.S. (2005) Statistical media optimization studies for growth and PHB production by *Ralstonia eutropha*. *Process Biochem.*, 40: 2173-2182.
15. Braunegg, G., Bona, R., Koller, M. (2004) Sustainable Polymer Production. *Polym. Plast. Technol. Eng.*, 43: 1779-1793.
16. Mohapatra, S., Mohanta, P.R. Sarkar, B., Daware, A., Kumar, C., Samantaray, D.P., Production of Polyhydroxyalkanoates (PHAs) by *Bacillus Strain* Isolated from Waste Water and Its Biochemical Characterization. *Proc. Natl. Acad. Sci., India, Sect. B Biol. Sci.*, 87:459-466.
17. Otari, S.V., Ghosh, J.S. (2009) Production and characterization of the polymer polyhydroxy butyrate-co-polyhydroxy valerate by *Bacillus megaterium* NCIM 2475.

- Curr Res J Biol Sci.*, 1:23–26
18. Yung, H.Y., Christopher, J.B., Charles, F.B., Paolo, B., Laura, B.W., Mohd Ali Hassan., Mohd Yusof, Z.A., ChoKyun, R., Anthony, J.S.(2010) Optimization of growth media components for polyhydroxyalkanoate (PHA) production from organic acids by *Ralstonia eutropha*. *Appl Microbiol Biotechnol.* 87:2037–2045.
 19. Anderson, A.J., Dawes, E.A.(1990) Occurrence, metabolism, metabolic role and industrial uses of bacterial polyhydroxyalkanoates. *Microbiol. Rev.*, 54:450–472.
 20. Sei, K.H., Yong, K.C., Beom, S.K., Ho, N.C.(1994) Optimization of Microbial Poly (3-hydroxybutyrate) Recovery Using Dispersions of Sodium Hypochlorite Solution and Chloroform. *Biotechnol. Bioeng.* 44:256-261.
 21. Reddy, S. V., Thirumala, M., T. V. K. Reddy., Mahmood, S.K. (2008) Isolation of bacteria producing polyhydroxyalkanoates (PHA) from municipal sewage sludge. *World. J. Microbiol. Biotechnol.*, 24: 2949-2955.
 22. Mulchandani, A., Luong, J.H.T., Groom, C. (1989) Substrate inhibition kinetics for microbial growth and synthesis of PHB by *Alcaligenes eutrophus* ATCC 17697. *Appl Microbiol Biotechnol.* 30:11–7.
 23. Raje, P., Srivastava, A.K. (1998) Updated mathematical model and fed batch strategies for poly-b-hydroxybutyrate (PHB) production by *Alcaligenes eutrophus*. *Bioresource Technol.* 64:185–92.
 24. Arnold, L., Demain, J. and Davis, E. (1999). Polyhydroxyalkanoates. Manual of Microbiology and Biotechnology. Washington, Am Soc Microbiol, USA, 2, pp 616-627.
 25. Zakaria, M.R., Ariffin, H., Johar, N.A.M., Aziz, S.A., Nishida, H., Shirai, Y. and Hassan, M.A. (2010). Biosynthesis and characterization of poly (3-hydroxybutyrate-co-3-hydroxybutyrate) copolymer from wild type *Comamonas* sp. EB172. *Polym Degrad Stab.* 95:1382-1386.
 26. Poorna Chandrika, S., Sabarinathan, D., Anburajan, P., K. Preethi (2017) Bioprocess optimization of PHB homopolymer and copolymer P3 (HB-co-HV) by *Acinetobacter junii* BP25 utilizing rice mill effluent as sustainable substrate, *Environ. Technol.*, DOI:10.1080/09593330.2017.1330902.
 27. Aarthi, N., VenkataRamana, K.(2012) Polyhydroxybutyrate production in *Bacillus mycoides* DFC1 using response surface optimization for physico-chemical process parameters. *3 Biotech.*, 2:287–296 DOI 10.1007/s13205-012-0054-8
 28. John, H.L., Slepecky, R.A. (1961) Assay of poly- β -hydroxybutyric acid. *J Bacteriol.* 82: 33–36.
 29. Shilpi, K., Ashok, K.S. (2005) Statistical media optimization studies for growth and PHB production by *Ralstonia eutropha*, *Process Biochem.* 40:2173–2182.
 30. Bharathi, B., Gowdhaman, D., Ponnusami, V. (2016). Isolation and Identification of Polyhydroxybutyrate(PHB) Producing *Bacillus cereus* BB613-A Novel Isolate. *Int J Chemtech Res.*, 9:224-228.
 31. Noha, S. E., Khaled Mohamed A., Mohammad Aboulwafa, Nadia, A.H.(2016) cost-effective production of the bio-plastic poly- β -hydroxybutyrate using *Acinetobacter baumannii* isolate p39 *J Microbiol Biotech Food Sciences* ., 5: 552-556
 32. Sathiyarayanan, G., Seghal Kiran, G., Joseph, S., Saibaba, G.(2013) Optimization of polyhydroxybutyrate production by marine *Bacillus megaterium* MSBN04 under solid state culture *Int J Biol Macromol.*, 60: 253–261
 33. Nisha, V. R., Carlos, R. S., Ashok, P.(2010) A Statistical Approach for Optimization of

- Polyhydroxybutyrate Production by *Bacillus sphaericus* NCIM 5149 under Submerged Fermentation Using Central Composite Design. *Appl Biochem Biotechnol.*, 162:996–1007.
34. Qiong Wu, Honghua Huang, Guohong Hu, Jinchun Chen, KP Ho, Guo-Qiang Chen.(2001) Production of poly-3-hydroxybutyrate by *Bacillus* sp. JMa5 cultivated in molasses media *Antonie van Leeuwenhoek*, 80: 111–118.
35. Tokiwa, Y., Ugwu, C.U. (2007) Biotechnological production of (R)-3-hydroxybutyric acid monomer. *J Biotechnol.*, 132:264-272.
36. Noha, S. E., Khaled, M. A., Mohammad, M.A., Nadia, A.H. (2013) Optimization of bioplastic (poly- β -hydroxybutyrate) production by a promising *Azomonas macrocytogenes* bacterial isolate P173. *Afr. J. Microbiol. Res.*, 7:5025-5035.
37. Aslim, B., Yksekda, Z.N., Beyatli, Y. (2001) Determination of growth quantities of certain *Bacillus* species isolated from soil. *Turk Electr J Biotechnol* (Sp. Issue):24–30
38. Hamieh, A., Olama, Z., Holail, H. (2013) Microbial production of polyhydroxybutyrate, a biodegradable plastic using agro-industrial waste products. *G Adv Res J Microbiol.*, 2:54–64
39. Paolo Visca, Harald Seifert, Kevin J Towner. *Acinetobacter* Infection – an Emerging Threat to Human Health. *IUBMB Life*. 2011; 63:1048–1054.
40. Ramya, R., SangeethaDevi, R., Manikandan, A., RajeshKannan, V.(2017) Standardization of biopolymer production from seaweed associative bacteria R. R. et al. / *Int. J. Biol. Macromol.*, 102:550–564.
41. Abhishek, D.T., Sureshkumar, S., Ravipatap, S. (2013) Statistical optimization of physical process variables for bio-plastic (PHB) production by *Alcaligenes* sp. *Bio mass Bioenergy.*, 55:243-250.
42. Gulab Singh, Anish Kumari, Arpana Mittal, Anita Yadav, Neeraj, K.A.(2013) Poly- γ -Hydroxybutyrate Production by *Bacillus subtilis* NG220 Using Sugar Industry Waste Water. *Biomed Res Int.*, Article ID 952641, 10 pages <http://dx.doi.org/10.1155/2013/952641>.
43. VishnuvardhanReddy,S., Thirumala, M., Mahmood,S.K.(2009) A novel *Bacillus* sp. accumulating poly (3-hydroxybutyrate-co-3-hydroxyvalerate) from a single carbon substrate. *J Ind Microbiol Biotechnol.*, 36:837–843.
44. Thunoli, P.P., Sindhu, R., Parameswaran, B., Vandana, S., Gopalan Raghu,K., Ashok P. (2015) Production and characterization of PHB from a novel isolate *Comamonas* sp.from a dairy effluent sample and its application in cell culture. *Biochem. Eng. J.*, 101: 150–159.
45. Sharjeel, A.Z., Ali Raza, Tanveer Hussain. (2016) Production kinetics of polyhydroxyalkanoates by using *Pseudomonas aeruginosa* gamma ray mutant strain EBN-8 cultured on soybean oil. *3 Biotech.*, 6:142 DOI 10.1007/s13205-016-0452-4
46. Pinaki, D., Vivek, R. (2017) Improved fed-batch production of high-purity PHB (poly-3hydroxy butyrate) by *Cupriavidus necator* (MTCC 1472) from sucrose-based cheap substrates under response surface optimized conditions. *3 Biotech.*, 7:310 DOI 10.1007/s13205-017-0948-6.
47. Limpon, B. (2013) Polyhydroxybutyrate Accumulation in *Bacillus megaterium* and Optimization of Process Parameters Using Response Surface Methodology. *J Polym Environ.*, 21:415–420 DOI 10.1007/s10924-012-0529-z
48. Sowmya P. M., Linu, B., Lekshmi, N., Sherine Sonia C., Rosamma, P., Bright Singh I. S. (2016) Production and

- characterization of polyhydroxybutyrate from *Vibrio harveyi* MCCB 284 utilizing glycerol as carbon source. *J Appl Microbiol.*, DOI: 10.1111/jam.13359.
49. Gouda, M.K., Swellam, A.E., Omar, S.H. (2001) Production of PHB by a *Ba-cillus megaterium* strain using sugarcane molasses and corn steep liquor as sole carbon and nitrogen sources. *Microbiol Res.*, 156 :201–7.
50. Shilpi, K., Ashok, K.S.(2005) Statistical media optimization studies for growth and PHB production by *Ralstonia eutropha* *Process Biochem.*, 40: 2173–2182. Doi:10.1016/j.procbio.2004.08.011
51. Sindhu, R., Ammu, B., Binod, P., Deepthi, S.K., Ramachandran, K.B., Soccol, C.R., Pandey, A. (2011) Production and characterization of poly-3-hydroxybutyrate from crude glycerol by *Bacillus sphaericus* NII 0838 and improving its thermal properties by blending with other polymers. *Braz Arch Biol Technol* 54: 783-794.
52. wang, Jin., Yu, Han-Qing. (2007) Biosynthesis of polyhydroxybutyrate (PHB) and extracellular polymeric substances (EPS) by *Ralstonia eutropha* ATCC 17699 in batch cultures. *Applied microbiology and biotechnology.* 75: 871-8. 10.1007/s00253-007-0870-7.
53. Chen, Q., Nijenhuis, A., Preusting, H., Dofling, J., Janssen, D.B. and Witholt, B. (1995). Effects of octane on the fatty acid composition and transition temperature of *Pseudomonas oleovorans* membrane lipids during growth in two-liquid phase continuous culture. *Enzyme and Microbial Technology* 17: 647 –652.
54. Lee WH, Azizan MNM, Sudesh K. Magnesium affects poly (3-hydroxybutyrate-co-4- hydroxybutyrate) content and composition by affecting glucose uptake in *Delftia acidovorans*. *Malays J Microbiol.* 2007; 3: 31–34.

***In-Vivo* Evaluation of Rifampicin Loaded Nanospheres: Biodistribution and *Mycobacterium* Screening Studies**

Vishnu Vardhan Reddy Beeram¹, Krupanidhi S^{1*}&Venkata Nadh R²

¹Department of Biotechnology, Vignan's University, Vadlamudi, Guntur-522213, India.

email: srivyshu.pharma@gmail.com; Mobile: +91-9705070901

²GITAM University – Bengaluru Campus, Karnataka- 561 203, India,

email: doctornadh@yahoo.co.in; Mobile: +91-9902632733

*Corresponding Author email: krupanidhi.srirama@gmail.com

Abstract:

Rifampicin PLGA nanospheres are formulated with a specific goal in order to decrease the dose, adverse effects and to enhance targeted drug delivery. Rifampicin nanospheres were prepared and evaluated by emulsion solvent evaporation method. *In vivo* bio distribution studies reveal that there was a long term accumulation of rifampicin nanospheres in the lungs over other organs. The increase in C_{max} values confirmed that inhalable PLGA nanospheres are suitable for targeting and providing sustained release of anti-tubercular drugs to lungs. So inhalation is a selected administration route of Rifampicin PLGA nanospheres. The *in vivo* screening of *M. tuberculosis* showed good activity as well as its activity against multidrug-resistant *M. tuberculosis* and against *M. tuberculosis* isolates in a potentially latent state, makes Rifampicin PLGA nanospheres as an attractive drug dosage form for the therapy of tuberculosis. It can be concluded that there is a significant potential for effective oral delivery as well as nasal delivery of the Nanospheres for the treatment of tuberculosis.

Keywords: Rifampicin Nanospheres, *M. tuberculosis*, *In vivo* Bio distribution studies.

Introduction

Tuberculosis is a contagious disease that transmits through air by the bacterium *Mycobacterium tuberculosis* (MTB) (1). Despite

the pathogen being pulmonary targeted, it's pathogenicity spreads over entire body. In addition, tuberculosis displays a vibrant range from non infectious to hazardous ailment (2, 3).

Development of specific delivery system with sustained release of drug can able to maintain the adequate therapeutic concentration in the site of action (4). Use of bio decomposable and biocompatible polymers to develop nanospheres is remarkable achievement in controlled drug delivery system.

Poly lactic co glycolic acid (PLGA) polymer its co-polymers have achieved a perspective in preparing an array of delivery systems incorporated with various drugs for sustained release, being their biodegradable and biocompatible characters with minimum toxicity (5) in particular as anti tubercular drug (ATD) carrier (6).

Current research was aimed to investigate pre clinically for efficacy release of pulmonary targeted ATD rifampicin from PLGA nano carrier in comparison with intravenous route therapy of the same using the conventional formulation.

Materials and Methods

Materials

Rifampicin and polyvinyl alcohol (PVA) were obtained from Sigma Chemical Co. Poly (lactide-co-glycoside) was purchased from Boehringer Ingelheim, Germany. Remaining chemicals used in this study are of analytical grade.

Formulation of Rifampicin PLGA Nanoparticle by Emulsion Solvent Evaporation Method :

Different variants of rifampicin stacked nanoparticles (NPs) were prepared by changing the formulation variables (like polymer and surfactant) and process variables (like sonication time). In the formulations, 100 mg of rifampicin was dissolved with various concentrations of PLGA and surfactant in 300 ml ethanol. Then the organic phase was emulsified by adding different concentrations of PVA using ultrasonicator for 35 seconds. The emulsion was included drop wise into beaker containing different concentration of PVA solution which acts as continuous phase and mixture was maintained for continuous stirring. The emulsion was left on gentle stirring for 3 hrs to allow for solvent evaporation. Then, suspended nanoparticles were collected by ultracentrifugation at 30,000 rounds per minutes (RPM) for 15 min at 3° C. The NPs were washed three times with cold double-deionized water and then freeze-dried for 38 h (7).

Pharmacokinetic Studies : Rodents like Wistar albino rat of male gender (160-180g) were selected for investigation. Rats were resided in polypropylene cages in a proper aerated room under atmospheric circumstances of 22±2°C and 45-65% relative humidity, with on and off light with equal duration in a day. Selected rats were adjusted to laboratory conditions one week prior to the date of experimentation. Standard diet food and water were given at sufficient levels. Rats were fasted overnight prior to the day of experiment with a provision of water.

On the next day, Rifampicin nanospheres were administered to rats (n= 6) by intravenous route through tail vein at the dose of 2.4 mg/rat. Rats are bled at time periods 5,15,30 min,1,2,4,6,8,12 and 24 h following administration. After centrifugation, the plasma was divided and frozen at -20°C for further studies (7).

Bio-distribution studies : Male Wistar rats (n=6) weighing 160–180g were used for the bio distribution studies. The experimental proposal was accepted and performed as per the guidelines

of Institutional Animal Ethical Committee (IAEC) (MIP/IAEC/2015-16/M1/07) of the Institute. Nanospheres at a dose of 25mg/rat were administered once by inhalational route. About required dose of drug loaded nanospheres were charged and nebulized for 30 sec using an in house apparatus to obtain inhaled dose of 25mg/rat. Before dosing, the rats were trained for 3 days to accept or restraint the application of an infant inhalation mask attached to our in-house apparatus.

After inhalation, rats were bled at different time intervals selected for Bio distribution studies. After blood collection, animals were sacrificed by using CO₂ euthanasia and organs like lungs, liver and kidney were collected. The organ weights were recorded. Lungs were kept in saline prepared with phosphate buffer at a slight acidic pH and stored at -20°C until analysis. The collected organs are sliced and homogenized at 6000 RPM for 20 min. Centrifugation was done to the collected tissue samples at 4000 RPM for 10 min and the collected supernatant was analyzed by HPLC.

Collection of bronchi -alveolar ravage : From the sacrificed rats lungs were isolated in conjunction with trachea by dissecting thoracic region. The lungs were frequently lavaged with ice cold phosphate buffer saline (PBS) (with 0.5M EDTA) through cannulated trachea. Broncho alveolar fluids were pooled, made centrifuge and the collected macrophages were numbered and stored at -20°C till the analysis.

The analysis of drug was done by HPLC and the concentration of drug was obtained from calibration graphs. Inspecting the data visually, maximum plasma concentration (C_{max}) and time to achieve it time to maximum plasma concentration (T_{max}) were determined.

The plasma concentration values were transformed logarithmically and by applying linear regression T_{1/2} was estimated. The plasma concentration versus time curve (zero moment) and the first moment curve area under the moment curve (AUMC) were estimated. The area under the curve (AUC), area under the concentration-

time curve from time zero to time of last sample intake (AUC_{0-t}) and area under the moment curve-time curve from time zero to time of last sample intake ($AUMC_{0-t}$) were calculated as per the trapezoid rule. The first moment was calculated as concentration times time ($C_p \times t$). The AUMC is the area under the ($C_p \times t$) versus time curve. The AUC determines the bioavailability of the drug for the given same dose in the formulation. Total calculations were done by software Phoenix WinNonlin non-compartmental analysis program.

Sample preparation for analysis

Blood sample: The blood samples collected at respective time intervals during pharmacokinetic and bio distribution studies were taken in heparinised micro-centrifuges. Blood samples were centrifuged at 4000 rpm for 10 min to separate plasma and it was maintained at -20°C until analysis.

Aliquots of 150 μl of plasma were mixed with methanol (300 μl) as de-proteinizing agent and the obtained dispersal is whirl pooled around 2 min. The samples were centrifuged at 15000 RPM for 10min at 4°C and the supernatant is collected.

Rifampicin was extracted with 3 ml of chloroform-butanol (70:30%v/v) and 3 ml portions of chloroform-butanol (70:30% v/v) and vortexed for about 1 min followed by centrifuging at 4000 RPM of 10 min duration. The superficial layer was decanted and the process was repeated for in triplicate and superficial liquid was collected. The collected supernatants were diluted and analyzed by HPLC.

Tissue sample : Tissue homogenates (20% w/v) with aqueous medium were prepared in cold 150M KCL. Supernatant liquid collected from homogenates by centrifugation at 15000 RPM for 10 min at 4°C was kept aside for further studies. Then, 300 μl of the methanol was admixed to 150 μl of the clear homogenates and the dispersal was vortexed for 2 min. The samples were then centrifuged at 15,000 RPM for about 10 min at 4°C . An equal volume of water is added to the obtained supernatant. The samples were further filtered using 0.2 μm nylon filters and were instilled to the HPLC system (8-11).

Bio-analytical HPLC method : The collected serum and tissue samples were analyzed by HPLC (Analytical technologies Ltd) comprising C-18 column & UV detector. The mobile phase consists of Triethanolamine acetate: acetonitrile (97: 3% v/v) eluted by isocratic method and detected at 262 nm, analysed at 30°C by injecting 20 μl by maintaining a flow rate of 0.9ml/min. A wash method program which increased the % methanol was included at the end of drug elution to ensure washout of all interfering excipients. Spectral purity analysis of the drugs peak over a range of 200–400 nm was performed. The accuracy and precision of the developed method for determination of drug was comparable to the isocratic methods described in United State Pharmacopoeia (USP).

Data Analysis

The area under the total plasma concentration time curve from zero time to infinity was calculated by equation $AUC_{0-\infty}$ = area under the plasma concentration-time curve extrapolated to infinity

$$AUC_{0-\infty} = AUC_{0-t} + C_t/K_e$$

Where C_t is the rifampicin concentration observed at last time and K_e is the apparent elimination rate constant obtained from the terminal slope of the individual plasma concentration (12-18). Durations of serum drug concentration following inhalational route were analyzed by software Phoenix Win Nonlin non-compartmental analysis program of version 5.1.

Mycobacterial infection study in rat

MTB H37Rv ATCC 27294, a strain sensitive to all the standard antimycobacterial agents, was used for all animal infection in the experiments. Bacterial cultures were prepared as described previously published article (8). Wistar rats were infected via the respiratory route to obtain low-grade bacillary lung infection (100 bacilli) using a modified Madison aerosol chamber (9). Bacterial lung loads were estimated to determine suitable infection conditions for drug efficacy experiments. After infection, the animals were housed for the duration of the study in a bio-safety level 3 facilities. By using microbial enumeration,

dependent variable, the number of animals required, per treatment group was three in experiments for drug evaluation. The course of mycobacterial infection was monitored by enumeration of colony forming units (CFU) from excised lungs at 1, 2, 3, 4, 6, and 12 weeks of post infection.

Statistical analysis : All the experiments were performed in triplicate. Results were collected as mean and standard deviation (mean \pm SD). Significance in difference was measured with p value as p < 0.05.

Results

The mean bio distribution pharmacokinetic study parameters of F13 rifampicin nanospheres formulation administered through Intravenous (IV) and Inhalation are summarized in the Table 1, Figure 1 & 2. The C_{max}, T_{max} and clearance of F13 through Inhalation route were 42.34 μ g/mL, 14 hr and 0.82(ml/hr) respectively, similarly those of IV route were 20.46 μ g/mL, 14 hr and 3.44 respectively.

In short term study (Table-3), the potency of rifampicin nanospheres at 25 mg/kg body weight was compared with those of rifampicin pure drug.

rifampicin nanospheres slightly more active than pure drug rifampicin. Long-term treatment (Table-3) with rifampicin nanospheres at 25 mg/kg Shown statistically very significant when compared to negative control in the lungs and spleen (p<0.05). The results elucidated that there was a significant decrease in colony forming unit (CFU) of lungs and spleen in all treated groups during both period in contrast to negative control group. After 18 days of treatment, rifampicin nanospheres minimized the bacterial content by 0.54 log₁₀ CFU. The activity of rifampicin nanospheres and rifampicin pure drug in the lungs and spleen was statistically not significant (p = ns) when compared with negative control after 18 days of treatment. After 42 days of treatment, rifampicin nanospheres minimized the bacterial content 4.62 log₁₀ CFU. (9.68 14.30-9.68 log₁₀ CFU). The efficacy of rifampicin nanospheres in the lungs and spleen differs statistically from those of rifampicin pure drug (P > 0.001) after 42 days of treatment. The results are shown in (Table 2&3 and Figure no 3).

Discussion

By comparing the C_{max} results between IV and Inhalation administration of Rifampicin Nanospheres it shows that more concentration of drug was accumulated in the lungs while

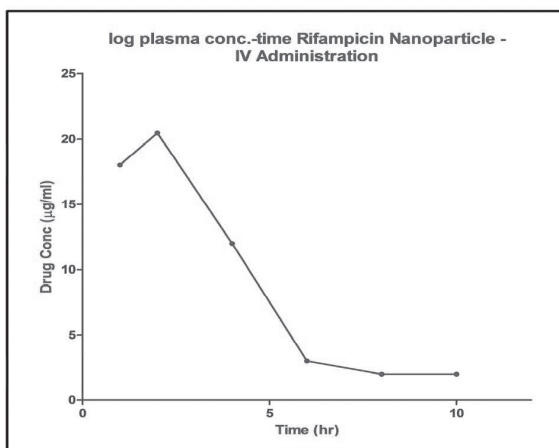


Fig. 1 : XY plot for Rifampicin Nanoparticle –IV administration

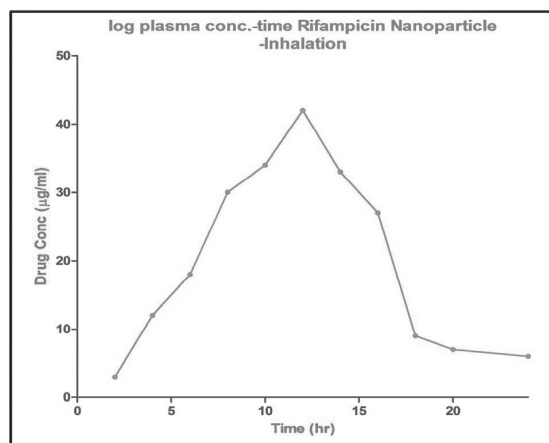


Fig. 2: XY plot for Rifampicin Nanoparticle – Inhalation administration

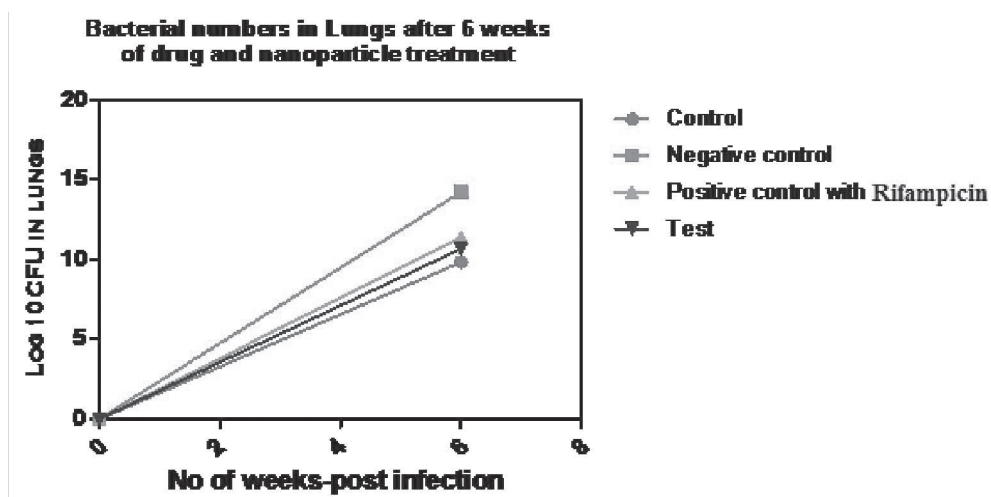


Fig. 3: Determination of Bacterial numbers in lungs after 6 weeks of treatment

Table 1: Bio distribution studies of Rifampicin Nanospheres (F13) – IV & Inhalation administration

Tissue	T+(hr)	C _{max} (µg/ml)	AUC _{0-∞} (µg/ml/hr)	V _d (ml)	Clearance (ml/hr)
IV Administration					
Lungs	1	20.46±1.05	802.3±5.29	244.8±3.95	3.44±0.31
Liver	2	24.98±1.17	1120.16±8.46	184.61±2.10	2.82±0.56
Kidney	3	22.02±0.94	690.39±5.93	218.43±42	3.02±0.14
Inhalation					
Lungs	14	42.34±2.46	1996±8.32	136.33±2.48	0.82±0.04
Liver	20	10.84±1.8	484±4.26	489±5.73	2.84±0.19
Kidney	24	4.32±0.86	118±3.16	756.6±6.38	2.34±0.23

Table 2: Growth of *M.tuberculosis* in culture medium and their control in different conditions

Compound	Concentration	Log ₁₀ CFU±SD (per ml)	% growth of microorganism compared with controls
Only culture	-	11.62±0.22	100
Pure Rifampicin	25 mg/kg	9.40±0.12**	78.40
Rifampicin NP	Equivalent to 25 mg/kg	6.42±0.26***	68.40

Values are expressed as mean ± SD. n=3; Values are statistically significant at p<0.05; Significant-p<0.05;** Very significant -p<0.01;***-p<0.001; ns-non-significant;

Table 3: *M. tuberculosis* number in lungs and spleen of albino rat

Treatment batch	<i>M. tuberculosis</i> number (Log ₁₀ CFU±SD) after different treatment schedules			
	18days		42 days	
	Lungs	Spleen	Lungs	Spleen
Control group	6.40 ± 0.12	2.16 ± 0.12	9.42 ± 0.42	4.12 ± 0.10
Negative control	7.42 ± 0.32 ^{a**}	2.74 ± 0.10 ^{a**}	14.30 ± 0.54 ^{a***}	5.68 ± 0.22 ^{a***}
Positive control with Rifampicin 25 mg/kg	7.40 ± 0.20 ^{b ns}	2.54 ± 0.14 ^{b ns}	10.40 ± 0.30 ^{b***}	3.64 ± 0.24 ^{b***}
Test group with Rifampicin Nanospheres Equivalent to 25 mg/kg	7.82 ± 0.22 ^{b ns}	2.48 ± 0.10 ^{b ns}	9.68 ± 0.22 ^{b***}	2.28 ± 0.22 ^{b***}

Values are expressed as mean ± SD. n=3; Values are statistically significant at p<0.05; Significant-**-p<0.01; Very Significant-***-p<0.001; ns-non-significant; a-Group compared to control; b-Groups compared to negative control;

administering the formulation through Inhalation. From the T_{max} comparison data between IV and Inhalation administration it shows the sustainability time of rifampicin nanospheres in lungs i.e., it confirms the sustained action of rifampicin nanospheres in lungs. By comparing the AUC₀₋₄ from Table 1, it concludes that maximum concentration of drug was present in lungs through inhalation than any other organ. The organ clearance ratio of drug from lungs through inhalation was less than the IV administration, which confirms the sustained release of rifampicin from nanospheres in the lungs. From the above pharmacokinetic distribution data it shows that rifampicin nanospheres shows more accumulation of drug in lungs through inhalation administration than IV, which indicates nanospheres is having targeted and sustained release of drug results in lungs. By this it can be confirmed that inhalable nanospheres are suitable for targeting with negligible toxicity and providing sustained release of anti-tubercular drugs especially rifampicin in lungs. The result showed the rifampicin nanospheres leads to maximum deposition of drug in lungs through inhalation which leads to maintain

high therapeutic concentration by improving good pulmonary tuberculosis chemotherapy.

In vivo mycobacterium screening studies show that on long term therapy rifampicin nanospheres shows better control of growth of microorganism i.e. CFU when compared to short term therapy i.e. for 18 days after administration. After 6 weeks of treatment the bacterial counts in the lungs were reduced to very low numbers in all treatment groups (range, 14.30 to 9.68 log₁₀ CFU Rifampicin Nanospheres Vs untreated controls), as was the case for the spleens (p<0.001). In summary, its good activity *in vivo* models, as well as its activity against multidrug-resistant *MTB* and against *MTB* isolates in a potentially latent state, makes Rifampicin Nanospheres an attractive drug dosage form for the therapy of tuberculosis. These data indicate that there is significant potential for effective inhalational delivery of Rifampicin Nanospheres for the treatment of tuberculosis.

Conclusion

In vivo bio distribution studies show that nanospheres form is the best formulation for Rifampicin, Nanospheres accumulates maximum

dose in the lungs than other organs over prolonged period of time. The plasma levels are more for inhalable PLGA Nanospheres and are suitable for targeting and providing sustained release of anti-tubercular drugs to lungs. So inhalation can be selected as administration route of Rifampicin PLGA Nanospheres. From the *in vivo* screening of *M.tuberculosis*, it shows good activity *in vivo* models, as well as its activity against multidrug-resistant *MTB* and against *MTB* isolates in a potentially latent state, makes Rifampicin PLGA Nanospheres an attractive drug dosage form for the therapy of tuberculosis. These data indicate that there is significant potential for effective intravenous as well as nasal delivery of Nanospheres for the treatment of tuberculosis.

REFERENCES

1. World Health Organization (WHO, 2015). Global Tuberculosis Report 2015.
2. Barry, C. E. (2009). The spectrum of latent tuberculosis: rethinking the biology and intervention strategies. *Nat. Rev. Microbiol.* 7: 845–855.
3. Esmail, H., Barry, C. E., Young, D. B. and Wilkinson, R. J. (2014). The ongoing challenge of latent tuberculosis. *Phil. Trans. R. Soc. B* 369: 387-422.
4. Anderson J.M. and Shive M.S. (1997). Biodegradation and biocompatibility of PLA and PLGA microspheres, *Adv. Drug. Delivery Rev.* 28: 5–24.
5. Dutt M. and Khuller G.K. (2001). Chemotherapy of Mycobacterium tuberculosis infection in mice with a combination of isoniazid entrapped in poly (DL lactide-co-glycolide) microparticle. *J. Antimicrob. Chemother.* 4: 829-835.
6. AitMoussa L., Khassouani C.E., Hue B., Jana M., Begaud B. and Soulaymani R. (2002). Determination of the acetylase phenotype in Moroccan tuberculosis patients using isoniazid as metabolic probe. *Int J Clin Pharm Ther.* 40: 548-53.
7. Maikelohrmann, Michael Kappl., Hans-Juergen Butt., Nora Anne Urbanetz. and Bernhard Christian Lippold. (2007). Adhesion forces in interactive mixtures for dry powder inhalers – Evaluation of a new measuring method. *Eur. J. Pharm. Biopharm.* 67: 579 - 586.
8. SanilbnYakubua., Khaled H. Assi. and Henry Chrystync. (2013). Aerodynamic dose emission characteristics of dry powder inhalers using an Andersen Cascade Impactor with a mixing inlet. *Int. J. Pharm.* 455: 213– 218.
9. Francesco Martinelli., Anna Giulia Balducci., Alessandra Rossi., Fabio Sonvico. and Paolo Colombo. (2015). Pierce and inhale design in capsule based dry powder inhalers: Effect of capsule piercing and motion on aerodynamic performance of drugs. *Int. J. Pharm.* 487:197–204.
10. Yoen-JuSon., Worth Longest P. and Michael Hindle. (2013). Aerosolization characteristics of dry powder inhaler formulations for the excipient enhanced growth (EEG) application: Effect of spray drying process conditions on aerosol performance. *Int. J. Pharm.* 443:137– 145.
11. Sarah Zellnitz., Jakob Dominik RedlingerPohna. and Michael Kapplb. (2003). Characterization and deposition studies of engineered lactose crystals with potential for use as a carrier for aerosolised salbutamol sulfate from dry powder inhalers. *Eur. J. of Pharm. Sci.* 19: 211–221.
12. Cordula Weiss., Peter McLoughlin. And Helen Cathcart. (2015). Characterization of dry powder inhaler formulations using atomic force microscopy. *Int. J. Pharm.* 494: 393 - 407.
13. FlorisGrasmeijer., Paul Hagedoorn., Henderik W Frijlink. And Anne H de Boer. (2012). Characterization of high dose aerosols from dry powder inhalers. *Int. J. Pharm.* 437: 242– 249.

14. Ehab F Elkady. and Marwa A Fouad. (2011). Forced degradation study to develop and validate stability-indicating RP-LC method for the determination of ciclesonide in bulk drug and metered dose Inhalers. *Talanta*, 87: 222– 229.
15. De Boer A.H., Winter H.M.I. and Lerk C.F. (1996) Inhalation characteristics and their effects on in vitro drug delivery from dry powder inhalers Part 1. Inhalation characteristics, work of breathing and volunteers' preference in dependence of the inhaler resistance. *Int. J. Pharm*, 130: 231-244.
16. De Boer A.H., Gjaltema D, Hagedoorn P. (1996). Inhalation characteristics and their effects on in vitro drug delivery from dry powder inhalers Part 2: Effect of peak flow rate (PIFR) and inspiration time on the in vitro drug release from three different types of commercial dry powder inhalers. *Int. J. Pharm*, 138: 45-56.
17. Tan Suwandecha., Wibul Wong poowarak., Kittinan Maliwan. and Teerapol Srichana. (2014). Effect of turbulent kinetic energy on dry powder inhaler performance. *Powder Technology*, 267: 381–391.
18. Nora Y.K Chewa., Hak Kim Chana., David F Bagsterb. and Jay Mukhraiya. (2002). Characterization of pharmaceutical powder inhalers: estimation of energy input for powder dispersion and effect of capsule device configuration. *Aerosol Science*, 33: 999–1008.

System Modeling of AkT using Linear and Robust Regression Analysis

Shruti Jain

Department of Electronics and Communication Engineering, Jaypee University of
Information Technology, Himachal Pradesh.

*For Correspondence - jain.shruti15@gmail.com

Abstract

This paper presents the review of different types of modeling like deterministic and probabilistic. Main stress of this paper is on Probabilistic modeling. Probabilistic modeling is further divided into three types : predictive, regression and correlation modeling. The analysis was done using three different input proteins and four different output proteins. A model was made using different analysis techniques which presents the r^2 values for one of the marker protein called AkT. This paper investigates two linear regression models : *ordinary least square* analysis and *partial least square* analysis. In this paper we are also comparing different robust regression analysis techniques with partial least square method and plotted the residual and predicted values of the different techniques, PLS yields the best result in terms of squared R and plots. For all these calculations we have used Systat 13 software.

Keywords: AkT, Linear Regression Analysis, Robust Regression Analysis, Partial Least Square.

INTRODUCTION

Communication between the response of cells with extracellular signals such as hormones, growth factors, and cytokines is mediated by receptors [1-3]. The magnitudes of the responses vary with cell type, but the pathways downstream of cytokine receptors are conserved and highly interconnected.

In this work our purpose is to study the different modeling techniques. The analysis was

done using three different input proteins (Tumor necrosis factor (TNF) [4-8], Epidermal growth factor (EGF) [9-13], and insulin) [12-20] and four different output proteins (phosphatidylserine exposure (PE), membrane permeability (MP), nuclear fragmentation (NF) and caspase substrate cleavage (CCK)) [1-3]. Analysis was done using different robust regression methods (RRM) and linear regression methods (LRM). RRM is further divided into two least median squares (LMS) and least trimmed squares (LTS) while analysis for LRM is also done by two approaches i.e. ordinary least square (OLS) and partial least square (PLS). All these analysis presents the r^2 values for one of the marker protein called AkT [21-25]. AkT is also known as protein kinase B(PKB). AkT is the main signaling pathway for EGF/ Insulin. AkT activates many different proteins which lead to cell survival/ cell death. AkT leads to cell survival by activating (electronically means 1/ON) NFkB, BAD etc proteins while AkT leads to cell death by deactivating (electronically means 0/OFF) FKHR, caspase proteins. In this paper we work on the response of HT-29 human colon carcinoma cells [26-30] for ten different concentrations of TNF- α , EGF and insulin in ng/ml [31-32]. Later in the paper we have find the correlation matrixes using normalized Euclidean distance, spearman correlation matrix, gamma correlation matrix and Pearson correlation matrix.

MATERIALS AND METHODS

For data analysis we have different approaches. Basically we have two types of input data : categorical (numerical or binary) and continuous data [33-36]. For every analysis we

have to model the system. There are two types of modeling : deterministic modeling and probabilistic modeling. Deterministic modeling has no randomness, it is suitable when predicted error is negligible, and for hypothesize there is exact relationship. Probabilistic modeling is with randomness, hypothesize has 2 components i.e deterministic and random error. Probabilistic modeling is further divided into three different models: predictive, correlation and regression model. Predictive modeling is further divided into different types : logistic, multiple, decision tree, neural network, survival modeling (cox regression) shown in Fig 1.

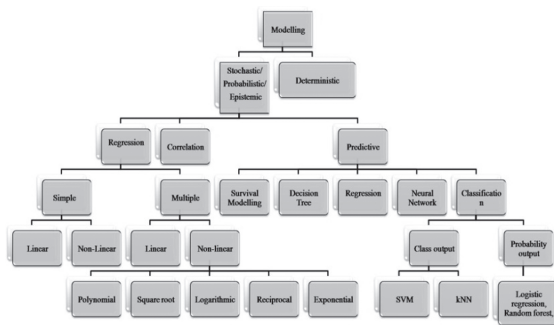


Fig 1: Different types of Modeling

Regression analysis/modeling is divided into four categories :

- *No of independent variables* : one (simple) or more than one (multiple).
- *Type of dependent variable* : categorical or continuous
- *Shape of the regression line* : straight line, polynomial etc.
- *Dimensionality in data* : For high dimensionality we use regression regularization method : lasso, ridge, and elastic net.

Based on above characterization of regression types we will discuss different types of analysis :

Linear regression (LR) : As the name suggests the shape of regression line is linear whose intercept is a and slope of line is b . For LR the dependent variable (y) is continuous while

independent variable (x) can be continuous or discrete. We can consider the error term 'e or \hat{a} '. LR is expressed as:

$$\underbrace{y}_{\text{actual (observed)}} = \underbrace{ax+b}_{\text{explained (predicted)}} + \underbrace{\varepsilon}_{\text{error}} \quad (1)$$

Equation 1 can be represented as :

$$\underbrace{y}_{\text{observed}} = \underbrace{\hat{y}}_{\text{predicted}} + \underbrace{\varepsilon}_{\text{error}} \quad (2)$$

For predicted values equation 1 can be written as :

$$\hat{y} = \hat{a}x + \hat{b} \quad (3)$$

where slope is represented as :

$$\hat{a} = \frac{SS_{xy}}{SS_{xx}} = \frac{\sum (x - \bar{x})(y - \bar{y})}{\sum (x - \bar{x})^2} \quad (4)$$

and intercept is represented by equation 5,

where \bar{x} and \bar{y} are the sample means.

$$\hat{b} = \bar{y} - \hat{a}\bar{x} \quad (5)$$

If the x parameters are more than one i.e. x_1, x_2, \dots than the regression analysis is known as multiple regression (MR) but if the x parameter is one than it is LR. MR equation can be represented as :

$$y = a + b_1x_1 + b_2x_2 + b_3x_3 + \dots + b_nx_n + e \quad (6)$$

Ordinary least square (OLS) method and partial least square analysis (PLS) method is used for calculation of LR while forward selection (FS), backward elimination (BE) and step wise approximation (SWA) is used for MR analysis.

OLS minimizes the SS of the vertical deviations from each data point to the line. OLS is calculated by minimizing the sum of square distance between the sample data and the predicted values. For OLS we have to consider some points:

- Regression coefficient must be linear
- No relation between predictors and residuals

- No correlation between residuals
- All residuals must have a constant variance and normally distributed.
- No correlation between predictors.

PLS method is used when factors/ variables are many and highly collinear or multi-collinear. It is mostly used in the industry for soft modeling. PLS is used for LR using continuous predicted values and MR for categorical predicted values or many other combinations. For PLS, initially the values are squared, then added up so as there is no cancellation of positive and negative terms. Finally, the minimum (least) square value is considered.

We have three different types of sum of squares (SS) :

- a. regression sum of squares (SS_{reg}) which is a measure of explained variation,

$$SS_{reg} = \sum (\hat{y} - \bar{y})^2 \quad (7)$$

- b. residual sum of squares or error sum of squares (SS_{err}) which is a measure of unexplained variation and

$$SS_{err} = SS_{residual} = \sum (y - \hat{y})^2 = \sum \hat{\epsilon}^2 \quad (8)$$

- c. total sum of squares (SS_{total}) which is a measure of total variation.

$$SS_{total} = SS_{reg} + SS_{err} \quad (9)$$

where

$$SS_{total} = \sum (y - \bar{y})^2 \quad (10)$$

The ratio of SS_{reg} to SS_{total} is known as coefficient of determination (r^2) is expressed as :

$$r^2 = \frac{SS_{reg}}{SS_{total}} = \frac{SS_{reg}}{SS_{reg} + SS_{err}} \quad (11)$$

$$r^2 = 1 - \frac{SS_{err}}{SS_{total}} \quad (12)$$

The r^2 lies in the range of 0 and 1, greater the value of r^2 more accurate the model.

The outlier can be identified through scatter plot. For MR, scatter plot method is not working. The outliers in the data are not identified by OLS method. The RR techniques are devised as a remedy to this situation.

Robust Regression (RR) : There are two types of RR methods : LMS, and LTS. For these analyses we will determine squared R, and plot for residuals v/s predicted values.

LMS : From equation 8 we can say that minimizing the SS_{er} or SS_{resi} is equal to minimizing the mean of square residuals. If we divide SS_{res} to the number of observations (n) it will produce average SS_{resi} which helps in rescaling of z-axis without changing maximum value. If we replace sum with median which generate mode RRA instead of mean SS_{resi} .

$$\min SSR = \sum_{i=1}^n (y_i - (ax_i + b))^2 \quad (13)$$

or

$$\min Average SSR = \frac{1}{n} \sum_{i=1}^n (y_i - (ax_i + b))^2 \quad (14)$$

Formally, the Least Median of Squares fit is determined by solving the following optimization problem:

$$\min med SSR = Median \left\{ (y_i - (ax_i + b))^2 \right\} \quad (15)$$

LTS : The standard least squares method, minimizes the SS_{resi} over n points, the LTS method minimize the SS_{resi} over a subset, k , of those n points. The $n-k$ points which are not used will not affect the fit.

Logistic regression (LoR) : For LoR the dependent variable (y) is categorical (0 or 1) and it can be expressed as :

LoR = event occurrence probability (p) / No event occurrence probability ($1-p$) (16)

$$LoR = \frac{p}{1-p} \quad (17)$$

Taking \ln on both sides

$$\ln (LoR) = \ln (p / (1-p)) = \text{logit} (p) \quad (18)$$

LoR is usually used for classification problems.

There is no linear relationship between dependent and independent variable in LoR. Step wise method is maximum used for LoR. LoR uses maximum likelihood estimates because it uses large data size instead of small data size which can be used by OLS. If the dependent variable is ordinal than LoR is known as ordinal LoR but if the dependent variable is multiclass than LoR is known as Multinomial LoR. If the independent variables are not correlated than it is no multi co linearity.

There is *Endogeneity* property in which regression analysis holds. It occurs when the relationship is either circular or backwards (it signifies that if there is any change in dependent variable that will change in the independent variable).

Polynomial Regression (PR) : If the power of independent variable (x) is greater than one then equation 1 is known as PR which is represented as : $y = a + b * x^2$ (19)

Stepwise Regression (SR) : SR uses multiple independent variables. It can handle higher dimension of data set. It is similar to MR which uses FS, BE and SAR techniques for analysis. FS initiates with the significant predictor and then adds variable for each step. BE initiates with all predictors and removes the least significant variable for each step. SAR adds and removes predictors as required.

Ridge Regression (RR) : RR is used when the independent variables are correlated i.e. multi-collinear. In this analysis we have two components : First components is known as loss which is least square term and second is penalty which is lambda of the summation of square of coefficient $\hat{\alpha}^2$. RR solves the multicollinearity problem through shrinkage parameters $\hat{\alpha}$ (lambda).

$$\hat{\alpha} = \arg \min_{\beta \in R^p} \underbrace{\|y - X\beta\|_2^2}_{Loss} + \lambda \underbrace{\|\beta\|_2^2}_{Penalty} \quad (20)$$

Least Absolute Shrinkage and Selection Operator (Lasso) Regression : It is similar to RR, It is capable of reducing the variability and improving the accuracy of LR models.

$$\hat{\alpha} = \arg \min_{\beta \in R^p} \underbrace{\|y - X\beta\|_2^2}_{Loss} + \lambda \underbrace{\|\beta\|_1}_{Penalty} \quad (21)$$

Lasso and RR differs if we use absolute value in $\hat{\alpha}$ term inspite of square. It uses L1 regularization technique. If it is multi-collinear than Lasso uses only one and rest it shrinks others to zero.

ElasticNet Regression (ENR) : EN is hybrid of Lasso and RR techniques. L1 and L2 regularizer is used to train ENR . EN is useful when there are multiple features which are correlated. Lasso is likely to pick one of these at random, while elastic-net is likely to pick both.

$$\hat{\alpha} = \arg \min_{\beta} (\|y - X\beta\|^2 + \lambda_1 \|\beta\|^2 + \lambda_2 \|\beta\|_1) \quad (22)$$

We have two more types of regression analysis which are less used : Bayesian and Ecological Regression

RESULTS AND DISCUSSION

The different research objectives formulated for the present work were described as:

i) The collection of a database: The data was collected from multiple files. In this paper the work has been carried out on images available from Weiss [2]. The data consists of different images of AkT. If the data is numeric or continuous the regression analysis was done but if the data is categorical than chi square test or different data mining techniques was applied.

ii) The pre processing technique was applied which consists of cleaning, transformation etc. In this paper we clean the data by removing outliers from the data or using different plots. Figure 2 shows the predicted vs. residuals plot of LMS and LTS which shows the outlier in the plot while Figure 3 shows the predicted vs. residuals plot of PLS which shows no outlier in the graph. So PLS is the best regression method to use. The multiple R, square multiple R, adjusted square multiple R and standard R for three techniques LMS, LTS and PLS for our one data sets in which TNF, EGF and Insulin is 0 ng/ml shown in Table 1.

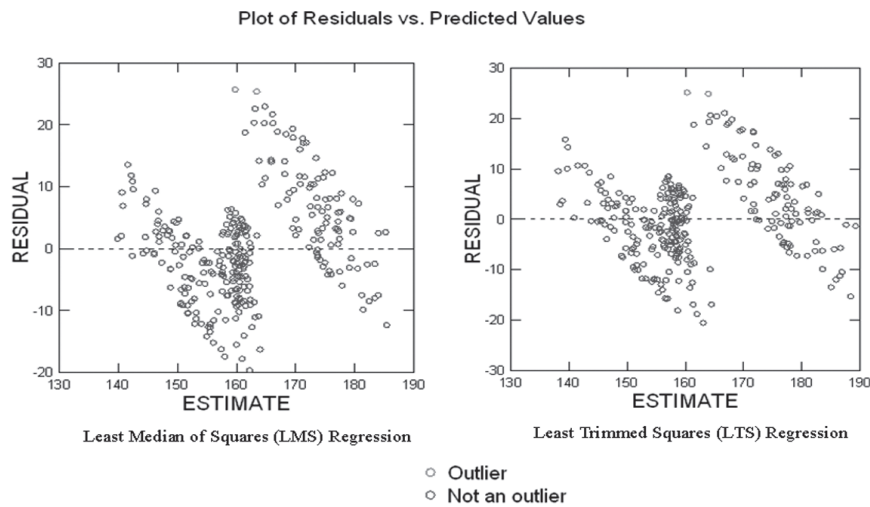


Fig 2: Residuals vs. Predicted Value plots for LMS and LTS Regression

We can also use attributes method which is shown in Fig 4. We have also worked on different plots : box plot (shown in Fig 5), quantile- quantile plot (Q-Qplot) (shown in Fig 6), probability- probability plot (P-P plot) (shown in Fig 7). Normalization and aggregation technique can also be applied so as to clean the data.

(iii) After pre-processing of data, features of the data were selected. There are different methods of selecting the features : direct method (minimum features were selected which are sufficient for modelling), indirect method (PCA, SVD, ICA) and heuristic method (step wise backward elimination, step wise forward selection,). Modelling was done according to the data. If the data is categorical than data mining approach (binning, histogram analysis, clustering, entropy based, equal with and equal frequency) was done and if the data is

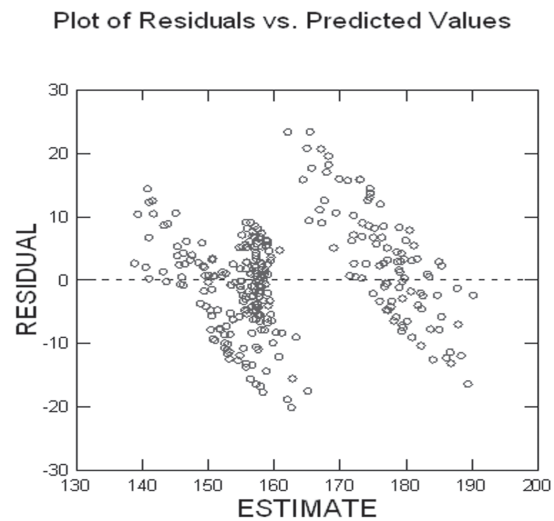


Fig 3 : Residuals vs. Predicted Value plots for PLS Regression

Table 1: Different r^2 values for Outlier Free Data

	LMS Regression	LTS Regression	PLS Regression
Multiple R	0.837	0.844	0.836
Squared Multiple R	0.701	0.712	0.7
Adjusted Squared Multiple R	0.697	0.708	0.695
Standard R	7.905	7.682	7.896

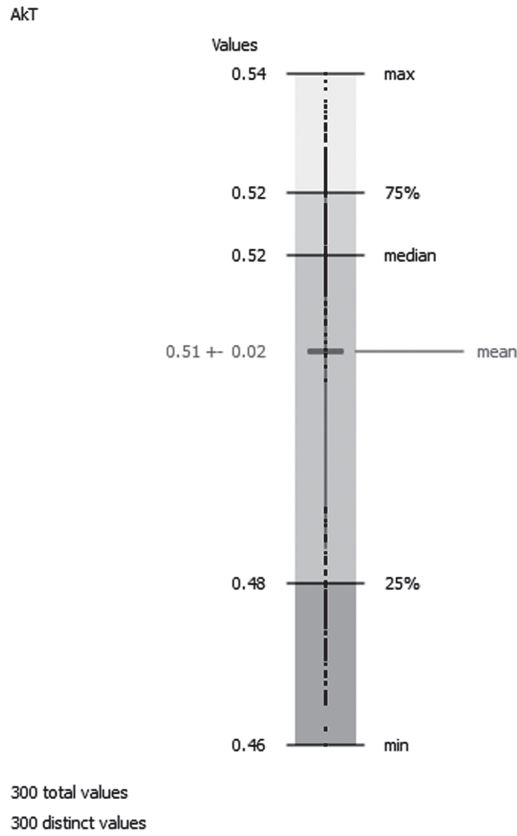


Fig 4 : Attibutes of AkT

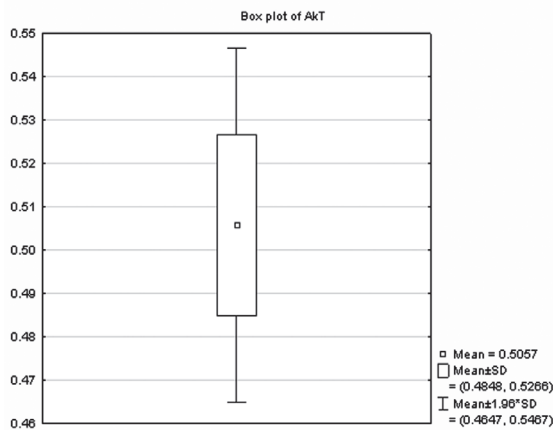


Fig 5 : Box plot of AkT

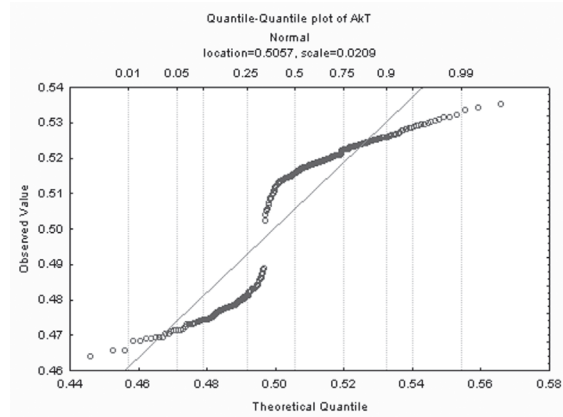


Fig 6: Q-Q plot of AkT

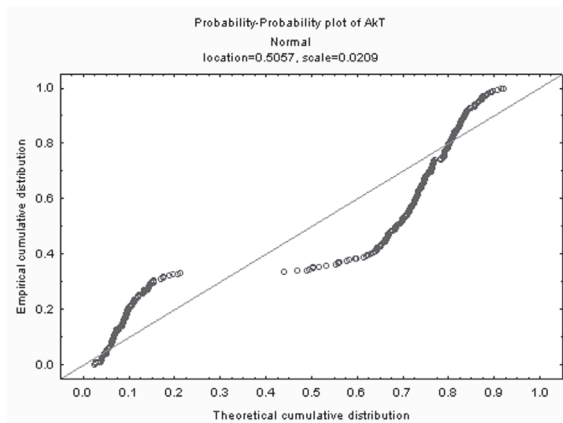


Fig 7 : P-P plot of AkT

continuous than regression analysis (linear, multiple and log linear) was used.

In this paper we have used LMS, LTS and PLS regression analysis to minimize the median and the trimmed mean of the squares residuals respectively. For all these calculations we have used Systat 13 software. In this section we have shown all the results for our one data sets in which TNF, EGF and Insulin is 0 ng/ml. Table 2 shows the different parameters estimates for LMS and LTS regression while Table 3 shows the coefficient, standard error, standard coefficient, tolerance, *t* value and *p* value using PLS technique.

Table 2 : Parameter Estimates using LMS and LTS Regression

	LMS Regression	LTS Regression
CONSTANT	114.123	117.124
PS Exposure	0.75	0.732
Membrane permeability	0.136	0.07
DNA Cleavage	-1.288	-1.447
CCK	0.342	0.512
Scale Estimates	7.846	7.206
Robust R- square	0.78	0.766

Table 3: Parameter Estimates using Partial Linear Square Regression

Effect	Coefficient	Standard Error	Std. Coefficient	Tolerance	t	p- Value
CONSTANT	112.158	11.738	0	.	9.555	0
PS Exposure	0.977	0.083	3.453	0.012	11.733	0
Membrane permeability	0.122	0.078	0.193	0.067	1.569	0.118
DNA Cleavage	-1.325	0.075	-4.408	0.017	-17.751	0
CCK	0.238	0.088	1.118	0.006	2.69	0.008

(iv) Classification can be done by different methods [35-38] which results in Confusion Matrix, Gain and Lift Chart : used for campaign targeting problems, Kolmogorov Smirnov Chart : measures performance of classification models, AUC – ROC : Receiver operating characteristic curve, Gini Coefficient : class problem = $(2 \times \text{AUC} - 1)$. Its value should be above 60% than model is known as good, Concordant – Discordant Ratio : classification problem, Root Mean Squared Error and Cross Validation.

Differences between observations those were not explained by the model will be treated as error term. If the r^2 value is 0.7 it signifies that 70% of the variance of observed value of the dependent variable explain by the model and rest 30% remains unexplained. The p -value explains the emerging of independent variables their own which are not helpful in describing a real value. A p -value of 0.05 means that there is a 5% chance of relationship generated randomly and a 95% chance relationship is real.

We have also found the different correlation matrix which shows how the independent variables are related to one another. The coefficient of output variable explains how much increase of one in its value will affect the independent variable keeping all other dependent variable constant. Table 4, table 5, table 6 and table 7 shows the normalized Euclidean distance, spearman correlation matrix, gamma correlation matrix and Pearson correlation matrix respectively.

CONCLUSION

This paper explains the different regression analysis which was applied on AkT protein. For this analysis we have considered three different input proteins and four output. In this paper we have done analysis for Ong/ml concentration of TNF, EGF and insulin. We have used different plots to remove outliers as preprocessing. Out of different regression techniques, PLS gives the best results. At the end different correlation matrixes were shown for different types like spearman, gamma, Pearson etc. Later in future author will try for other concentrations of input proteins.

Table 4 : Normalized Euclidean Distances

	DATA	PSEXP	MEM	DNA	CCK
DATA	0				
PSEXP	79.205	0			
MEM	36.61	98.173	0		
DNA	96.446	22.829	117.482	0	
CCK	67.338	44.925	69.555	65.38	0

Table 5 : Spearman Correlation Matrix

	DATA	PSEXP	MEM	DNA	CCK
DATA	1				
PSEXP	0.459	1			
MEM	0.383	0.839	1		
DNA	0.476	0.889	0.845	1	
CCK	0.475	0.899	0.852	0.887	1

Table 6 : Gamma Correlation Matrix

	DATA	PSEXP	MEM	DNA	CCK
DATA	1				
PSEXP	0.23	1			
MEM	0.206	0.62	1		
DNA	0.263	0.669	0.629	1	
CCK	0.255	0.69	0.639	0.668	1

Table 7 : Pearson Correlation Matrix

	DATA	PSEXP	MEM	DNA	CCK
DATA	1				
PSEXP	0.419	1			
MEM	0.377	0.963	1		
DNA	0.279	0.983	0.958	1	
CCK	0.366	0.994	0.965	0.991	1

REFERENCES :

- [1] S Jain. 2012, Communication of signals and responses leading to cell survival / cell death using Engineered Regulatory Networks. PhD Dissertation, Jaypee University of Information Technology, Solan, Himachal Pradesh, India.
- [2] R Weiss. 2001, Cellular computation and communications using engineered genetic regulatory networks. PhD Dissertation, MIT.
- [3] S Gaudet, JA Kevin, AG John, PA Emily, LA Douglas, and SK Peter. A compendium of signals and responses triggered by prodeath and prosurvival cytokines. Manuscript M500158-MCP200, 2005.
- [4] B Thoma, M Grell, K Pfizenmaier and P Scheurich. Identification of a 60-kD tumor necrosis factor (TNF) receptor as the major

- signal transducing component in TNF responses. *J Exp Med*. 1990; 172, 1019-23.
- [5] S Jain, PK Naik and SV Bhooshan. Mathematical modeling deciphering balance between cell survival and cell death using Tumor Necrosis Factor α . *Research Journal of Pharmaceutical, Biological and Chemical Sciences*. 2011 ; 2(3): 574-83.
- [6] S Jain, PK Naik, R Sharma, A Computational Modeling of cell survival/ death using VHDL and MATLAB Simulator, *Digest Journal of Nanomaterials and Biostructures*. 2009: 4 (4): 863- 79.
- [7] S Jain, PK Naik, R Sharma, A Computational Modeling of Apoptosis Signaling using VHDL and MATLAB Simulator, *International Journal of Information and Communication Technology*. 2009 2(1-2): 7-12.
- [8] S Jain, PK Naik and SV Bhooshan. A System Model for Cell Death/ Survival using SPICE and Ladder Logic. *Digest Journal of Nanomaterials and Biostructures*. 2010; 5(1), 57-66.
- [9] JA Kevin, AG John, G Suzanne, SK Peter, LA Douglas, YB Michael. A systems model of signaling identifies a molecular basis set for cytokine-induced apoptosis. *Science*. 2005; 310, 1646-53.
- [10] N Normanno, A De Luca, C Bianco, L Strizzi, M Mancino, MR Maiello, A Carotenuto, G De Feo, F Caponigro and DS Salomon. Epidermal growth factor receptor (EGFR) signaling. *Cancer Gene*. 2006; 366, 2–16.
- [11] S Jain, Implementation of Marker Proteins Using Standardised Effect, *Journal of Global Pharma Technology*. 2017: 9(5), 22-27.
- [12] S Jain, Compedium model using frequency / cumulative distribution function for receptors of survival proteins: Epidermal growth factor and insulin, *Network Biology*. 2016: 6(4), 101-110.
- [13] S Jain and DS Chauhan. Mathematical Analysis of Receptors For Survival Proteins. *International Journal of Pharma and Bio Sciences*. 2015; 6(3), 164-176.
- [14] S Jain, PK Naik and SV Bhooshan. Mathematical modeling deciphering balance between cell survival and cell death using insulin. *Network Biology*. 2011; 1(1):46-58.
- [15] S Jain, PK Naik, System Modeling of cell survival and cell death : A deterministic model using Fuzzy System, *International Journal of Pharma and BioSciences*. 2012: 3(4), 358-73.
- [16] S Jain, PK Naik, Communication of signals and responses leading to cell death using Engineered Regulatory Networks, *Research Journal of Pharmaceutical, Biological and Chemical Sciences* . July – Sep 2012 : 3(3), 492-508 JM Lizcano and DR Alessi. The insulin signalling pathway. *Curr Biol*. 2002; 12, 236-38.
- [17] MF White. Insulin Signaling in Health and Disease. *Science*. 2003; 302, 1710–11.
- [18] S Jain , Regression Modeling of Different Proteins using Linear and Multiple Analysis, *Network Biology*. 2017: 7 (4). 80-93.
- [19] S Jain, PK Naik, Computational Modeling of Cell Survival using VHDL, *BVICAM's International Journal of Information Technology (BIJIT)*. 2010: 2 (1): 47-51.
- [20] S Jain, PK Naik and SV Bhooshan, Computational Modeling of Cell Survival/ Death Using BiCMOS, *International Journal of Computer Theory and Engineering*. 2010: 2 (4). 478-81.
- [21] P.J. Coffey, J. Jin, and J. R. Woodgett, Protein kinase B (c-Akt): a multifunctional mediator of phosphatidylinositol 3-kinase activation. *Biochem. J*. 335 (1998):1-13.
- [22] B.A. Hemmings, Akt signaling: linking membrane events to life and death decisions. *Science*. 275(1997), 628–630.
- [23] A. Brunet, A. Bonni, M. J. Zigmund, M. Z. Lin, P. Juo, L. S. Hu, Akt promotes cell

- survival by phosphorylating and inhibiting a Forkhead transcription factor. *Cell*, 96 (1999), 857–868.
- [24] S Jain, Parametric and Non Parametric Distribution Analysis of AkT for Cell Survival/Death, *International Journal of Artificial Intelligence and Soft Computing*. 2017 : 6(1), 43- 55
- [25] S Jain and DS Chauhan. Linear and Non Linear Modeling of Protein Kinase B/ AkT. *In: Proceeding of the International Conference on Information and Communication Technology for Sustainable Development, Ahmedabad, India. 2015, p.81-88.*
- [26] S Jain, PK Naik and SV Bhooshan. Petri net Implementation of Cell Signaling for Cell Death. *International Journal of Pharma and Bio Sciences*. 2010; 1(2) , 1-18.
- [27] S Jain, PK Naik, SV Bhooshan, Model of Protein Kinase B for Cell Survival/Death and its Equivalent Bio Circuit , *In: Proceedings of the 2nd International Conference on Methods and Models in Science and Technology (ICM2ST-11), Jaipur, Rajasthan, India Organized by Institution of Engineers, Technocrats and Academician Network (IETAN). November 19-20, 2011, pp 69-73.*
- [28] S Jain, Regression analysis on different mitogenic pathways, *Network Biology*. June 2016: 6(2), 40-46 .
- [29] S Jain, *Mathematical Analysis using Frequency and Cumulative Distribution functions for Mitogenic Pathway, Research Journal of Pharmaceutical, Biological and Chemical Sciences*. May - Jun 2016 : 7(3), 262-72.
- [30] S Jain. Mathematical Analysis and Probability Density Function of FKHR pathway for Cell Survival /Death. *In: Proceedings of the Control System and Power Electronics – CSPE, Bangalore. 2015. p 84-93.*
- [31] S Jain, SV Bhooshan, PK Naik, Model of Mitogen Activated Protein Kinases for Cell Survival/Death and its Equivalent Bio-Circuit, *Current Research Journal of Biological Sciences*. 2010: 2(1): 59-71.
- [32] S Jain, PK Naik and SV Bhooshan. Nonlinear Modeling of cell survival/ death using artificial neural network. 2011. *In: The Proceedings of International Conference on Computational Intelligence and Communication Networks, Gwalior, India. 2011; p 565-68.*
- [33] S Bhusri, S Jain and J Virmani. Breast Lesions Classification using the Amalgamation of morphological and texture features. *International Journal of Pharma and BioSciences*. 2016; 7(2), 617-24.
- [34] S Bhusri, S Jain, J Virmani. Classification of breast lesions using the difference of statistical features. *Research Journal of Pharmaceutical , Biological and Chemical Sciences*. 2016; 7 (4), 1365-72.
- [35] S Rana, S Jain and J Virmani. SVM-Based Characterization of Focal Kidney Lesions from B-Mode Ultrasound Images. *Research Journal of Pharmaceutical, Biological and Chemical Sciences*. 2016; 7(4), 837- 46.
- [36] Amandeep, S Jain, S Bhusri, CAD System for Non Small Cell Lung Carcinoma using Laws' Mask Analysis, *In – Proc of the 11th INDIACom: 4th 2017 International Conference on Computing for Sustainable Global Development, BVICAM, New Delhi, March 1st - 3rd , 2017, pp 6285-6288.*
- [37] S Rana, S Jain , J Virmani, Classification of Kidney Lesions using Gabor Wavelet Texture Features. *In: Proc of the 10th INDIACom 3rd 2016 International Conference on Computing for Sustainable Global Development. p 2528-2532.*
- [38] S Rana, S Jain , J Virmani, Classification of Focal Kidney lesions using Wavelet-Based Texture Descriptors, *International Journal of Pharma and Bio Sciences*, 7(3) B, 646-652, July-Sep 2016.

Molecular Taxonomy of Associated Microbes From Sea Slug *Kalinga Ornata* and its bioactivity

M. Mohanraj¹, N. Sri Kumaran^{1,2,*} and S. Bragadeeeswaran¹

¹Faculty of Marine Science, Centre of Advanced Study in Marine Biology, Annamalai University, Parangipettai – 608 502, Tamil Nadu, India

²Department of Marine Biotechnology, AMET University, Kanathur, Chennai 603112, Tamil Nadu, India

* For Correspondence - s.kumaran08@gmail.com

Abstract

This study was carried to investigate the molecular taxonomy of associated microbes from sea slug *Kalinga ornata* and its bioactivity from Indian coastal waters. In this study, totally 27 associated microbes isolated from sea slug *K. ornata*. Morphologically 5 different isolates were selected for sequencing and submitted to NCBI. Further these 5 sequences were analysed for the phylogenetic relationship and percentage of the nucleotide contents with few isolates sequences extracted via FASTA format from NCBI. The sequenced isolate was assigned to *Psychrobacter celer*, *Bacillus flexus*, *Acinetobacter radioresistens*. The isolated associated bacteria displayed hopeful antimicrobial properties. These results depict that not only the sea slug exhibits biologically active metabolites but also its associated microbes show potent antimicrobial activity against tested pathogens. The haemolytic activities of associated microbes were tested against chicken, goat and cow erythrocytes. The result proved that the sea slug associated microbes are rich in producing the metabolites and it possesses cytotoxic activity. The current study shows that bacterial isolates from *K. ornata* possess bioactive properties. All the tested isolates were potential inhibition against human bacterial pathogens. Thus, this investigation highlights the importance of bacteria associated with the *K. ornata* as a valuable resource for the discovery of novel bioactive molecules.

Keywords: sea slug, molecular taxonomy, sequencing, antagonistic, haemolytic

Introduction

The Ocean is great diversity source of structurally unique natural products that are mainly accumulated in living organisms. Several of these compounds show pharmacological activities and are helpful for the invention and discovery of bioactive compound, primarily for deadly diseases like cancer, acquire immuno deficiency syndrome, etc. Recently isolation of natural product from marine organisms increases rapidly, and now exceeds with few hundreds of new compounds being discovered every year (Faulkner, 2002; Proksch and Muller, 2006).

Antibiotics are defined as chemical substances fashioned by microorganisms and they have a major impact on the development of medical science. Microorganisms not only cause infection but also produce organic compounds that can treat a variety of infectious disease (Chellaram and Edward, 2009). Marine microorganisms are of considerable current interest as a new and promising source of biologically active compounds. They produce a variety of metabolites, some of which can be used for drug development (Grossart *et al.*, 2004 and Chellaram and Premanand, 2010).

In many cases, microorganisms are known or suspected to be the biosynthetic source of

marine invertebrate natural products (Haygood *et al.*, 1999; Kelecom, 2002). The successfully screened antimicrobial compounds by marine bacteria usually assayed under straight forward growth conditions. However, as the primary role of antimicrobial activity can be to antagonise competitors, bacteria may also produce antimicrobial compounds when they sense the presence of competing organisms (Patterson and Bolis, 1997).

Many marine animals are protected by arsenals of defensive compounds, which have been exploited in the discovery of pharmaceuticals (Putz and Proksch, 2010). These chemicals can be divided into two groups: proteins and peptides (large molecules) and secondary metabolites (small molecules). Small molecules are highly diverse in terms of their chemical structures, and they are more commonly associated with soft-bodied, "defenceless" animals, such as ascidians, sponges, and nudibranch molluscs (Blunt *et al.*, 2011).

Many invertebrate animals, like sponges, tunicates, bryozoans, molluscs and oligochaetes are symbiotically associated with microorganisms belonging to the Bacteria and Archaea domains. In some cases, the source of the cytotoxic compounds isolated from marine invertebrates are the symbiotic bacteria. For instance, the tunicate *Lissoclinum patella* is symbiotically associated with the cyanobacteria *Prochloron* sp., which produces the cytotoxic compounds patellamides A and C, each with clinical potential. Davidson *et al.* (2001) observed that bryozoan *Bugula neritina* and its symbiont "*Candidatus endobugula sertula*" is the source of bryostatins, which show excellent potential as therapeutic agents against leukemias, lymphomas, melanomas and solid tumors. Molluscs lacking shells are sometimes defended instead by secondary metabolites (Benkendorff, 2010). Often, the molecules seem to have a dietary origin (Gavagnin *et al.*, 1994; Fontana, 2006). Therefore, attention is being focused on the investigation of the efficacy of marine molluscs based drugs. Since the conventional drugs used to ameliorate this phenomenon are either too

expensive or toxic and not commonly available to the rural folks that constitute the major populace of the world, this study seeks to assess the importance of bacteria associated with the *K. ornata* as a valuable resource for the discovery of novel bioactive molecules.

Materials and Methods

Isolation of bacteria associated with marine sea slug : The Sea slugs *K. ornata* were collected from Mudasalodai landing centre, East Coast of India. The sea slug samples soon after collection were transferred to a sterile polyethylene bag and transported at 4°C to the laboratory for the isolation of associated microbes on reaching the laboratory, the invertebrate was brought to room temperature and cut aseptically into small pieces (2 × 2 cm) using a sterile scissors. The pieces were freed from adhering particles by vortexing twice for 20 sec with 2mL of sterile sea water. The sterile sea water was decanted which were once again replaced with sterile sea water with continued vortexing between washing finally, sample in sterile sea water was homogenized using sterile mortar and pestle in a laminar flow chamber. The homogenate was serially diluted up to 10⁻⁶ dilution and then spread plated on Zobell marine agar plates. The plates were incubated at room temperature for 24-48 hrs. The colonies were selected on the basis of morphology and the pure cultures are maintained in the same medium in slants at 4°C for further study.

Cultivation of bacteria isolate for screening :

The isolated bacteria were sub cultured on nutrient agar plates and incubated at 28±2°C for two days. A loop full of bacterial culture was transferred into nutrient broth and incubated on a shaker at 30°C for 48 hrs. At the end of the incubation period, broth cultures were used for screening. In all the media preparation 50 % sterilized seawater and 50 % of distilled water was used for media preparation.

Identification of bacteria by 16S rRNA partial sequencing :

The genomic DNA was extracted from the marine sea slug associated potent strains was PCR amplified for 16S rRNA genes using the

universal bacterial primers, 27F (5'-AGAGTTTGA TCG TGG CTC AG-3') and 1492R (5' GGT TAC CTT GTTACG ACT T-3'). This primer combination amplified a 1500 bp 16S rRNA fragment amplification reaction was performed in a 0.2 mL optical grade PCR tube. 50 nanogram of DNA extract was added to a final volume of 50 µL of PCR reaction mixture containing 1.5 mM MgCl₂, 1X Reaction buffer (without MgCl₂) (Fermentas), 200 µM of each dNTP'S (Fermentas), 100 M of each primer and 1.25 U Taq DNA polymerase (fermentas). PCR was performed in an automated thermal cycler with an initial denaturation at 95°C for 5 min, followed by 30 cycles of 95°C for 30 sec. (denaturation), 52°C for 45 sec. (annealing), 72°C for 10 min (final extension). PCR product was run on 1% agarose in TAE buffer (40 mM Tris; 20 mM acetic acid, 1 mM EDTA (pH 8.0) to confirm the right product (1500bp). The PCR product was purified using the QIAGEN PCR amplification kit for sequencing and for further analysis. The partial 16S rRNA gene sequencing was done using Perkin Elmer applied biosystems and ABI Primes software was used to align the sequence and compared sequences were retrieved by the queries generated by BLAST of genbank database. Phylogenetic analysis was performed with the MEGA 4.0 program (Molecular evolutionary genetic analysis, (version 4.0) (Tamura *et al.*, 2007). The tree topologies were evaluated by bootstrap analyses based on 1000 replicates and phylogenetic trees were inferred using the neighbour joining method and submitted to NCBI genbank.

Screening for antimicrobial activity

Antagonistic assay for bacteria against bacterial pathogens : Antagonistic assay was done by agar well diffusion method in aerobic condition. Isolated bacterial specimens were tested for antibacterial activity. Bacterial pathogens such as *Escherichia coli*, *Klebsiella oxytoca*, *Klebsiella pneumonia*, *Proteus mirabilis*, *Salmonella typhi*, *Salmonella paratyphi*, *Staphylococcus aureus*, *Vibrio cholerae* and *V. parahaemolyticus* were obtained from the Rajah Muthiah Medical College, Annamalai University,

Annamalai Nagar, Tamil Nadu, India. The pathogens were spreaded on Muller Hinton agar plates. Then wells were made and 50µL of culture of each strain were inoculated into a separate well. Antagonistic activity was detected after an incubation of 24-48 hrs at 38°C. The zone of clearance on agar plates were used as an indicator for the antibacterial activity. The strain which showed the maximum zone of clearance was chosen for further study. The presence of zone of clearance on agar plates was used as an indicator of bioactive potential of the strain (Portrait *et al.*, 1999)

Hemolytic assay on blood agar plate : The hemolytic activity was assayed using blood agar plates by following the method of Lemes-Marques and Yano (2004). Chicken, cow and goat blood agar plates were prepared by adding 5 mL of blood and 95 mL of sterile blood agar aseptically poured immediately on to the Petri dishes. After solidification, wells were cut into the agar plate using a corkscrew borer (8 mm diameter). Wells were loaded with 50 iL (1 mg/mL) of samples. The plates were observed for hemolysis after overnight incubation at room temperature.

Results

A total of twenty seven strains were isolated from sea slug of *K. ornata*, the Specimens are investigated phenotypically. Five isolates were selected to characterize phylogenetically. Comparative 16S rRNA gene sequence analysis affiliated the isolates to diverse phylogenetic groups. The 16S rRNA gene sequencing data were confirmed by the phenotypic characterization. It was found that most bacteria could be assigned to *Psychrobacter celer*. The 16S rRNA gene sequence of marine bacteria NAM1- KF577981.1; NAM2- KF577982.1; NAM4- KF577983.1; NAM5- KF577984.1 and NAM6- KF577985.1 was deposited in NCBI database from the sea slug associated bacteria. The phylogenetic analysis of *Psychrobacter celer* NAM1 (KF577981.1) sequences shows 100% maximum identity with *Psychrobacter celer* strain PHCDB19 (Fig 1). The *Bacillus flexus* NAM2 (KF577982.1) sequences shows 99% maximum identity with *Bacillus flexus*

strain PHCDB20 (Fig 2). The *Psychrobacter celer* NAM4 (KF577983.1) sequences shows 55% maximum identity with *Psychrobacter* sp. (Fig 3). The *Acinetobacter radioresistens* NAM5 (KF577984.1) sequences shows 64% maximum identity with *Acinetobacter* sp1070 (Fig 4). The *Psychrobacter celer* NAM6 (KF577985.1) sequences shows 73% maximum identity with some *Psychrobacter* sp. (Fig 5). The GC and AT content was showed in NAM1 G+C content = 53.56%, A+T content = 46.44%. Table 1. Express nucleotide contents in sea slug associated bacteria. The nucleotide A, C, G and T content were showed 25.30%, 23.02%, 30.53% and 21.15% respectively. In NAM2, G+C content = 53.75% and A+T content = 46.25%. The nucleotide A, C, G and T content were showed 25.25%, 22.22%, 30.93% and 20.99% respectively. In NAM4, G+C content = 52.85%, A+T content = 47.15%. The nucleotide A, C, G and T content were showed 26.07%, 21.69%, 31.16% and 21.08% respectively. In NAM5, G+C content = 52.71% and A+T content = 47.29%. The nucleotide A, C, G and T content were showed

26.25%, 21.64%, 31.06% and 21.04% respectively. In NAM6, G+C content = 52.43%, A+T content = 47.57%. The nucleotide A, C, G and T content were showed 25.96%, 21.70%, 30.73% and 21.60% respectively.

In the present study, the isolated *K. ornata* associated bacteria displayed hopeful antimicrobial properties. These results depict that not only the sea slug exhibits biologically active metabolites but also its associated microbes show potent antimicrobial activity (Plate 1.). Fig. 6. shows antagonistic assay of sea slug associated bacteria against bacterial pathogens. The results of the antibacterial assay reveal that the NAM1 extracts showed maximum susceptibility against *K. pneumoniae* (9.37±0.13 mm), *K. oxytoca* (8.57±0.11 mm) and *V. cholerae* (8.15±0.15 mm) whereas minimum inhibition zone were observed in *S. paratyphi* (5.5±0.23 mm), *S. aureus* (5.53±0.36 mm) and *P. mirabilis* (1.03±0.01). The extracts of NAM 2 exhibited a high zone of inhibition against *K. pneumoniae* (8.49±0.16 mm) *K. oxytoca* (7.51±0.24 mm) *S. aureus* (7.38±0.23

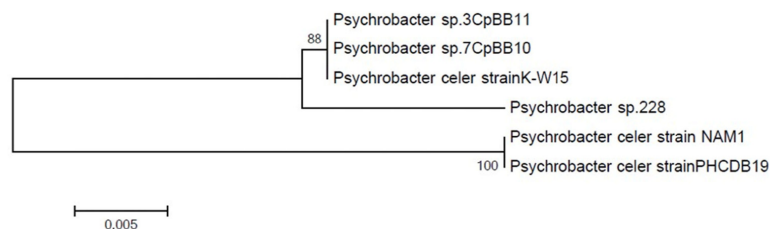


Fig. 1. Phylogenetic tree of *Psychrobacter celer* NAM1

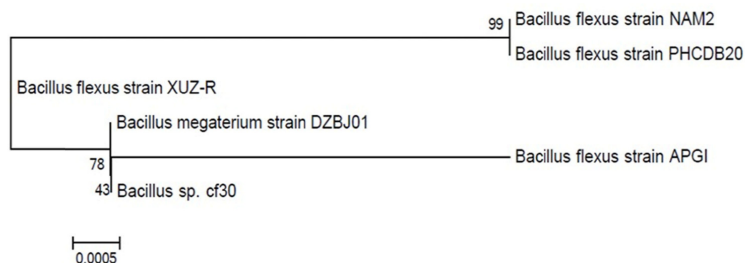


Fig. 2. Phylogenetic tree of *Bacillus flexus* (NAM2)

mm) nevertheless minimum values of susceptibility were recorded in *E. coli* (4.3 ± 0.22 mm), *V. parahaemolyticus* (3.39 ± 0.27 mm), *S. typhi* (3.34 ± 0.20 mm). NAM 3 extracts showed strong antimicrobial activity against *K. pneumoniae* (10.3 ± 0.22 mm) *S. typhi* (8.26 ± 0.17 mm) and *K. oxytoca* (8.19 ± 0.22 mm) but displayed least amount of activity in *V. parahaemolyticus* (5.22 ± 0.21 mm) *S. pyogenes* (5.15 ± 0.13 mm) and *P. mirabilis* (3.55 ± 0.29 mm). NAM4 extracts demonstrated a high inhibition range of 7.49 ± 0.41

mm (*Escherichia coli*), 6.66 ± 0.50 mm (*S. paratyphi*) and 6.46 ± 0.30 mm (*S. pyogenes*) whereas the least inhibitions zones of 3.65 ± 0.26 mm (*K. pneumoniae*), 3.34 ± 0.43 mm (*P. mirabilis*) and 4.33 ± 0.27 mm (*K. oxytoca*). In the present study, the NAM 5 extract evidenced higher inhibition zone against *V. parahaemolyticus* (8.47 ± 0.18 mm), *V. cholera* (8.22 ± 0.08 mm) and *S. pyogenes* (5.52 ± 0.35 mm). While low level of antibacterial activity was observed in *S. aureus* (4.58 ± 0.18 mm), *S. typhi* (4.47 ± 0.33 mm) and *P. mirabilis* (2.48 ± 0.24 mm).

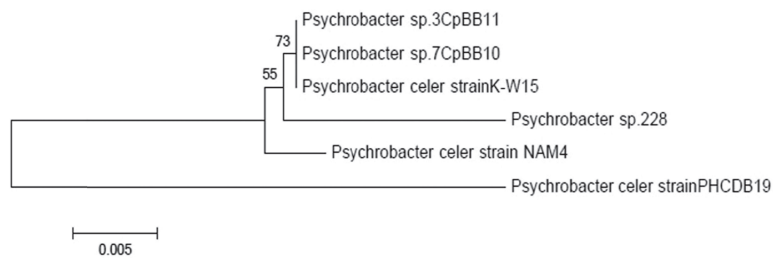


Fig. 3. Phylogenetic tree of *Psychrobacter celer* (NAM4)

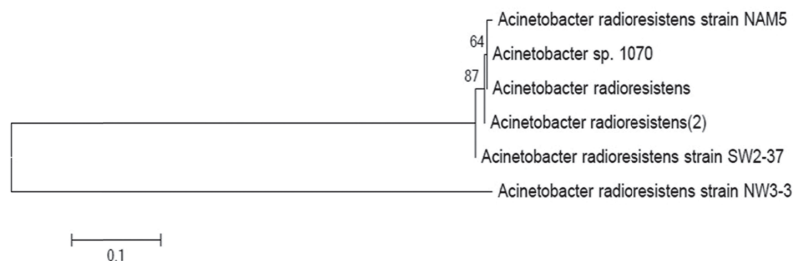


Fig. 4. Phylogenetic tree of *Acinetobacter radioresistens* (NAM5)

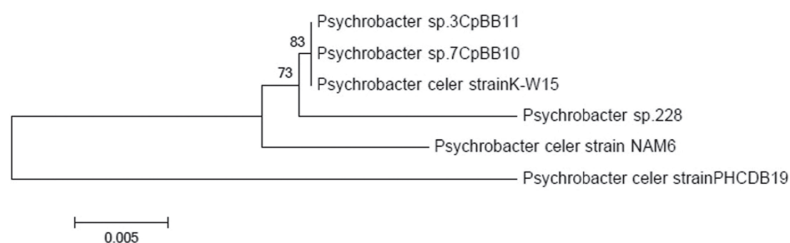


Fig. 5. Phylogenetic tree of *Psychrobacter celer* (NAM6)

In the present investigation, the haemolytic activity of associated microbes in sea slug *K. ornata* were tested against chicken, goat and cow. The result proved that the sea slug associated microbes are rich in producing the metabolites and it possess cytotoxic activity (Fig 7). In this assay five microbes were tested against blood agar diffusion method. In the present study chicken blood agar assay NAM1 associated bacteria showed maximum susceptibility of 4.07 ± 0.19 mm and followed by NAM6 4.07 ± 0.06 . The minimum susceptibility were recorded in NAM5 3.32 ± 0.28 . In the case of goat blood agar assay, NAM2 associated bacteria showed

maximum inhibition of 4.58 ± 0.23 mm and minimum were recorded in NAM5 2.62 ± 0.20 mm. In cow blood agar assay, the maximum susceptibility were observed in NAM4 5.37 ± 0.21 mm and the minimum were recorded in NAM5 3.46 ± 0.25 mm.

DISCUSSION

Marine organisms have been found to produce a great diversity of novel bioactive secondary metabolites and be potential source for new drug discovery. Biological activities which have been frequently observed in marine invertebrates and micro-organisms include

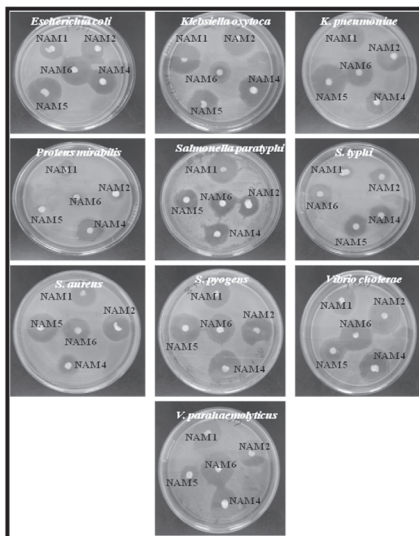


Plate 1. Antagonistic assay of sea slug associated bacteria against bacterial pathogens

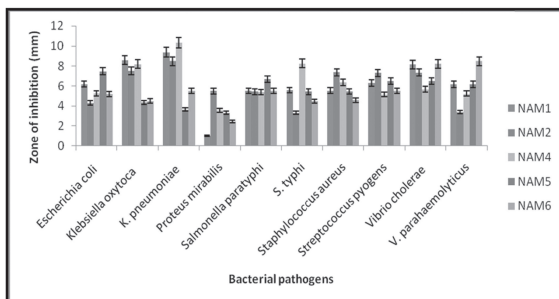


Fig. 6. Antagonistic assay of sea slug associated bacteria against bacterial pathogens

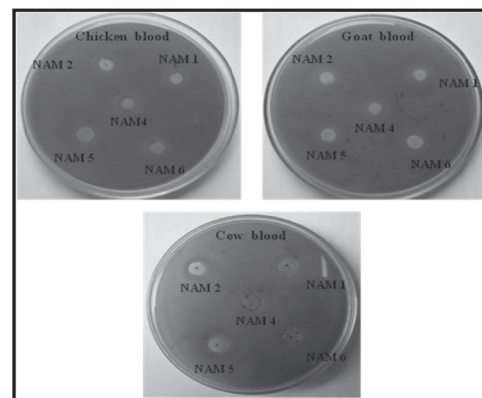


Plate 2. Hemolytic assay of sea slug associated bacteria on blood agar plate

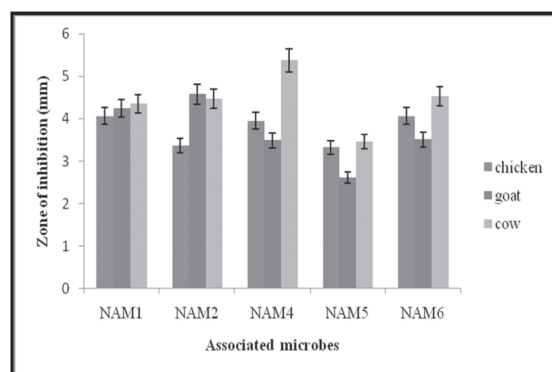


Fig. 7. Hemolytic assay of sea slug associated bacteria on blood agar plate

Table 1. Nucleotide contents in sea slug associated bacteria

	A (%)	T (%)	G (%)	C (%)	A-T (%)	G-C (%)
NAM1	25.30	21.15	30.53	23.02	46.44	53.56
NAM2	25.25	20.99	30.93	22.22	46.25	53.75
NAM4	26.07	21.08	31.16	21.69	47.15	52.85
NAM5	26.25	21.04	31.06	21.64	47.29	52.71
NAM6	25.96	21.70	30.73	21.60	47.57	52.43

antibiosis agent against bacterial pathogen. The fact that many marine invertebrate secondary metabolites have presented antibiotic and cytotoxic activities is not only a consequence of their intrinsic activity but also because research towards the search for new drugs has focused mainly on these bio assays (Newmen *et al.*, 2003).

It has been estimated that over 99% of the marine mollusc associated microbes have yet to be cultured in the laboratory with bacteria isolated from the mollusc containing diverse *Bacillus* species being one of the most divergent forms (Kennedy *et al.*, 2009). Dopazo *et al.* (1988) reported the coral associated isolates were tested for antagonistic effect by double agar overlay method.

A total of twenty seven strains were isolated from sea slug of *K. ornata*, the specimens are investigated phenotypically. Five isolates were selected to characterize phylogenetically. Comparative 16S rRNA gene sequence analysis affiliated the isolates to diverse phylogenetic groups. The 16S rRNA gene sequencing data were confirmed by the phenotypic characterization. It was found that most bacteria could be assigned to *Psychrobacter celer*.

Screening has resulted in five strains with inhibitory activities, mainly on NAM1 against *K. pneumoniae* (9.37±0.13 mm) next to *K. oxytoca* showed (8.57±0.11 mm) and *V. cholerae* (8.15±0.15 mm) whereas minimum inhibition zone was observed in *Proteus mirabilis* (1.03±0.01 mm). From this, *K. pneumoniae* has showed

prominent result. In NAM2 the highest zone of inhibition against *K. pneumoniae* (8.49±0.16 mm) nevertheless minimum values of susceptibility were recorded in *S. typhi* (3.34±0.20 mm). The NAM 3 extracts showed strong antimicrobial activity against *K. pneumoniae* (10.3±0.22 mm) but displayed least amount of activity in *P. mirabilis* (3.55±0.29 mm). The NAM4 extracts demonstrated a high inhibition range of 7.49±0.41 (*Escherichia coli*), whereas the least inhibitions zones of 3.34±0.43 mm (*P. mirabilis*). In the present study, the NAM 5 extract evidenced higher inhibition zone against *V. parahaemolyticus* (8.47±0.18 mm), while low level of antibacterial activity was observed in *P. mirabilis* (2.48±0.24 mm). Comparing the entire associated microbe the NAM3 was performed and showed the maximum inhibition. Likewise, the maximum inhibition zones were observed for three coral associated species against human pathogens as reported by Jeyasekaran *et al.* (2002). A total of five isolates were tested for their Hemolytic activity on blood agar plates. Most haemolysis positive strains were revealed that *P. celer* against cow blood agar plates. Lyudmila *et al.* (2008) reported the marine molluscs associated bacteria were showed high antimicrobial, hemolytic and surface activities. It is well known, that surface activity is often accomplished by hemolysis and sometimes by antimicrobial activity, and therefore, both activity assays above has been used to search surfactant producing bacteria. Williams *et al.* (2007) showed the associated bacteria isolated from *Stichodactyla haddoni* against microbial pathogens.

In this study eight associated bacterial species were recorded. The culture extracts from the associated bacterial species showed sensitivity against human bacterial and fungal pathogens. Similarly in our present study, five associated bacterial species were isolated and ten clinical pathogenic bacterial strains were used and tested on the isolates of associated organism. It is coinciding with the previous reports. Burgess *et al.* (1999) explained the discovery of new classes of antibiotics is necessary due to the increased incidence of multiple resistance among pathogenic microorganisms to drugs that are currently in clinical use.

Conclusion

The current study shows that bacterial isolates from the *K. ornata* possess bioactive properties. All the tested isolates were potential inhibition against human bacterial pathogens. Thus this investigation highlights the importance of bacteria associated with the *K. ornata* as a valuable resource for the discovery of novel bioactive molecules. Further chemical isolation and characterization of active compounds from these bacterial extracts is under investigation, and findings will be reported in due course. Interesting finding from the antimicrobial sensitivity of associated bacteria must play a role in host defense, and thus constitute a valuable source of immuno competent effector cells for *in vitro* analyses.

Acknowledgements

The authors are thankful to the Dean, Centre of Advanced Study in Marine Biology, Faculty of Marine Sciences, Annamalai University, Parangipettai, Tamil Nadu, India, for facilities provided. Author N. Sri Kumaran thanks to AMET University management for encouragement.

Declaration of interest : We declare that we do not have conflict of interest.

Reference

1. Faulkner, D.J., 2002. Marine natural products. *Nat. Prod. Rep.*, 19: 1-48.

2. Proksch, P. and W.E.G. Muller, 2006. *Frontiers in Marine Biotechnology*. Horizon Bioscience, Norfolk, U.K. 98 pp.
3. Chellaram, C. and J.K.P. Edward, 2009. Antinociceptive assets of coral associated gastropod *Drupa margariticola*. *Int. J. Pharmacol.*, 5: 236-239.
4. Chellaram, C. and T. Premanand, 2010. Antitumor assay using artemia Toxicity of five *Cyprae* sp. (Mollusca; Gastropoda) from Gulf of Mannar Coastal Waters. *Current Scenario in Microbial Biotechnology. Excel Publication*, New Delhi, 60-64.
5. Grossart, H.P., A. Schlingloff, M. Bernhard, M. Simon and T. Brinkhoff, 2004. Antagonistic activity of bacteria isolated from organic aggregates of the German Wadden sea. *FEMS. Microbial. Ecol.*, 47: 387-396.
6. Chellaram, C. and T. Premanand, 2010. Antitumor assay using artemia Toxicity of five *Cyprae* sp. (Mollusca; Gastropoda) from Gulf of Mannar Coastal Waters. *Current Scenario in Microbial Biotechnology. Excel Publication*, New Delhi, 60-64.
7. Haygood, M.G., E.W. Schmidt, S.K. Davidson and D.J. Faulkner, 1999. Microbial symbionts of marine invertebrates: Opportunities for microbial biotechnology. *J. Mol. Microbiol. Biotechnol.*, 1(1): 33-43.
8. Kelecom, A., 2002. Secondary metabolites from marine microorganisms. *An. Acad. Bras. Cien.*, 74(1): 151-170.
9. Patterson, G.L. and C.M. Bolis, 1997. Fungal cell wall polysaccharides elicit an antifungal secondary metabolite (phytoalexin) in the cyanobacterium *Scytonema ocellatum*. *J. Phycol.*, 33: 54-60.
10. Putz, A. and P. Proksch, 2010. Chemical defence in marine ecosystems. *Annual Plant Rev.*, 39: 162-213.

11. Blunt, J.W., B.R. Copp, M.H.G. Munro, P.T. Northcote and M.R. Prinsep, 2011. Marine natural products. *Nat. Prod. Rep.*, 28: 196-268.
12. Davidson, S.K., A.W. Allen, G.E. Lim, C.M. Anderson and M.G. Haygood, 2001. Evidence for the biosynthesis of bryostatins by the bacterial symbiont *Candidatus Endobugula sertula* of the bryozoan *Bugula neritina*. *Appl. Environ. Microbiol.*, 67:4531-4537.
13. Benkendorff, K., 2010. Molluscan biological and chemical diversity: Secondary metabolites and medicinal resources produced by marine molluscs. *Biol. Rev. Camb. Philos. Soc.*, 85: 757-775.
14. Gavagnin, M., A. Marin, E. Mollo, A. Crispino, G. Villani and G. Cimino, 1994. Secondary metabolites from the Mediterranean Elysioidea: Origin and biological role. *Comp. Biochem. Physiol. B. Biochem. Mol. Biol.*, 108: 107-115.
15. Fontana, A., 2006. Biogenetic proposals and biosynthetic studies on secondary metabolites of opisthobranch molluscs. *Prog. Mol. Subcell. Biol.*, 43: 303-332.
16. Tamura, K., J. Dudley, M. Nei and S. Kumar, 2007. MEGA4: Molecular evolutionary genetics analysis (MEGA) software version 4.0. *Molecular Biology and Evolution*, 24: 1596-1599.
17. Lemes-Marques, E.G. and T. Yano, 2004. Influence of environmental conditions on the expression of virulence factors by *Listeria monocytogenes* and their use in species identification. *FEMS. Microbiol. Lett.*, 239: 63-70.
18. Newman, D.J., G.M. Cragg and K.M. Snader, 2003. Natural products as sources of new drugs over the period 1981-2002. *J. Nat. Prod.*, 66: 1022-1037.
19. Kennedy, J., P. Baker, C. Piper, P.D. Cotter, M. Walsh, M.J. Mooij, M.B. Bourke, M.C. Rea, P.M. O'Connor, R.P. Ross, C. Hill, F. O'Gara, J.R. Marchesi and A.D. Dobson, 2009. Isolation and analysis of bacteria with antimicrobial activities from the marine sponge *Haliclona simulans* collected from Irish waters. *Mar. Biotechnol.*, 11: 384-396.
20. Dopazo, C.P., M.L. Lemos, C. Lodeiros, J. Bolinches, J.L. Barja and A.E. Toranzo, 1988. Inhibitory activity of antibiotic producing marine bacteria against the fish pathogens. *J. Appl. Bacteriol.*, 65: 97-101.
21. Jeyasekaran, G., K. Jayanath and R. Jeya Shakil, 2002. Isolation of marine bacteria, antagonistic to human pathogens. *Indian J. Mar. Sciences*, 31: 39-44.
22. Lyudmila, A., Romanenko, Masataka Uchinob, Natalia, Kalinovskayaa, Valery and Mikhailova, 2008. Isolation, phylogenetic analysis and screening of marine mollusc-associated bacteria for antimicrobial, hemolytic and surface activities. *Microbiological Research*, 163: 633-644.
23. Williams, G. P, S. Babu, S. Ravikumar, K. Kathiresan, S. Arul Prathap, S. Chinnapparaj, M.P. Marian and S. Liakath Alikhan, 2007. Antimicrobial activity of tissue and associated bacteria from benthic sea anemone *Stichodactyla haddoni* against microbial pathogens. *Journal of Environmental Biology*, 28(4): 789-793.

Targeting Cancer cell metabolism via Target of Rapamycin

Ankita Awasthi¹, Vikrant Nain¹, Himanshi Singh¹ Pavan Kumar¹, Rekha Puria^{1*},

1. School of Biotechnology, Gautam Buddha University, Greater NOIDA,
Gautam Budh Nagar-201312, India

* For Correspondence - rpuria@gbu.ac.in

Abstract

Cancer cells acquire many metabolic rearrangements to provide energy and macromolecules required for continuous growth and proliferation. Warburg suggested that cancerous cells rely only on glycolysis for energy and biosynthesis of macromolecules. It's still unexplainable that how this metabolic switch allows predominance of cancer cell in the hypoxic and metabolically highly active conditions around the cancerous cells. Understanding of signaling particularly, role of Ser/Thr PI3 kinase Target of Rapamycin TOR, "central regulator of growth" in cancer cell metabolism has ignited interest in comprehending the precise mechanism linking cancer cell environment to metabolic rearrangements ensuring cancer proliferation. The focus of present review is to summarize the role of TOR in metabolic rearrangements prevalent in glycolysis and TCA occurring in cancerous cell. The insights from mechanistic of mTOR signaling in cancer cell metabolism have led to identification of several downstream candidates to be explored in anticancer therapeutics. Thus usage of drug directly targeting macromolecular biosynthesis in combination with environment responder, mTOR inhibitor, is more promising in cancer therapeutics.

Introduction

Cell growth is a phenomenon that relies on ability of cell to biosynthesize macromolecules and drive energy. It's an incompletely understood complex phenomenon that involves direct

communication between extra and intracellular environment. Any communication gap between the two, because of mechanistic failure at any step either results in cell death or uncontrolled proliferation of cells. Randomly growing cells need to establish their predominance in available variable environmental conditions to promote tumorigenesis. To accommodate these observations, Warburg in 1927 predicted that cancerous cells heavily rely on glycolysis rather than oxidative metabolism. These cells generate lactate from glucose inspite of adequate oxygen supply and utilize glucose for macromolecular synthesis (anabolism). Its established now that aerobic glycolysis, uptake of glutamine and glycine allows cancer cells to produce energy and biosynthesize macromolecule (Teicher *et al.* 2012). A thorough understanding of growth response to diverse environmental cues is mandatory for development of efficient cancer therapeutics.

Of late, mTOR has become a favorite candidate in cancer therapeutics. It regulates cell growth in response to different environmental conditions (energy, stress, hypoxia, growth factors etc.) by regulating processes such as translation, transcription, autophagy etc. It catalyzes number of growth process by participating as component of two Complexes mTORC1 and mTORC2. mTORC1 primarily regulates temporal aspect while mTORC2 regulates spatial aspect of growth (Suzuki and Inoki 2011). Interestingly, mTOR is activated in more than 80% of cancers. Its association with cancers is validated by

presence of several oncogenic mutations in components that act upstream of mTOR as well as in mTOR itself (Murugan *et al.* 2013). mTORC1 facilitates alteration of cell metabolism best suited to promote tumorigenesis. It plays role in almost all process e.g., glycolysis, lipogenesis, nucleotide biosynthesis, protein synthesis etc, required for continuous synthesis of macromolecules in growing cancer and provides an explanation to Warburg effect. Here our focus is to summarize the role of mTOR in metabolic rearrangements in cancer which can be exploited in development of new therapeutic interventions with the ability of targeted therapy.

Role of mTOR in cell growth metabolism : mTORC1 primarily controls cell growth by regulating the activity of eIF4 and S6 kinase, the two well established substrates of TOR kinase. These two substrates precisely regulate protein synthesis, ribosome biogenesis, stress response etc. The pathophysiology of cancer is supported by 3 major metabolic pathways i.e., A. Glycolysis, B. Pentose Phosphate Pathway (PPP) and C. Lipogenesis. Largely mTORC1 regulates these pathways by controlling the expression of transcription factors HIF1 α and SREBP. Basically it drives glucose uptake and glycolysis through upregulation of HIF1 α , induced under low oxygen concentration. It not only induces the expression of enzymes involved in glycolysis instead also promotes uptake of glucose by regulation of expression of glucose transporters (Pinheiro *et al.* 2010). Moreover, activated mTORC1 induces the expression of lipid and sterol biosynthetic genes by stimulating the activity of SREBP. Interestingly SREBP also increases the expression of G6PD rate limiting enzyme of oxidative branch of PPP in mTORC1 dependent manner (Wang *et al.* 2014). This indirectly helps in nucleotide synthesis. Recently it has also been shown that mTORC1 regulates pyrimidine biosynthesis in an S6K1 dependent manner. Hyperactive mTOR phosphorylates S6K1 which in turn phosphorylates CAD, a multifunctional enzyme that catalyzes the three steps in pyrimidine synthesis. Further the role of ACLY in

histone acetylation is mediated by SREBP. This implicates global role of mTORC1 in regulation of expression of various genes by chromatin modification. SREBP also plays crucial role in regulation of genes associated with lipogenesis. mTOR also responds to energy stress via AMPK. Increased AMP/ATP ratio induces AMPK which in turn phosphorylates raptor and suppress mTORC1 in response to depleted energy levels (Gwinn *et al.* 2008). An ATP dependent TTT-RUVBL1/L complex remains dissociated, and prevents interaction between Rag and mTORC1 required for lysosomal localization and amino acid based mTORC1 activation (Kim *et al.* 2013). Interestingly, a recent study has demonstrated the role of mTOR in reprogramming cellular metabolism from glycolysis to oxidative phosphorylation upon relocalization onto mitochondria (Lu *et al.* 2015). Basically this can increase sensitivity of cancerous cells to various metabolic inhibitors.

Regulation of Glycolysis by mTOR : Glycolysis provides the much needed energy and macromolecules for tumorigenesis. It's a oxidative process where glucose is broken into two 3C pyruvate through series of steps catalyzed by number of enzymes. mTORC1 increases expression of the primary glucose transporter Glut1 and several of the enzymes involved in catalyzing various steps of glycolytic pathway in HIF1 α dependent manner. HIF1 α being oxygen sensitive, gets rapidly degraded under normal oxygen concentration. Nevertheless, hyperactive TORC1 with increased translation downstream of 4E-BP eIF-4E branch ensures accretion of HIF1 α (Ruggero *et al.* 2004). Though most of the enzymes of glycolysis are associated with tumor growth, however role of each in cancer is not well defined.

Hexokinase : It catalyzes the first and rate limiting step of glycolytic pathway i.e., conversion of glucose to to glucose 6-phosphate. Of four mammalian isozymes, HK2 is often hyperactivated in malignant tumors. Its localization onto mitochondrial membrane ensures its ability to couple ATP synthesis to Glucose phosphorylation.

glucose 6-phosphate thus generated is utilized in continuing with glycolysis. This also participates in nucleotide synthesis by contributing in pentose phosphate pathway which is utilized for synthesis of ribose sugars (Kumar *et al.* 1996). Activity of HK2 is regulated by miR125a/b and miR143. Interestingly, mTOR regulates the expression of miR143 which means hyperactivation of mTOR may promote expression of HK2 via downregulation of miR143(Grabiner *et al.* 2014).

Glucose 6 phosphate isomerase (GPI) : GPI or phosphor glucose isomerase catalyzes the reversible isomerization of glucose 6-phosphate to fructose 6-phosphate in glycolysis. GPI is released by tumor cells. It act as autocrine motility factor, induces mitogenic, motogenic and differentiation functions implicated in various aspects of tumor progression and metastasis(Bao *et al.* 2014). It plays crucial role in synthesis of PAP and glycerolipid. Loss of function mutants of GPI results in accumulation of glucose 6-phosphate. It has been observed that an increased concentration of G6P acts as inducer of mTOR signaling in cardiomyocytes. Further GPI deficiency results in increase in PA levels, which has an established role in mTOR signaling(You *et al.* 2014).

Phosphofructokinase : Phosphofructokinase catalyzes rate limiting phosphorylation of fructose-6-phosphate to fructose-1,6-bisphosphate by using ATP as energy source. It is regulated allosterically by 2,3-diphosphoglycerate. Very little information is available about its direct role either in tumorigenesis or mTOR mediated cancer pathology(Yi *et al.* 2012).

Aldolase : Six carbon sugars are cleaved by an aldolase to produce two 3 carbon triose phosphate glyceraldehyde 3-phosphate and dihydroxyacetone phosphate. Disruption of Aldolase inhibits cell proliferation by 90% in Ras transformed NIH-3T3 cells. However, this inhibition is neither linked to glycolytic flux nor to levels of intracellular ATP rather probably is outcome of disruption of actin-cytoskeleton dynamics(Lew and Tolan 2012). Since mTORC2 plays role in actin cytoskeleton

dynamics, the possible regulatory role of mTORC2 cannot be ignored.

Triose phosphate Isomerase : Triosephosphate isomerase reversibly catalyzes the conversion of dihydroxyacetone phosphate to glyceraldehyde 3-phosphate. No direct correlation of activity of this enzyme with hyperactive mTOR has been reported till date. However, in study it was proposed that upregulation of TPI could possibly retrieve tumor cells from a resting or dormant fashion back to cell cycle, and thus sensitize tumor cells to chemotherapy (Fonvielle *et al.* 2005).

Glyceraldehyde 3-phosphate dehydrogenase (GAPDH) : GAPDH catalyzes the oxidation of glycerate 3-phosphate to 1,3 bisphosphoglycerate resulting in ATP synthesis. Overexpression of GAPDH has been observed in various tumor and malignant cell lines e.g., human prostate cancer, lung cancer etc(Guo *et al.* 2013).GAPDH plays significant role in regulating mTOR activity in response to glucose flux. GAPDH can interact with Rheb. Rheb GTP interaction with mTOR is mandatory for responding to amino acid levels in cell (nutrient sensing). When concentration of glucose is low GAPDH remains associated with Rheb so no free Rheb is available to interact with mTOR. However under conditions of high glucose influx GAPDH is primarily involved in carrying out glycolysis and does not interact with Rheb(Lee *et al.* 2009). Thus free Rheb GTP binds to mTOR and promotes cell growth. Basically GAPDH serves as a connecting link between glycolysis and mTORC1 signalling.

Phosphoglycerate kinase : It catalyzes reversible reaction of conversion of substrate 1,3-Biphosphoglycerate to 3 phosphoglycerate with generation of ATP. Out of two isoforms of PGK, PGK1 and PGK2, PGK1 is regulated by hypoxia inducible factor 1 α . Increased PGK1 is found in number of different cancers. Recently, PGK1 was identified as substrate of nuclear p85^{S6K1} in phosphoproteomic screen for identification of targets and function of nuclear p85^{S6K1}(Jastrzebski *et al.* 2011).

Phosphoglycerate mutase : It catalyzes the interconversion of glycerate 3-phosphate (3PG) and glycerate 2-phosphate (2PG). Altered expression of mutase is observed in different types of cancer. Overexpression of PGAM1 is associated with 66.7% of hepatocellular Carcinoma, Wherein it provides metabolic advantage to cancer cell proliferation and tumor growth. PGAM1 coordinates glycolysis and anabolic biosynthesis partially by controlling intracellular levels of substrate 3PG and product 2PG. 3PG inhibits 6PGD by directly binding to the active site of 6PGD and competing with its substrate 6PG. Attenuation of PGAM1 results in abnormal accumulation of 3PG, which in turn inhibits 6PGD and consequently leads to the oxidative PPP and anabolism (Peng *et al.* 2016).

Enolase : Enolase also known as phosphor pyruvate hydratase catalyzes the penultimate step of glycolysis by converting 2- phosphoglycerate to phosphoenolpyruvate. Promoter contains hypoxia responsive element. EnoA is upregulated at the mRNA and/or protein level in several tumors including brain, breast etc. In cancer cells, EnoA is overexpressed and localizes on their surface where it acts as a key protein in tumor metastasis, promoting cellular metabolism in anaerobic conditions and driving tumor invasion through plasminogen activation and extracellular matrix degradation No direct link of its regulation via mTORC1 has been observed.

Pyruvate Kinase : PK catalyzes the irreversible phosphoryl group transfer from phosphoenol pyruvate to ADP, yielding pyruvate and ATP. Pyruvate kinase is a tetramer that is allosterically activated by PEP and negatively regulated by ATP. PKM2 isoform is exclusively expressed in embryonic, proliferating and tumor cells and it plays an essential role in tumor metabolism and growth. mTOR acts as a central activator of Warburg effect by inducing PKM2 and other glycolytic enzymes under normoxic conditions. mTOR upregulation of PKM2 expression through HIF1 α mediated transcription activation and c-myc heterogenous nuclear ribonucleoprotein (hnRNPs) dependent regulation

of PKM2 gene splicing. Disruption of PKM2 suppressed oncogenic mTOR mediated tumorigenesis(Sun *et al.* 2011). PKM2 stimulated glycolysis contributes to the development of tumors caused by hyperactive mTOR and therefore this interaction may be targeted in anticancer therapeutics.

Lactate dehydrogenase : Glucose is preferentially converted into lactic acid through aerobic glycolysis. Lactate dehydrogenase catalyzes formation of lactic acid from pyruvate. It's a tetrameric enzyme composed of two subunits (LDHA and LDHB). The exact mechanism by which mTOR regulates the activity of LDH is unknown. However, recent studies have shown that mTOR positively regulates activity of LDHB and signal transducer and activator of transcription 3 (STAT3). STAT3 is a transcription activator of LDHB, downstream of mTOR(Zha *et al.* 2011)

Pyruvate Dehydrogenase : It's a link between glycolysis and TCA cycle. It catalyzes the conversion of pyruvate to acetyl-CoA via decarboxylation. Activity of PDH is regulated by Pyruvate dehydrogenase kinase (PDK1). The ability of HIF1 α to suppress TCA is primarily because of regulation of PDK1. Thus under hypoxic conditions an activated HIF1 α activates PDK1 which suppresses PDH by phosphorylation dephosphorylation of three serine residues (ser264, ser271 and ser203) (Seifert *et al.* 2007; Denko 2008; Shi *et al.* 2011)

TCA : Role of TCA cycle in promotion of cancer is not well illustrated. The opponent of Warburg has always suggested an active role of TCA in energy production in cancerous cells. Truncation of TCA cycles due to various physiological or genetic factors does not lead to its complete suppression. Rather utilization of alternative carbon sources, e.g., glutamine ensures replenishment of TCA steps and ensures generation of energy and macromolecules (DeBerardinis *et al.* 2007; Le *et al.* 2012; Nain *et al.* 2014). Interestingly one of the crucial steps in completion of TCA cycle is utilization of glutamine to produce alfa ketoglutarate and activity of

enzyme GDH which catalyzes this conversion is regulated by TOR complex. Basically TOR plays crucial role in TCA by promoting glutamine anaplerosis by activating glutamate dehydrogenase. TORC1 represses the activity of GDH inhibitor, SIRT4 (mitochondria localized sirtuin) by promoting proteasome mediated destabilization of cAMP-responsive element binding 2 (CREB2) (Cibelli *et al.* 1999; Csibi *et al.* 2013). Glutamine is also considered as positive regulator of mTORC1. It facilitates uptake of leucine and promotes mTORC1 assembly and lysosomal localization. Also explains addiction of cancer cells to glutamine. Role of mTOR complex in facilitating other steps of TCA or ETC, ATP synthase activity are not well illustrated.

Lipogenesis and Pentose Phosphate pathway:

Recent studies has unraveled prominent role of mTOR in regulating lipogenesis and Pentose Phosphate pathway, important mechanism by which number of tumor cells meet the unique metabolic demands of proliferating cancerous cells. SREBP, transcription factor facilitates these two processes. Akt(upstream regulator of mTOR) regulates SREBP partially by promoting stability of its processed form through inhibition of glycogen synthase kinase (GSK3). GSK3 targets SREBP for proteasomal degradation by its phosphorylation (Jope *et al.* 2007; Xu *et al.* 2009; Dong *et al.* 2016).

SREBP also stimulates the fatty acid synthesis by regulating ACLY at mRNA level. It promotes utilization of acetyl CoA generated upon degradation of citrate to acetyl CoA and oxaloacetate. This requires activity of enzyme ACLY, which has been reported to be upregulated in different types of cancer (Zaidi *et al.* 2012; Khwairakpam *et al.* 2015). AKT/PI3k pathway is responsible for regulation of phosphorylation and activation of ACLY to meet increased demand of fatty acid synthesis generated by membrane biogenesis of growing cells. ACLY is required for histone acetylation which suggests a potential role for global regulation of chromatin downstream of mTORC1 (Covarrubias *et al.* 2016). Further exposure of cancer cell lines to mTOR kinase inhibitor INK128 has been shown to reduce the

expression of acetyl CoA carboxylase and fatty acid synthase along with suppressed lipogenesis (Liu *et al.* 2015; Li *et al.* 2016).

mTORC1, regulates pentose phosphate pathway by regulating the expression of glucose-6-phosphate dehydrogenase via SREBP. G6PD is rate limiting enzyme of oxidative branch of pentose phosphate pathway. Thus mTORC1 promotes the utilization of glucose 6 phosphate for synthesis of ribose sugars to be consumed in nucleotide biosynthesis (Ye *et al.* 2012; Stincone *et al.* 2015). Hyperactivation of TOR regulates pyrimidine synthesis by regulation of phosphorylation of enzyme CAD through its downstream effector S6k1 (Magnuson *et al.* 2012; Ben-Sahra *et al.* 2013). Further, G6PD activity results in synthesis of NADPH. High metabolic activity in tumor cells result in generation of high ROS which can actually damage cells. Thus high activity of PPP results in higher NADPH which can be exploited to reduce glutathione in the protection against ROS(Krüger *et al.* 2011; Chadwick *et al.* 2013)

mTOR Inhibitors in cancer therapeutics : Crucial role of mTOR in metabolic rearrangements implicate the role of mTOR inhibitors in control of cancerous growth by sabotaging altered metabolism in cancer cells (Fig1). Rapamycin or its analog rapalogs with better pharmaceutical properties exhibit strong anticancer properties. In combination with FKBp12, rapalogs specifically bind FRB domain of Tor kinase and inhibits its activity. Everloimus and temsirolimus (rapalogs) have been approved by FDA for treatment of RCC (Zhang *et al.* 2013).The restricted activity of rapalogs at prescribed concentrations against mTORC1 has limited their ability to circumvent growth of many different types of cancer. Activation of feedback loops and prosurvival pathways by TORC2 supports the proliferation of cancer cells even in presence of rapamycin/rapalogs. The new class of molecular inhibitors with efficacy against both mTORC1 and mTORC2, posses the ability to globally suppress TOR mediated cell growth activities (Wang *et al.* 2009; Xiong *et al.* 2013).

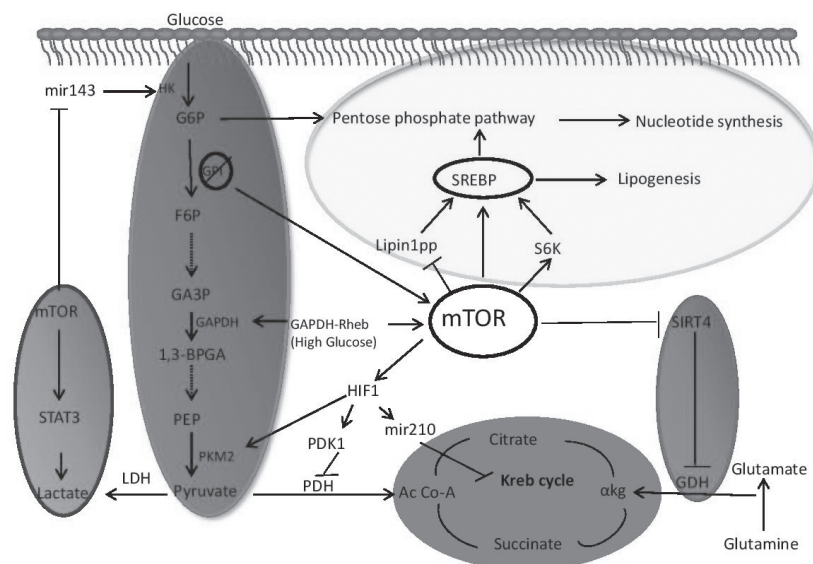


Fig1: mTOR in cancer cell metabolism

Torin1, Torin2 have been shown to possess anticancer properties superior to rapalogs. Nevertheless, high complex cross talk between survival pathways and strong immunosuppression does not rule out the probability of generation of drug resistant mechanism (Thoreen *et al.* 2009; Moorman and Shenk 2010; Hussain *et al.* 2015).

An apparent better alternative is combination therapy e.g. uses of dual inhibitors for PI3K/mTOR. Several clinical trials are going on to search for combination of drugs with high anticancer activity and low toxicity. TKIs are known to reduce tumor cell growth by suppressing glycolysis, reducing lactate production and expression of Glut1, HIF1 α and HIF2 α (Chiavarina *et al.* 2012; Arreola *et al.* 2014). The use of nontoxic doses of TKIs in combination with known glycolytic inhibitor with low cytotoxicity or with inhibitors specific to components of metabolism which are not directly regulated by mTOR are being tested for their ability to suppress tumorigenesis with high efficacy and low toxicity leading to less side effects.

The advent of various genetic engineering approaches has made it feasible to specifically

manipulate the sequence and structure of desired genes at high frequency. The expression of mTOR in cancerous cells can be curtailed by designing and targeting regulatory RNA (miRNA, siRNA) or engineered nucleases (ZFN, TALENS or CRISPR-CAS9) designed against mTOR. (Puria *et al.* 2012). Nonetheless genetically modified bacterial strains with ability to recognize and grow precisely at tumor site, are future devices for delivery of gene expression manipulating tools (Regulatory RNA or engineered nucleases) in cancer cells.

Concluding remarks : Reprogramming of bioenergetics of cancer cells from glycolysis to oxidative phosphorylation hold promise of efficient cancer therapy. Reduced pyruvate flux into mitochondria oxidative phosphorylation enables cancer cells to avoid ROS generation from oxidative phosphorylation and improved survival even during metastasis. An induced glycolysis acts as a constant source of energy for proliferating cancer cells. Further expression of alternative routes ensures supply of macromolecules to growing cells. mTOR pathway plays vital role in altered cancer cell metabolism. mTOR regulates the expression of PFK2M and hexokinase largely

responsible for activated uptake and metabolism of glucose. Further mTOR responds to glutamine levels, a source of intermediate for TCA cycle. In addition mTOR mediated expression of miRNA 143 has been shown to promote glucose metabolism in human lung cancer. Actually the understanding of role of mTOR signalling in cancer cell metabolism has expanded the avenues for targeted therapy. Though drugs specific to mTOR are known, an enhanced cytotoxicity has always been a concern. Further it is evident that single factor cannot be responsible for drastic metabolic switch acquired by these cells and cancer cells growing at different regions (periphery, deep inside or during metastasis) faces differential nutrient environment. As mTOR is a sensor of extracellular and intracellular cues, its response should vary under such different conditions. We believe that an understanding of mTOR signalling under varied conditions prevalent during the progression of cancer ultimately resulting in metabolic rearrangements will actually lead to identification of targets with less cytotoxicity and better efficacy.

Acknowledgment

Department of Biotechnology, Ministry of Science & Technology, India to RP is duly acknowledged. Compliance with Ethical Standards.

Conflict of Interest Authors declare no conflict of interest.

References

1. Arreola, A., C. L. Cowey, J. L. Coloff, J. C. Rathmell, and W. K. Rathmell, 2014 HIF1a and HIF2a exert distinct nutrient preferences in renal cells. *PLoS One* 9: 5.
2. Bao, Q., H. Niess, R. Djafarzadeh, Y. Zhao, B. Schwarz *et al.*, 2014 Recombinant TIMP-1-GPI inhibits growth of fibrosarcoma and enhances tumor sensitivity to doxorubicin. *Target. Oncol.* 9: 251–261.
3. Ben-Sahra, I., J. J. Howell, J. M. Asara, and B. D. Manning, 2013 Stimulation of de Novo Pyrimidine Synthesis by Growth Signaling Through mTOR and S6K1. *Science* 339: 1323–1328.
4. Chadwick, A. L., A. Howell, F. Sotgia, and M. P. Lisanti, 2013 Carbonic anhydrase 9 (CA9) and redox signaling in cancer-associated fibroblasts: Therapeutic implications. *Cell Cycle* 12: 2534.
5. Chiavarina, B., U. E. Martinez-Outschoorn, D. Whitaker-Menezes, A. Howell, H. B. Tanowitz *et al.*, 2012 Metabolic reprogramming and two-compartment tumor metabolism: Opposing role(s) of HIF1a and HIF2a in tumor-associated fibroblasts and human breast cancer cells. *Cell Cycle* 11: 3280–3289.
6. Cibelli, G., S. Schoch, and G. Thiel, 1999 Nuclear targeting of cAMP response element binding protein 2 (CREB2). *Eur. J. Cell Biol.* 78:.
7. Covarrubias, A. J., H. I. Aksoylar, J. Yu, N. W. Snyder, A. J. Worth *et al.*, 2016 Akt-mTORC1 signaling regulates Acly to integrate metabolic input to control of macrophage activation. *Elife* 5:.
8. Csibi, A., S. M. Fendt, C. Li, G. Poulogiannis, A. Y. Choo *et al.*, 2013 The mTORC1 pathway stimulates glutamine metabolism and cell proliferation by repressing SIRT4. *Cell* 153: 840–854.
9. DeBerardinis, R. J., A. Mancuso, E. Daikhin, I. Nissim, M. Yudkoff *et al.*, 2007 Beyond aerobic glycolysis: Transformed cells can engage in glutamine metabolism that exceeds the requirement for protein and nucleotide synthesis. *Proc. Natl. Acad. Sci.* 104: 19345–19350.
10. Denko, N. C., 2008 Hypoxia, HIF1 and glucose metabolism in the solid tumour. *Nat. Rev. Cancer* 8: 705–713.
11. Dong, Q., F. Giorgianni, S. Beranova-Giorgianni, X. Deng, R. N. O’Meally *et al.*, 2016 Glycogen synthase kinase-3-mediated phosphorylation of serine 73 targets sterol response element binding protein-1c (SREBP-1c) for proteasomal degradation. *Biosci. Rep.* 36: e00284–e00284.

12. Fonvielle, M., S. Mariano, and M. Therisod, 2005 New inhibitors of rabbit muscle triose-phosphate isomerase. *Bioorg. Med. Chem. Lett.* 15: 2906–2909.
13. Grabiner, B. C., V. Nardi, K. Birsoy, R. Possemato, K. Shen *et al.*, 2014 A diverse array of cancer-associated MTOR mutations are hyperactivating and can predict rapamycin sensitivity. *Cancer Discov.* 4: 554–563.
14. Guo, C., S. Liu, and M. Z. Sun, 2013 Novel insight into the role of GAPDH playing in tumor. *Clin. Transl. Oncol.* 15: 167–172.
15. Gwinn, D. M., D. B. Shackelford, D. F. Egan, M. M. Mihaylova, A. Mery *et al.*, 2008 AMPK Phosphorylation of Raptor Mediates a Metabolic Checkpoint. *Mol. Cell* 30: 214–226.
16. Hussain, A. R., M. Al-Romaizan, M. Ahmed, S. Thangavel, F. Al-Dayel *et al.*, 2015 Dual Targeting of mTOR Activity with Torin2 Potentiates Anticancer Effects of Cisplatin in Epithelial Ovarian Cancer. *Mol. Med.* 21: 466–478.
17. Jastrzebski, K., K. M. Hannan, C. M. House, S. S. C. Hung, R. B. Pearson *et al.*, 2011 A phospho-proteomic screen identifies novel S6K1 and mTORC1 substrates revealing additional complexity in the signaling network regulating cell growth. *Cell. Signal.* 23: 1338–1347.
18. Jope, R. S., C. J. Yuskaitis, and E. Beurel, 2007 Glycogen synthase kinase-3 (GSK3): Inflammation, diseases, and therapeutics. *Neurochem. Res.* 32: 577–595.
19. Khwairakpam, A. D., M. S. Shyamananda, B. L. Sailo, S. R. Rathnakaram, G. Padmavathi *et al.*, 2015 ATP Citrate Lyase (ACLY): A Promising Target for Cancer Prevention and Treatment. *Curr Drug Targets* 16: 156–163.
20. Kim, S. G., G. R. Hoffman, G. Poulgiannis, G. R. Buel, Y. J. Jang *et al.*, 2013 Metabolic Stress Controls mTORC1 Lysosomal Localization and Dimerization by Regulating the TTT-RUVBL1/2 Complex. *Mol. Cell* 49: 172–185.
21. Krüger, A., N.-M. Grüning, M. M. C. Wamelink, M. Kerick, A. Kirpy *et al.*, 2011 The Pentose Phosphate Pathway Is a Metabolic Redox Sensor and Regulates Transcription During the Antioxidant Response. *Antioxid. Redox Signal.* 15: 311–324.
22. Kumar, A., A. S. Goel, T. M. Hill, S. D. Mikolajczyk, L. S. Millar *et al.*, 1996 Expression of human glandular kallikrein, hK2, in mammalian cells. *Cancer Res.* 56: 5397–5402.
23. Le, A., A. N. Lane, M. Hamaker, S. Bose, A. Gouw *et al.*, 2012 Glucose-independent glutamine metabolism via TCA cycling for proliferation and survival in b cells. *Cell Metab.* 15: 110–121.
24. Lee, M. N., S. H. Ha, J. Kim, A. Koh, C. S. Lee *et al.*, 2009 Glycolytic flux signals to mTOR through glyceraldehyde-3-phosphate dehydrogenase-mediated regulation of Rheb. *Mol. Cell. Biol.* 29: 3991–4001.
25. Lew, C. R., and D. R. Tolan, 2012 Targeting of several glycolytic enzymes using RNA interference reveals aldolase affects cancer cell proliferation through a non-glycolytic mechanism. *J. Biol. Chem.* 287: 42554–42563.
26. Li, S., Y.-T. Oh, P. Yue, F. R. Khuri, and S.-Y. Sun, 2016 Inhibition of mTOR complex 2 induces GSK3/FBXW7-dependent degradation of sterol regulatory element-binding protein 1 (SREBP1) and suppresses lipogenesis in cancer cells. *Oncogene* 35: 642–650.
27. Liu, D., Y. Xiao, B. S. Evans, and F. Zhang, 2015 Negative feedback regulation of fatty

- acid production based on a malonyl-CoA sensor-actuator. *ACS Synth. Biol.* 4: 132–140.
28. Lu, C. L., L. Qin, H. C. Liu, D. Candas, M. Fan *et al.*, 2015 Tumor cells switch to mitochondrial oxidative phosphorylation under radiation via mTOR-mediated hexokinase II inhibition - A Warburg-reversing effect. *PLoS One* 10: 3.
29. Magnuson, B., B. Ekim, and D. C. Fingar, 2012 Regulation and function of ribosomal protein S6 kinase (S6K) within mTOR signalling networks. *Biochem. J.* 441: 1–21.
30. Moorman, N. J., and T. Shenk, 2010 Rapamycin-Resistant mTORC1 Kinase Activity Is Required for Herpesvirus Replication. *J. Virol.* 84: 5260–5269.
31. Murugan, A. K., A. Alzahrani, and M. Xing, 2013 Mutations in critical domains confer the human mTOR gene strong tumorigenicity. *J. Biol. Chem.* 288: 6511–6521.
32. Nain, V., R. Buddham, R. Puria, and S. Sahi, 2014 Role of TCA cycle truncation in cancer cell energetics. *Current Trends in Biotechnology and Pharmacy* 8: 428-438.
33. Peng, X. C., F. M. Gong, Y. Chen, M. Qiu, K. Cheng *et al.*, 2016 Proteomics identification of PGAM1 as a potential therapeutic target for urothelial bladder cancer. *J. Proteomics* 132: 85–92.
34. Pinheiro, C. H. da J., L. R. Silveira, R. T. Nachbar, K. F. Vitzel, and R. Curi, 2010 Regulation of glycolysis and expression of glucose metabolism-related genes by reactive oxygen species in contracting skeletal muscle cells. *Free Radic. Biol. Med.* 48: 953–960.
35. Ruggero, D., L. Montanaro, L. Ma, W. Xu, P. Londei *et al.*, 2004 The translation factor eIF-4E promotes tumor formation and cooperates with c-Myc in lymphomagenesis. *Nat. Med.* 10: 484–486.
36. Seifert, F., E. Ciszak, L. Korotchkina, R. Golbik, M. Spinka *et al.*, 2007 Phosphorylation of serine 264 impedes active site accessibility in the E1 component of the human pyruvate dehydrogenase multienzyme complex. *Biochemistry* 46: 6277–6287.
37. Shi, LZ., R. Wang, G. Huang, P. Vogel, G. Neale *et al.*, 2011 HIF1a-dependent glycolytic pathway orchestrates a metabolic checkpoint for the differentiation of TH17 and Treg cells. *J. Exp. Med.* 208: 1367–1376.
38. Stincone, A., A. Prigione, T. Cramer, M. M. C. Wamelink, K. Campbell *et al.*, 2015 The return of metabolism: Biochemistry and physiology of the pentose phosphate pathway. *Biol. Rev.* 90: 927–963.
39. Sun, Q., X. Chen, J. Ma, H. Peng, F. Wang *et al.*, 2011 Mammalian target of rapamycin up-regulation of pyruvate kinase isoenzyme type M2 is critical for aerobic glycolysis and tumor growth. *Proc. Natl. Acad. Sci.* 108: 4129–4134.
40. Suzuki, T., and K. Inoki, 2011 Spatial regulation of the mTORC1 system in amino acids sensing pathway. *Acta Biochim. Biophys. Sin. (Shanghai)*. 43: 671–679.
41. Teicher, B. A., W. M. Linehan, and L. J. Helman, 2012 Targeting cancer metabolism. *Clin. Cancer Res.* 18: 5537–5545.
42. Thoreen, C. C., S. A. Kang, J. W. Chang, Q. Liu, J. Zhang *et al.*, 2009 An ATP-competitive mammalian target of rapamycin inhibitor reveals rapamycin-resistant functions of mTORC1. *J. Biol. Chem.* 284: 8023–8032.
43. Wang, T., U. Lao, and B. A. Edgar, 2009 TOR-mediated autophagy regulates cell death in *Drosophila* neurodegenerative disease. *J. Cell Biol.* 186: 703–711.
44. Wang, Y. P., L. S. Zhou, Y. Z. Zhao, S. W. Wang, L. L. Chen *et al.*, 2014 Regulation of

- G6PD acetylation by SIRT2 and KAT9 modulates NADPH homeostasis and cell survival during oxidative stress. *EMBO J.* 33: 1304–1320.
45. Xiong, Y., M. McCormack, L. Li, Q. Hall, C. Xiang *et al.*, 2013 Glucose–TOR signalling reprograms the transcriptome and activates meristems. *Nature* 496: 181–186.
46. Xu, C., N. G. Kim, and B. M. Gumbiner, 2009 Regulation of protein stability by GSK3 mediated phosphorylation. *Cell Cycle* 8: 4032–4039.
47. Ye, J., A. Mancuso, X. Tong, P. S. Ward, J. Fan *et al.*, 2012 Pyruvate kinase M2 promotes de novo serine synthesis to sustain mTORC1 activity and cell proliferation. *Proc. Natl. Acad. Sci.* 109: 6904–6909.
48. Yi, W., P. M. Clark, D. E. Mason, M. C. Keenan, C. Hill *et al.*, 2012 Phosphofructokinase 1 Glycosylation Regulates Cell Growth and Metabolism. *Science* (80-.). 337: 975–980.
49. You, J.-S., H. C. Lincoln, C.-R. Kim, J. W. Frey, C. a Goodman *et al.*, 2014 The role of diacylglycerol kinase α and phosphatidic acid in the mechanical activation of mammalian target of rapamycin (mTOR) signaling and skeletal muscle hypertrophy. *J. Biol. Chem.* 289: 1551–63.
50. Zaidi, N., I. Royaux, J. V. Swinnen, and K. Smans, 2012 ATP citrate lyase knockdown induces growth arrest and apoptosis through different cell- and environment-dependent mechanisms. *Mol. Cancer Ther.* 11: 1925–35.
51. Zha, X., F. Wang, Y. Wang, S. He, Y. Jing *et al.*, 2011 Lactate dehydrogenase B is critical for hyperactive mTOR-mediated tumorigenesis. *Cancer Res.* 71: 13–18.
52. Zhang, H., D. Berel, Y. Wang, P. Li, N. A. Bhowmick *et al.*, 2013 A Comparison of Ku0063794, a Dual mTORC1 and mTORC2 Inhibitor, and Temsirolimus in Preclinical Renal Cell Carcinoma Models. *PLoS One* 8:.
53. Puria, R., Sahi. S, Nain. V, 2012 HER2+ breast cancer therapy: by CPP-ZFN mediated targeting of mTOR? *Technol Cancer Res Treat.* 11: 175-80.

From Natural products to therapeutically important antifungals

Neelabh and Karuna Singh*

Department of Zoology (MMV), Banaras Hindu University
Varanasi -221005, India

* For Correspondence - karunasingh5.bhu@gmail.com

Abstract

Although, there has been a significant progress in the field of pharmaceuticals and drug designing in the recent past, yet there is a vacuum in the development of broad spectrum antifungal drugs. Those drugs that are at our disposal are not free from side effects having several risks and associated toxicities on prolonged usage. Therefore, there has been an ever escalating demand of devising new drugs that are preferably natural and free from side effects. The current article deals with the most recent natural antifungals, their salient features and their targets in order to provide the readers a clear understanding of the importance of the natural drugs and to provide the motivation so as to devise new and effective analogs of these drugs thus helping us combat the fungal diseases in a better way.

Key words: natural, antifungal, diseases, chitin synthase inhibitors

Introduction

Each year over a billion people come in contact with the fungal infections and the evidences suggest that the rate is ever escalating (1, 2, 3, 4). Fungi are eukaryotic organisms, having the ability to infect any part of the human body, ranging from superficial infections of the skin to the disseminated life threatening diseases. Some fungi like *Cryptococcus neoformans* not known to cause serious diseases in the past, are now posing new challenges to human health. This

change in scenario can be attributed to the increased number of immunocompromised patients (people suffering from AIDS, undergoing chemotherapy or organ transplant etc.), use of central venous catheters and increased use of broad spectrum antibiotics (5).

Prior to 1970, medical science claimed of treating the fungal infections by and large with the medications in hand. Therefore, there were hardly any new antifungals devised apart from flucytosine in 1964 and the polyenes nystatin and amphotericin B in 1950's. Only in the early 1970's came the majority of the azoles which are currently being used against the life threatening fungal diseases. To add to the misery, the currently used antifungals have side effects like the problem of nephrotoxicity with amphotericin B (6) and growing resistant against the azoles (7), drug – drug interactions and fungistatic mode of action.

Therefore, it is the need of the hour to develop new antifungals which should preferably be natural and having broad spectrum. Pharmaceutical giants are striving hard to focus their research towards the nature based products. The increasing role of natural products in the drug discovery has stemmed from the diverse structure and the complex carbon skeleton of natural products. Moreover, the natural product based drugs show far more drug likeliness and biological friendliness in comparison to the synthetic drugs as they have been elaborated within living systems (8, 9). This can be emphasized by a report published in the Journal of Natural Products stating that 70 % of the drugs that have been developed in the past 25

years in United States are based on the natural products (10). In the current article the various nature based antifungals have been divided on the basis of their respective targets and have been explained accordingly. A brief outline of this article has been explained in Figure 1.

**Types of natural antifungals -
 1,3 beta glucan synthase inhibitors**

FR901469 : FR901469, known to be a 1,3 β glucan synthase inhibitor has been isolated from an unidentified fungus no. 11243 in the form of a hydrochloride salt (11). It is an echinocandin derivative having high water solubility. The MIC of this natural inhibitor has been calculated to be 0.63 and 0.16 $\mu\text{g/ml}$ against *Candida albicans* and *Aspergillus fumigatus* respectively using the broth micro-dilution method. These MICs give a

clear idea about the high antifungal activity of this product. It has a limitation in the form of its high haemolytic behaviour which is lesser than the amphotericin B but higher than echinocandin B (5). So, efforts are being made to design its analogs in order to address this shortcoming.

FR901379 : FR901379 is another echinocandin derivative which has been isolated from *Coleophoma empedri* F-11899. It is a cyclic hexapeptide, highly water soluble due to the presence of a sulfonate moiety (12, 13). It targets 1, 3 β glucan synthase, having an IC_{50} value of 0.7 $\mu\text{g/ml}$ in comparison to 2.6 $\mu\text{g/ml}$ of echinocandin B against *C.albicans*. However, this compound could not prolong the survival of a model infected with aspergillosis and the MLC associated was 62 $\mu\text{g/ml}$ indicating the need to form its analogs (5).

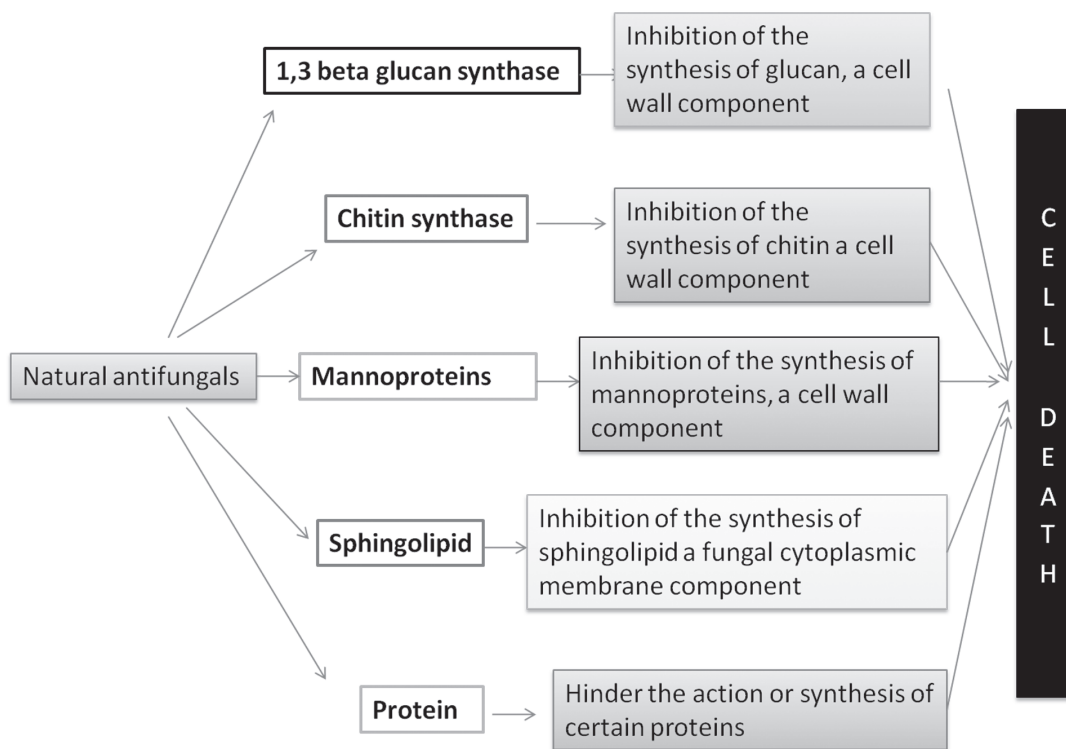


Fig.1: Action of natural antifungals on various cellular components of the fungi leading to cell death

Caspofungin : Caspofungin is the first of its class echinocandins which got the approval from Food and Drug Administration (FDA), USA. It is semi-synthetically derived from a fermentation product of the fungus *Glarea lozoyensis*. It is known to target the synthesis of 1,3 β glucan which is an integral component of the fungal cell wall thus causing an osmotic imbalance inside the fungal cell. Caspofungin in a head to head comparison was at par to the liposomal amphotericin B in case of neutropenic patients, amphotericin B deoxycholate in case of treatment of invasive candidiasis and far better than amphotericin B and similar to fluconazole in case of tolerability profile thus providing a viable alternate to liposomal amphotericin B, amphotericin deoxycholate and fluconazole at the same time (14).

Micafungin : Micafungin is the second drug of class echinocandin. It is a semi-synthetic drug which is formed by the chemical modification of the fermentation product of *Coleophoma empetri*. Micafungin is administered intravenously and targets the synthesis of 1-3 β glucan. Literature suggests that micafungin is similar to caspofungin in many respects like identical *in vitro* activity against *Candida albicans*, non-albicans species of *Candida*, and *Aspergillus* species (15). A favourable tolerability profile has been observed in case of this drug, no drug to drug interactions have been observed. Moreover, it does not need adjustment for renal or hepatic insufficiency (16).

Chitin synthase (Chs) inhibitors

Nikkomycin Z : Nikkomycin Z is a competitive inhibitor of chitin synthases in fungi. It is an antifungal peptide that has been produced as a by-product of *Streptomyces tendae* fermentation (17). Reports suggest that in case of *Saccharomyces cerevisiae*, nikkomycin inhibits only Chs 1 and 3 but not 2 whereas in case of *C. albicans* it inhibits all the 3 Chs having different IC_{50} for each of them. It has been concluded through studies conducted in different growth mediums that nikkomycin inhibits the formation of the septum and chitin by inhibiting the chitin synthases in a medium dependent manner (18).

Polyoxins : Polyoxins, produced by *Streptomyces cacaoi*, are a class of nucleoside antibiotics having nitrogen as a part of their heterocyclic ring. It targets the chitin synthase in order to block the production of chitin. Polyoxins have reportedly shown different activities against different organisms (19, 20, 21, 22). Polyoxin D is known to be fungistatic against *C. albicans* at concentrations as high as 500 to 2000 mg/ml and is also known to be a growth inhibitor in case of *C. neoformans* (23).

Mannoprotein synthesis inhibitor

Pradimicin/benanomycin family: Pradimicin and benanomycin are a new class of antifungals that have been isolated from actinomycetes. The primary character of these antifungals is that they possess a benzonathalene quinone skeleton substituted with an amino acid and a disaccharide side chain. This wide spectrum antifungal has a calcium dependent mode of action in which it forms a complex with the saccharide moiety present on the cell surface thus causing a leakage through the cell membrane and ultimately leading to death of the fungi (24).

Sphingolipid synthesis inhibitor : Lipoxamycin and hydroxylipoxamycin isolated from *Streptomyces sp.* have been reported to inhibit the fungal growth in case of various fungi but have a note worthy effect against *C. neoformans* and *C. albicans*. Although negative effect was shown by *Aspergillus fumigatus* against lipoxamycin tests but all the other filamentous fungi showed the inhibition during the disc diffusion tests (25, 26). Apart from the said compounds, viridofungin has also shown to inhibit the fungal growth (27). Further investigation showed that all these compounds inhibited serine palmitoyl transferase, an important enzyme in the course of formation of sphingolipid (28, 29, 30).

Another key enzyme that is responsible for the formation of ceramide during the synthesis of sphingolipid is ceramide synthase. Researchers have shown that a group of mycotoxins termed as fumonisins, primarily produced by *Fusarium verticillioides* and *Fusarium*

proliferatum (31) are responsible for the inhibition of this enzyme. Although, there are evidences that show that fumonisin B1 has the potential to inhibit the sphingolipid synthesis *in-vitro* but altogether due to the low penetrance power, fumonisins are not considered as good therapeutic agents (32, 33). Apart from fumonisins, australifungin isolated from *Sporormiella australis* is the first non sphingosine based inhibitor having a unique combination of α -diketone and β -ketoaldehyde. Although australifungin has shown MIC of 1mg/L or less than all the organisms it has been tested against yet it has a hindrance for therapeutic use as it hampers the ceramide synthesis in HepG2 cells (30).

Likewise, a third enzyme, inositol phosphorylceramide (IPC) synthase catalyzes the transfer of phosphoinositol from phosphatidylinositol to ceramide to form IPC. Aureobasidins specially aureobasidin A has been known to produce high antifungal inhibitions against *Candida* species but are not effective against *Aspergillus* species the reason still being unknown (34, 30).

Protein synthesis inhibitors : A lot of protein synthesis inhibitors which can prove to be of therapeutic importance have come up in the recent past. Sordarin, isolated from the fermentation of *Sordaria araneosa* shows high degree of activity against *Candida albicans*, *C. tropicalis*, *C. kefyr* and *Cryptococcus neoformans*, but showed negative effect against *C. krusei*, *C. glabrata* and *C. parapsilosis*. It shows a high level of specificity against elongation factor 2 (EF2) (35, 36).

Similarly, Zofimarin has shown potency against *C. albicans*, *S. cerevisiae*, *C. neoformans* and *Aspergillus* species also. A different antifungal compound BE 31405 has a unique tricyclic structure with a sugar and is reported to be active against *C. albicans*, *C. glabrata* and *C. neoformans* (30, 37).

Conclusion

The success of the natural products in the drug discovery is due to the biological compatibility and drug likeliness of the natural compounds as

compared to the synthetic compounds. The countries which are rich in biological diversity have a great scope of utilization of their natural products in the formulation of effective drugs. But, it is necessary to use controlled scientific methodologies without disturbing the biodiversity.

In the recent past, after the failure of the alternate drug discovery strategy, the science of drug discovery has changed its course back to the utilization of the natural resources. It is the need of the hour that the present day technology for instance smart screening methods, robotic separation with structural analysis, metabolic engineering, bioinformatics and synthetic biology should lend a co-operative hand in developing the nature based drugs thus culminating the ill effects of the synthetic drugs and more efficiently fighting the war against mycological diseases.

Conflict of Interest : None

Acknowledgement

One of the authors Mr. Neelabh would like to thank Indian council of Medical Research (ICMR) for providing Senior Research Fellowship (SRF).

References

1. Hsu, J. L., Ruoss, S. J., Bower, N. D., Lin, M., Holodny, M., and Stevens, D. A. (2011). Diagnosing invasive fungal disease in critically ill patients. *Crit. Rev. Microbiol.*, 37: 277-312.
2. Di Santo, R. (2010). Natural products as antifungal agents against clinically relevant pathogens. *Nat. Prod. Rep.*, 27: 1084-1098.
3. Brown, G. D., Denning, D. W., and Levitz, S. M. (2012). Tackling human fungal infections. *Science*, 336: 647-647.
4. Fungal Research Trust. How Common are Fungal Diseases? Updated 10/8/2011. Available at: <http://www.fungalresearchtrust.org/How Common are Fungal Diseases2.pdf> Accessed 7/17/2012
5. Barrett, D. (2002). From natural products to clinically useful antifungals. *Biochim. et Biophys Acta (BBA)-Mol Basis of Dis*, 1587: 224-233.

6. Georgopapadakou, N. H., and Walsh, T. J. (1994). Human mycoses: drugs and targets for emerging pathogens. *Science*, 264: 371-373.
7. Cartledge, J. D., Midgley, J., and Gazzard, B. G. (1997). Clinically significant azole cross-resistance in *Candida* isolates from HIV-positive patients with oral candidosis. *Aids*, 11: 1839-1844.
8. Balunas, M. J., and Kinghorn, A. D. (2005). Drug discovery from medicinal plants. *Life sciences*, 78: 431-441.
9. Drahl, C., Cravatt, B. F., and Sorensen, E. J. (2005). Protein Reactive Natural Products. *Angewandte Chemie Int. Ed.*, 44: 5788-5809.
10. Butler, R. (2007). 70% of new drugs come from Mother Nature. Available at: <http://news.mongabay.com/2007/03/70-of-new-drugs-come-from-mother-nature/> Accessed: 28/12/2015
11. Fujie, A., Iwamoto, T., Muramatsu, H., Okudaira, T., Nitta, K., Nakanishi, T., et al (2000). FR901469, a novel antifungal antibiotic from an unidentified fungus No. 11243. I. Taxonomy, fermentation, isolation, physico-chemical properties and biological properties. *J Antibiot.*, 53: 912-919.
12. Iwamoto, T., Fujie, A., Sakamoto, K., Tsurumi, Y., Shigematsu, N., Yamashita, M., et al (1994). WF11899A, B and C, novel antifungal lipopeptides. I. Taxonomy, fermentation, isolation and physico-chemical properties. *J Antibiot.*, 47: 1084-1091.
13. Iwamoto, T., Fujie, A., Nitta, K., Hashimoto, S., Okuhara, M., and Kohsaka, M. (1994). WF11899A, B and C, novel antifungal lipopeptides. II. Biological properties. *J Antibiot.*, 47: 1092-1097.
14. McCormack, P. L., and Perry, C. M. (2005). Caspofungin. *Drugs*, 65: 2049-2068.
15. Chandrasekar, P. H., and Sobel, J. D. (2006). Micafungin: a new echinocandin. *Clin. Infect. Dis*, 42, 1171-1178.
16. de la Torre, P., and Reboli, A. C. (2014). Micafungin: an evidence-based review of its place in therapy. *Core evidence*, 9: 27-39.
17. Tokumura, T., and Horie, T. (1997). Kinetics of nikkomycin Z degradation in aqueous solution and in plasma. *Biol and Pharma. Bulletin*, 20: 577-580.
18. Kim, M. K., Park, H. S., Kim, C. H., Park, H. M., and Choi, W. (2002). Inhibitory effect of nikkomycin Z on chitin synthases in *Candida albicans*. *Yeast*, 19: 341-349.
19. Hori, M., Eguchi, J., Kakiki, K. and Misato, T. (1974). Studies on the mode of action of polyoxins. Vi. *J. Antibiot.*, 27: 260-266.
20. Hori, M., Kakiki, K., and Misato, T. (1974). Interaction between polyoxin and active center of chitin synthetase. *Agri. Biol. Chem.*, 38, 699-705.
21. Isono, K., and Suzuki, S. (1966). Studies on polyoxins, antifungal antibiotics. *Agri. Biol. Chem.*, 30: 813-814.
22. Suzuki, S., Isono, K., Nagatsu, J., Mizutani, T., Kawashima, Y., and Mizuno, T. (1965). A new antibiotic, polyoxin A. *J. Antibiot.*, 18, 131.
23. Becker, J. M., Covert, N. L., Shenbagamurthi, P., Steinfeld, A. S., and Naider, F. (1983). Polyoxin D inhibits growth of zoopathogenic fungi. *Antimicrob. Agents Chemother.*, 23, 926-929.
24. August, J. T., Anders, M. W., Coyle, J. T., Ignarro, L. J., and Murad, F. (1998). *Advances in Pharmacology* vol 44 Academic Press.
25. Mandala, S. M., Frommer, B. R., Thornton, R. A., KURTZ, M. B., Young, N. M., Cabello, M. A., et al., (1994). Inhibition of serine palmitoyl-transferase activity by lipoxamycin. *J. Antibiot.*, 47, 376-379.

26. Whaley, H. A., Sebek, O. K., and Lewis, C. (1970). Production, isolation, characterization, and evaluation of lipoxamycin, a new antifungal agent. *Antimicrob. Agents Chemother.*, 10, 455-461.
27. Onishi, J. C., Milligan, J. A., Basilio, A., Bergstrom, J., Curotto, J., Huang, L., et al. (1997). Antimicrobial activity of viridofungins. *J. Antibiot.*, 50: 334-338.
28. Zweerink, M. M., Edison, A. M., Wells, G. B., Pinto, W., and Lester, R. L. (1992). Characterization of a novel, potent, and specific inhibitor of serine palmitoyltransferase. *J. Biol. Chem.*, 267: 25032-25038.
29. Horn, W. S., Smith, J. L., Bills, G. F., Raghoobar, S. L., Helms, G. L., Kurtz, M. B., et al (1992). Sphingofungins F and F: Novel serinepalmitoyl transferase inhibitors from *Paecilomyces variotii*. *J. Antibiot.*, 45: 1692-1696.
30. Mandala, S. M., Thornton, R. A., Frommer, B. R., Dreikorn, S., and Kurtz, M. B. (1997). Viridofungins, novel inhibitors of sphingolipid synthesis. *J. Antibiot.*, 50: 339-343.
31. Schmale, D. G., & Munkvold, G. P. (2009). Mycotoxins in crops: A threat to human and domestic animal health. *Plant Health Inst.*, 3, 340-353.
32. Wu, W. I., McDonough, V. M., Nickels, J. T., Ko, J., Fischl, A. S., Vales, T. R. and Carman, G. M. (1995). Regulation of lipid biosynthesis in *Saccharomyces cerevisiae* by fumonisin B1. *J Biol Chem.*, 270:13171-13178.
33. Vicente, M. F., Basilio, A., Cabello, A., and Pelaez, F. (2003). Microbial natural products as a source of antifungals. *Clin Microbiol Infect.*, 9: 15-32.
34. Zhong, W., Jeffries, M. W., and Georgopapadakou, N. H. (2000). Inhibition of Inositol Phosphorylceramide Synthase by Aureobasidin A in *Candida* and *Aspergillus* Species. *Antimicrob. Agents and Chemother.*, 44: 651-653.
35. Justice, M. C., Hsu, M. J., Tse, B., Ku, T., Balkovec, J., Schmatz, D., and Nielsen, J. (1998). Elongation factor 2 as a novel target for selective inhibition of fungal protein synthesis. *J. Biol. Chem.*, 273: 3148-3151.
36. Domínguez, J. M., and Martín, J. J. (1998). Identification of elongation factor 2 as the essential protein targeted by sordarins in *Candida albicans*. *Antimicrob. Agents and Chemother.*, 42, 2279-2283.
37. Okada, H., Kamiya, S., Shiina, Y., Suwa, H., Nagashima, M., Nakajima, S., et al (1998). BE-31405, a new antifungal antibiotic produced by *Penicillium minioluteum*. I. Description of producing organism, fermentation, isolation, physico-chemical and biological properties. *J. Antibiot.*, 51: 1081-1086.

NEWS ITEM

Scientific findings :

Scientists worked out Novel approach to postpone Age related Health Deterioration:

Researchers have discovered a technique for breaking down damaged mitochondria and removing them from cells. This method resulted in improved health and extended lifespan for the insects, and its developers hope it may one day lead to longevity therapies for humans.

Researchers studying middle-aged fruit flies have improved the insects' health substantially and slowing their aging significantly. They believe their technique could someday pave the way toward delaying the onset of Alzheimer's disease, Parkinson's disease, cancer, cardiovascular disease, stroke, and other age-related diseases in humans. Their approach targets the cellular power houses, called mitochondria, which control the cell growth and death. Mitochondria frequently sustain damage as part of the aging process, and cells can't always remove these damaged organelles, which then become toxic as they accumulate in the muscles and the brain and other organs. This buildup contributes to a broad variety of age-related diseases. In this study, published in Nature Communications, the researchers found that the mitochondria in fruit flies changed shape, elongating as the insects hit middle age. The team broke damaged mitochondria up and removed them, which caused the flies to be more energetic and live 12 to 20 percent longer. Perhaps even more excitingly, the scientists discovered key cellular components of the process of mitochondrion elongation and removal. When they increased the levels of a protein called Drp1, this broke down the mitochondria, allowing them to be removed through a process controlled by the Atg1 gene. The scientists also switched off a protein called Mfn so the mitochondria were unable to fuse together into larger pieces, which also improving the health and extending the lives of the flies.

Novel CRISPR therapeutic approach to undo DMD mutations : A new approach to CRISPR-

Cas9 gene-editing technology, called myoediting, successfully restored dystrophin production and contraction force in heart muscle cells of Duchenne muscular dystrophy (DMD) patients. The new strategy, developed by U.S. and German researchers, targets sites located in "hot spots" of mutations along the dystrophin gene, allowing its editing and repair. The study, "Correction of diverse muscular dystrophy mutations in human engineered heart muscle by single-site genome editing," was published in the journal Science Advances. DMD is associated with the degeneration of skeletal and heart muscle caused by more than 3,000 different mutations in the dystrophin protein, which is essential for correct muscle movement. Researchers had previously shown that the genome editing method CRISPR could correct genetic defects that characterize Duchenne in mouse models and human cells. The CRISPR-Cas9 system, originally discovered in bacteria as a defense mechanism, allows researchers to edit parts of the genome by adding, removing, or changing specific sections of the DNA sequence. However, due to the high number of mutations involved, a specific therapy would have to be developed for each mutation. The novel CRISPR method, called myoediting, can modify DNA so that a wide region of mutation hot spots is skipped from the final dystrophin protein, potentially correcting the majority of DMD mutations.

Reversal of cell aging is possible now :

Induced pluripotent stem (iPS) cells may be the key to reversing aging in hematopoietic stem cells. The technique is also particularly useful for combating blood-related cancers and other disorders. From revitalizing heartbeats and increasing longevity, to removing disorders via gene editing, blood-borne challenges are approached with new solutions as quickly as we can innovate them. While many of the solutions we currently have can tackle blood disorders reactively, researchers at the University of Lunds in Sweden

have devised a method that could address blood disorders proactively. Our blood changes as we age due to epigenetics, a process by which our gene expression is silenced or activated over time, without modification of the genetic code itself. With this in mind, the team of researchers at the University of Lunds took a look at the hematopoietic stem cells (HSC) of aged mice to see if they could unlock the mysteries of how our cells age. The iPS cells served as a “reset button”, reprogramming the blood stem cells and sparking a rejuvenation of sorts. Researchers observed that the progenitor HSC cells in the old mice began to produce blood cells functionally similar to those seen in younger mice. The group’s data suggests that HSC aging can be reversed by the introduction of iPS cells. It’s important to note, however, that these changes in blood cell production do not primarily occur due to mutations — but because of epigenetic changes in gene expression over time. With their encouraging results, the research team is hopeful they may be closer to developing therapies that could reduce the incidence of blood disorders, including the three main types of blood cancers and over 100 blood-related diseases

Novel Tuberculosis detecting devise is on board : There may soon be a cost-effective, time-saving gadget to detect mycobacterium tuberculosis. Researchers from IIT Delhi, Jamia Hamdard University and Indian Council for Medical Research have developed ‘iMC2 TB Test’, which promises to bring down the detection time from four days to an hour. At present, smear microscopy is used to diagnose pulmonary TB by analysis of sputum samples. The new gadget needs no expertise or heavy infrastructure to test sputum. The gadget is the brainchild of Seyed E Hasnain of IIT-D who is the VC of Jamia Hamdard, Ravikrishnan Elangovan of IIT-D and Nasreen Ehtesham of ICMR. The diagnostic kit costing up to Rs 500 would be designed to minimise exposure among clinical workers. Six samples could be tested at a time. The gadget is already being tested at Jamia Hamdard. The project has cost Rs 2.28 crore and comes under a centrally funded IIT-IISc joint programme.

Drastic decline of Phytoplankton population to 40% since 1950

Researchers find trouble among phytoplankton, the base of the food chain, which has implications for the marine food web and the world’s carbon cycle. The microscopic plants that form the foundation of the ocean’s food web are declining, reports a study published in Nature. The tiny organisms, known as phytoplankton, also gobble up carbon dioxide to produce half the world’s oxygen output—equaling that of trees and plants on land. But their numbers have dwindled since the dawn of the 20th century, with unknown consequences for ocean ecosystems and the planet’s carbon cycle. Researchers at Canada’s Dalhousie University say the global population of phytoplankton has fallen about 40 percent since 1950. That translates to an annual drop of about 1 percent of the average plankton population between 1899 and 2008. The scientists believe that rising sea surface temperatures are to blame. The researchers found the most notable phytoplankton declines in waters near the poles and in the tropics, as well as the open ocean. They believe that rising sea temperatures are driving the decline. As surface water warms, it tends to form a distinct layer that does not mix well with cooler, nutrient-rich water below, depriving phytoplankton of some of the materials they need to turn CO₂ and sunlight into energy.

Scientists from MIT discovered a novel way to freeze water at boiling point, first of its kind : In a scientific breakthrough, researchers discovered a way to freeze water at temperatures higher than 100 degrees Celsius (212 degrees Fahrenheit) successfully. Because of water’s unique properties, the technique could be vital for the development of “ice” wires, which provide stable conductors of electricity already in the configuration needed for use in electronics. In an academic article recently published in Nature Nanotechnology, the research team demonstrated how common substances like water can drastically change behavior when confined to a minuscule space measuring in billionths of a

meter. The article's lead author, MIT's Carbon P. Dubbs Professor in Chemical Engineering Michael Strano and his team of researchers utilized single carbon nanotubes to trap water molecules, distorting the substance's change between solid, liquid and gas states.

For the first time scientists measured anti matter

Scientists have made the most precise measurement of antimatter yet, and the results only deepen the mystery of why life, the universe, and everything in it exists. The new measurements show that, to an incredibly high degree of precision, antimatter and matter behave identically. Now, in a new study published today (April 4) in the journal *Nature*, Hangst's team has achieved an unprecedented standard: They've taken the most precise measurement of antihydrogen — or any type of antimatter at all — to date. In 15,000 atoms of antihydrogen (think doing that aforementioned mixing process some 750 times), they studied the frequency of light the atoms emit or absorb when they jump from a lower energy state to a higher one. [Beyond Higgs: 5 Elusive Particles That May Lurk in the Universe] The researchers' measurements showed that antihydrogen atoms' energy levels, and the amount of light absorbed, agreed with their hydrogen counterparts, with a precision of 2 parts per trillion, dramatically improving upon the previous measurement precision on the order of parts per billion.

Metastasis is influenced by DNA of Mitochondria

The mitochondrial genome of mice is only 16 kilobases long, comprising just 37 genes, yet its polymorphisms appear related to the metastatic potential of cancer, researchers report at the American Association of Cancer Research annual meeting in Chicago. Researchers swapped the nuclear and mitochondrial DNA among several mouse strains and observed changes in immune function, microbiome composition, metabolomics, and tumor spread that tracked with mitochondrial

type. The latest, unpublished findings build upon a 2017 report in *Cancer Research* by Welch's group that showed that the mitochondrial genome was tied to the speed of cancer growth and metastasis. In the latest experiments, the researchers took cancer cells with the mouse strains' original nuclear and mitochondrial genomic backgrounds and infused them into mice with either original or swapped mitochondrial DNA. This set-up gave the investigators a look at how mitochondrial DNA in tissues outside the tumor might affect cancer spread. Again, the team found that the amount of metastases was tied to mitochondrial type.

Indians traversed to Australia 4000 years ago

Genetic evidence suggests that just over 4 millennia ago a group of Indian travellers landed in Australia and stayed. The evidence emerged a few years ago after a group of Aboriginal men's Y chromosomes matched with Y chromosomes typically found in Indian men. Up until now, the exact details, though, have been unclear. But Irina Pugach from the Max Planck Institute for Evolutionary Anthropology may have recently solved the thousand-year-old case. 4,000 years before the First Fleet landed on our fair shores, Indian adventurers had already settled and were accepted into the Indigenous Australian culture. The study found a pattern of SNPs that is only found in Indian genetics, specifically the Dravidian speakers from South India.

Research draws speculation as to why ancient terrestrial deer like animal evolved to whales

Whales come from a species of ancient deer-like creatures known as *Indohyus*. They roamed southern Asia about 48 million years ago. An *Indohyus* was only about the size of a raccoon, and researchers believe that they fed on aquatic plants. So what coaxed these creatures back into the ocean 100 million years after their ancestors climbed out of it? A duo of researchers contend that this question has received far too little attention, until now. The results of their study has been published in a report in the journal

Paleobiology. To date, there have been two prevailing hypotheses. The scientists isolated 69 incidents in which a terrestrial species decided to live in or extract sustenance from the ocean after a mass extinction had taken place. In two of the largest such events, one that occurred 201 million years ago at the end of the Triassic and another at the end of the Cretaceous period, there was no grand exodus of land animals back into the sea.

New approach to trace contamination of paraffin oil in coconut oil

Using a novel approach, researchers at Indian Institute of Technology (IIT) Madras have for the first time been able to use mass spectrometry to analyse various saturated and unsaturated hydrocarbons directly from solutions. Ionising the constituent molecules of a hydrocarbon sample for detection using mass spectrometry has not been easy till date as hydrocarbons do not tend to lose or gain electrons to form ions. Using the novel technique — laser-assisted paper spray ionisation mass spectrometry — the research team led by Prof. T. Pradeep from the institute's Department of Chemistry could detect various hydrocarbons, importantly, paraffin oil contamination in coconut oil samples. Though it is common knowledge that vegetable oils are adulterated, the extent of contamination with paraffin oil was as much as 10%. The results were published in the journal *Analytical Chemistry*. Detecting ions using paper spray ionisation mass spectrometry is known already. In this method, a regular filter paper containing the sample is subjected to high electrical potential and the charged droplets and the ions derived from them are analysed using a mass spectrometry. But this method cannot be used for detecting hydrocarbons. So the researchers turned to the humble laser pointer used commonly during presentations to turn the stubborn hydrocarbons to emit ions for the measurement.

IISc researchers developed nanomotors which aids in study of cell organelles.

Nanomotors and their applications in biomedicine have gained huge interest in recent times and now researchers from Indian Institute of Science (IISc), Bengaluru, have successfully shown how to move them around inside living cells. In a paper published recently in *Advanced Materials*, the team demonstrated the manoeuvrability of magnetic-material-coated silica nanomotors inside different cell lines. Less than 3 microns in length, they can be used for targeted drug delivery, nanosensing and in therapeutics. The group fabricated two helical nanomotors with different dimensions for their experiments. They found that nanomotors could move inside the cells when a rotating magnetic field of less than eighty Gauss (much below the safe level for human beings) is given. The smaller ones (250 nm thick and 2.4 micron long) could move at a speed of around 500 nanometer per second, throughout the cell much easier than the big ones (400 nm thick and 2.8 microns long) due to the natural porosity of intracellular environment. Three types of cell lines — human cervical cancer cells, human embryonic kidney and endothelial cells from cattle — were used for the study.

Scientists worked out novel technique for In vitro segregation of liposomes

In a prelude to manifest an artificial cell team of researchers led by Siddharth Deshpande, a postdoctoral researcher at Cees Dekker's lab at Delft University of Technology in the Netherlands mechanically segregates liposomes, which are compositional equivalents of cell envelopes. All living cells are enclosed in a lipid envelope. Thus, a liposome, which is a lipid bubble filled with water, is the simplest mimic of a living cell. Generating pure liposomes in a controlled fashion in the lab is not simple. To achieve this goal, Dr. Deshpande designed tiny fluid chambers with dimensions in the order of one-millionth of a metre to form stable liposomes. He reported this bubble-blowing method called octanol-assisted liposome assembly (OLA) in *Nature* in 2016 and in *Nature Protocols* in 2018. The team's next mission was to split these liposomes into 'daughter' liposomes. In the past, researchers have used different

methods to divide liposomes. However, all these methods suffered from leaky daughter liposomes and asymmetric splitting. In their latest study, published in ACS Nano journal, he kept the approach simple. He designed a wedge in the microfluidic chamber that physically blocked the newly formed liposomes as they progressed down the channel. By adding a fluorescent dye to the water inside the liposomes, the researchers visualised their fate using a microscope.

World's tiny fern is reported from Western Ghats

Indian researchers have discovered the world's smallest land fern hiding in the Ahwa forests of the Western Ghats in Gujarat's Dang district. According to a recent study in Scientific Reports, an international journal that publishes multidisciplinary research, the fingernail-sized fern belongs to a group known as the adder's-tongue ferns, named after their resemblance to a snake's tongue. The size of the new Malvi's adder's-tongue fern *Ophioglossum malviae* – just one centimetre.

Study reported that bacterial resistance is attributed to just a tiny dose of antibiotics

Even low concentrations of antibiotics can cause high antibiotic resistance in bacteria, a growing problem in global health care, according to a study. In the study published in the journal Nature Communications, researchers investigated how prolonged exposure to low levels of antibiotics contributes to the development of bacterial antibiotic resistance. The researchers show that low concentrations of antibiotics, too, play a major part in the development of resistance. The study showed that, over time, bacteria exposed to low doses of antibiotics developed resistance to antibiotic levels that were more than a thousand times higher than the initial level to which the bacteria were subjected. It was also found that the mutations in the bacterial DNA that cause resistance are of a different type than if they have been exposed to high doses.

Sulphur laden fossil fuels cleaned by bacteria

Using novel bacterial strains, scientists have

successfully removed sulphur from fossil fuels such as petroleum and coal. Sulphur is one of the major pollutants emitted during the combustion of fossil fuels. Scientists from CSIR-Institute of Minerals and Materials Technology (CSIR-IMMT) in Bhubaneswar used four bacterial strains that use dibenzothiophene (an organic sulphur compound which is a major contaminant of fossil fuel) as an energy source thereby getting rid of the sulphur. The work published in the journal PLOS ONE.

Scientists unleashed first bionic kidney which replaces dialysis process

California in San Francisco have invented the world's first bionic kidney which can replace damaged kidneys. The world's first bionic kidney can be inserted in a body by a common surgical procedure and it has proved to work efficiently. It is now proving to be the perfect replacement for a damaged kidney. The bionic kidney consists of several microchips which is moved by the heart. The bionic kidney also filters out toxins from the blood in the same way as a normal kidney.

ACADEMIC NEWS

UGC's Landmark decision towards institutionalizing Institutions of Eminence (IoE)

In a landmark development in the Higher Education sector in India, the University Grants Commission (UGC) has notified two important regulations: (i) UGC (Institutions of Eminence Deemed to be Universities) Regulations, 2017 for private institutions; (ii) UGC (Declaration of Government Educational Institutions as Institutions of Eminence) Guidelines, 2017 for public Institutions. These two regulations reflect the Government's efforts and seriousness to establish twenty 'Institutions of Eminence' to achieve world class status, from amongst the existing Government/private institutions and new institutions from the private sector. The objective is to provide for greater Academic, Financial, Administrative and other regulatory autonomy to 10 public and 10 private higher educational institutions to emerge as world-class teaching and research institutions. The Institutions declared as Institutions of

Eminence will be free from the usual regulatory mechanism to choose their path to become institutions of global repute with emphasis on multi disciplinary initiatives, high quality research, global best practices and international collaborations.

PM Research fellowships to curb the cream of India's brain drain

Indian government rolls out Rs 80,000 a month PhD grant to plug brain drain. As part of its move to stop them from taking up research scholarships abroad, the Cabinet has cleared the PM Research Fellowships (PMRF) for students of higher education institutions like the IITs, IISERs and NITs, which will also be the country's most lavish paid scholarships to date. Under the scheme, students who have completed or are in final year of B.Tech or integrated M.Tech or M.Sc in science and technology streams at IISc, IITs, NITs, IISERs, IIITs will be offered direct admissions in PhD programmes in IITs and IISc. The minimum eligibility for aspirants will be a cumulative grade point average (CGPA) of 8.5. The minister said that the scheme will be rolled out from the 2018-19 academic session. Students, who would fulfil the eligibility criteria and get shortlisted, would be offered a fellowship of Rs 70,000 a month during the first two years, Rs 75,000 per month during the third year and Rs 80,000 per month during the fourth and the fifth year.

62 Higher Educational institutions granted full autonomy by UGC

The University Grants Commission (UGC) approved full autonomy for 62 higher educational institutions, including JNU, BHU, AMU, TERI and University of Hyderabad, which have maintained high standards of excellence. The decision was taken at a UGC meeting today where five central universities, 21 state universities, 26 private universities besides 10 other colleges were granted autonomy under the Autonomous Colleges Regulation. These Higher Educational Institutions

(HEIs) achieved a benchmark of 3.26 and above NAAC (National Accreditation and Assessment Council) ranking.

POST – DOC OPPORTUNITIES

1. Indian Institute of Technology, Madras offers Postdoctoral Fellowship for women with Break in career :

IIT Madras offers PDF for women with Break in career with Ph.D with an objective of maintaining awareness and interest in high quality academic research in various departments. Refer www.iitm.ac.in.

2. TIFR Postdoctoral Fellow Positions :

Postdoctoral positions funded for a minimum of 3 years are available in the research group of Dr. Sreelaja Nair in the Department of Biological Sciences at the Tata Institute of Fundamental Research in Mumbai, India. Refer www.tifr.res.in

3. Indian Institute of Science Education and Research, Pune Post-Doctoral Position :

The research involves using mouse and human cell lines as well as ex vivo cells questions regarding T cell activation, differentiation, commitments to different functional fates, survival and death will be addressed. Refer iiserpune.ac.in.

4. Indian Institute of Technology Gandhinagar Postdoctoral Fellow :

One Postdoctoral Position in Aspects of the hot QCD medium in the presence of Strong EM fields under Prof. Vinod Chandra. Refer iitgn.ac.in

5. Indian Institute of Science Education and Research - Tirupati Post - Doctoral Research Fellowship Program :

IISER Tirupati is starting an active Post-doctoral Research Fellowship Program to enable highly motivated young researchers to conduct research in the frontier areas of science and Technology. Refer iisertirupati.ac.in



**International Conference on
Innovations in Pharma and Biopharma Industry
(ICIPBI - 2017)**

**CHALLENGES AND OPPORTUNITIES FOR
ACADEMY AND INDUSTRY
(20-22 December, 2017)**

Special Sessions

**Regenerative Medicine Innovations as Future
Medicine of 21st Century
Cancer and Infectious Disease Research - New
Drug Discovery and Development
Data Science Workshop**



Organizers

**University of Hyderabad
Hyderabad**



With participation from
Association of Biotechnology and Pharmacy

Contact

**Convener, Conference Secretariat
School of Life Science
University of Hyderabad
Hyderabad, Telangana - 500046, India
Ph : +914023134730,
Email : icipbi2017@gmail.com**

Registered with Registrar of News Papers for India
Regn. No. APENG/2008/28877

Association of Biotechnology and Pharmacy

(Regn. No. 28OF 2007)

Executive Council

Hon. President

Prof. B. Suresh

Hon. Secretary

Prof. K. Chinnaswamy

President Elect

Prof. T. V. Narayana

Bangalore

General Secretary

Prof. K.R.S. Sambasiva Rao

Guntur

Vice-Presidents

Prof. M. Vijayalakshmi

Guntur

Treasurer

Prof. P. Sudhakar

Prof. T. K. Ravi

Coimbatore

Advisory Board

Prof. C. K. Kokate, Belgaum

Prof. B. K. Gupta, Kolkata

Prof. Y. Madhusudhana Rao, Warangal

Prof. M. D. Karwekar, Bangalore

Prof. K. P. R. Chowdary, Vizag

Dr. V. S.V. Rao Vadlamudi, Hyderabad

Executive Members

Prof. V. Ravichandran, Chennai

Prof. Gabhe, Mumbai

Prof. Unnikrishna Phanicker, Trivandrum

Prof. R. Nagaraju, Tirupathi

Prof. S. Jaipal Reddy, Hyderabad

Prof. C. S. V. Ramachandra Rao, Vijayawada

Dr. C. Gopala Krishna, Guntur

Dr. K. Ammani, Guntur

Dr. J. Ramesh Babu, Guntur

Prof. G. Vidyasagar, Kutch

Prof. T. Somasekhar, Bangalore

Prof. S. Vidyadhara, Guntur

Prof. K. S. R. G. Prasad, Tirupathi

Prof. G. Devala Rao, Vijayawada

Prof. B. Jayakar, Salem

Prof. S. C. Marihal, Goa

M. B. R. Prasad, Vijayawada

Dr. M. Subba Rao, Nuzividu

Prof. Y. Rajendra Prasad, Vizag

Prof. P. M. Gaikwad, Ahmednagar

Printed, Published and owned by Association of Bio-Technology and Pharmacy # 6-69-64 : 6/19, Brodipet, Guntur - 522 002, Andhra Pradesh, India. Printed at : Don Bosco Tech. School Press, Ring Road, Guntur - 522 007. A.P., India Published at : Association of Bio-Technology and Pharmacy # 6-69-64 : 6/19, Brodipet, Guntur - 522 002, Andhra Pradesh, India. Editors : Prof. K.R.S. Sambasiva Rao, Prof. Karnam S. Murthy